Front. Chem. Sci. Eng. 2025, 19(10): 96
https://doi.org/10.1007/s11705-025-2567-9

REVIEW ARTICLE

A review of experimental approaches, trends and opportunities in plasma-based gas conversion research

Sirui Li (✉)[1], Pranav Arun[1], Huub van den Bogaard[1], Thijs van Raak[1], Changjun Liu[2], Fausto Gallucci[1]

1 Sustainable Process Engineering, Department of Chemical Engineering and Chemistry, Eindhoven University of Technology, Eindhoven 5612 AP, The Netherlands
2 School of Chemical Engineering and Technology, Tianjin University, Tianjin 300072, China

Abstract Plasma-based gas conversion has emerged as a sustainable and promising approach for chemical production, attracting increasing attention in recent years. Significant progress has been achieved in areas such as nitrogen fixation, CO_2 conversion, methane activation, and others, driven by the contributions of researchers from diverse disciplines. Given that most research in this field is experimental, the methodologies employed play a pivotal role and demand careful consideration. However, due to the interdisciplinary nature of the field and variations in research objectives, available resources, and laboratory standards, experimental set-ups and approaches often differ significantly. Moreover, critical details regarding operational techniques and key methodologies are sometimes overlooked. This paper provides a comprehensive review of the methodologies and experimental approaches used in the study of plasma-based gas conversion for chemical production. It first examines experimental systems, including plasma reactor design, plasma-catalyst integration, and set-up configuration. Subsequently, operational schemes, conditions, and analytical procedures are discussed, with examples showcasing state-of-the-art advancements. Finally, discussion on emerging research trends and potential opportunities are presented, aiming to inspire further advancements and broaden the scope of this growing field.

Keywords plasma catalysis, plasma reactor, CO_2 utilization, nitrogen fixation, methane conversion

1 Introduction

The use of plasma-based gas conversion for chemical production is not a new concept, with its roots stretching back over 100 years. Early research dates to 1857 when Siemens introduced silent discharge for ozone generation, laying the foundation for later applications. The Birkeland-Eyde process, which synthesized nitric oxide via thermal arc plasma, was commercialized in the early 1900s, marking it the first industrial plasma process. Even plasma-catalysis—a topic receiving substantial attention today—can be traced back to 1921 when Ray and Anderegg combined plasma discharge with silver catalysts to oxidize carbon monoxide [1]. However, plasma technology has not been widely applied in the chemical industry. Over the past century, the industry has been largely dominated by thermochemical processes powered by inexpensive fossil fuels. In recent decades, with increasing environmental concerns and a global push for energy transition, there has been a shift toward renewable electricity and the electrification of the chemical production sector. Plasma technology, particularly non-thermal plasma, has emerged as a promising green alternative. It offers significant advantages, including mild operating conditions (e.g., atmospheric pressure and low temperature), instantaneous control, and flexibility in scales. These characteristics make plasma highly suitable for coupling with intermittent renewable energy sources, aligning with the "Power-to-X" concept to produce chemicals and store energy.

Driven by the growing interest from both academia and industry, plasma-based gas conversion research has seen a dramatic surge in the past 15 years. Researchers worldwide have made significant advancements, as reflected by the substantial growth in scientific publications in Fig. 1(a). Major research efforts focus on the activation of small molecules such as N_2, CO_2, and CH_4. The activation of these molecules typically requires high energy input from elevated temperatures in conventional processes. This has been considered as a key

Received March 4, 2025; accepted April 17, 2025; online June 25, 2025

E-mail: s.li1@tue.nl

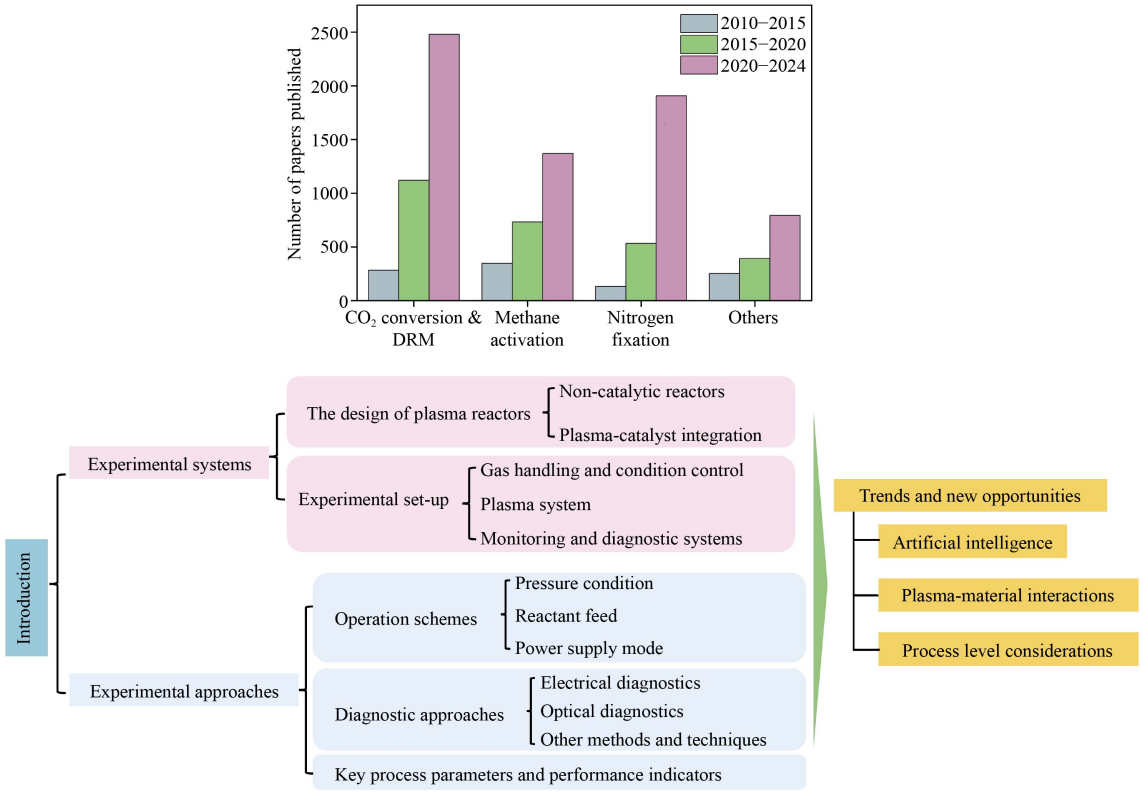

Fig. 1 (a) Number of journal paper publications on various gas-phase reactions over the year 2010–2024. Data retrieved from Google scholar database based on the keywords "plasma assisted" and "plasma catalysis with logical operators "AND" and "OR" to refine the search; (b) the structure of this review paper (DRM: dry reforming of methane; artificial intelligence, AI).

opportunity for plasma chemistry and plasma-catalysis. To date, several review papers have been published, covering topics such as nitrogen fixation, CO_2 conversion, and CH_4 activation with detailed background information, fundamental principles, the state of the art, and recent progress in the field. Table 1 summarizes

Table 1 Review papers published in the past five years (2020–2024) on plasma-based gas conversion

Topic	Title	Authors	Year	Ref.
CO_2 conversion	Plasma technology for CO_2 conversion: a personal perspective on prospects and gaps	Bogaerts et al.	2020	[2]
	A review of non-thermal plasma technology: a novel solution for CO_2 conversion and utilization	George et al.	2021	[3]
	CO_2 conversion using catalyst-free and catalyst-assisted plasma-processes: recent progress and understanding	Chen et al.	2021	[4]
	Non-thermal plasma catalysis for CO_2 conversion and catalyst design for the process	Xu et al.	2021	[5]
	Plasma catalysis: a feasible solution for carbon dioxide valorization?	Anoop et al.	2021	[6]
	Meta-analysis of CO_2 conversion, energy efficiency, and other performance data of plasma-catalysis reactors with the open access PIONEER database	Salden et al.	2023	[7]
	Recent trends in plasma-assisted CO_2 methanation: a critical review of recent studies	Ullah et al.	2023	[8]
	Plasma catalytic technology for CH_4 and CO_2 conversion: a review highlighting fluidized-bed (FB) plasma reactor	Chen et al.	2024	[9]
	Plasma-based CO_2 conversion	Bogaerts et al.	2024	[10]
Methane activation	Plasma-enhanced catalysis for the upgrading of methane: a review of modelling and simulation methods	Maitre et al.	2020	[11]
	Methane to methanol through heterogeneous catalysis and plasma catalysis	Li et al.	2021	[12]
	Current status and challenges of plasma and plasma-catalysis for methane coupling: a review	Maslova et al.	2024	[13]
	Plasma catalysis for hydrogen production: a bright future for decarbonization	Wang et al.	2024	[14]
	Non-thermal plasma enhanced catalytic conversion of methane into value added chemicals and fuels	Baig et al.	2024	[15]
	Plasma-driven catalysis: green ammonia synthesis with intermittent electricity	Rouwenhorst et al.	2020	[16]
Nitrogen fixation	Sustainable ammonia production by non-thermal plasmas: status, mechanisms, and opportunities	Zhou et al.	2021	[17]
	Recent advances in plasma-enabled ammonia synthesis: state-of-the-art, challenges, and outlook	Zeng et al.	2023	[18]
	From the Birkeland-Eyde process towards energy-efficient plasma-based NO_x synthesis: a techno-economic analysis (TEA)	Rouwenhorst et al.	2023	[19]
	Atmospheric-pressure plasmas for NO_x production: short review on current status	Abdelaziz et al.	2024	[20]
	Ammonia synthesis by nonthermal plasma catalysis: a review on recent research progress	Zhang et al.	2024	[21]

notable reviews as our recommendation for readers seeking additional insights. Table 2 listed the examples of the most studied reactions, presenting their current technological readiness level (TRL) and the typical range of reported energy consumption. While lower energy consumption has been observed in some cases, especially with recent advancements, the values listed represent the commonly reported value, providing a general overview of the state of the art.

While computational studies have contributed to the field, the majority of research focuses on experimental work, where methodologies play a critical role. Plasma-based gas conversion is inherently multidisciplinary, requiring expertise in plasma physics, plasma chemistry, chemical engineering, and electrical engineering. Researchers from different backgrounds may interpret the subject differently and employ diverse methodologies. Consequently, experimental set-ups, techniques, and performance metrics vary significantly. Furthermore, important details about research methodologies and practical techniques are often overlooked, particularly given the growing interest and rapid expansion of this field. To address these gaps, this paper provides a comprehensive review of the experimental methodologies employed in plasma-based gas conversion research with a focus on small molecule activation for chemical production. It aims to offer valuable insights to readers from diverse disciplines. Examples from the literature, primarily focused on CO_2 conversion due to its extensive research base, are used to illustrate key points. The structure of this paper is outlined in Fig. 1(b). This introduction offers an overview of the field, including its historical development, emerging trends, and key reactions of interest. Subsequent sections will present a detailed review of experimental systems, methodologies, and approaches. The paper concludes with a personal perspective on future trends and opportunities in this rapidly evolving field.

Table 2 Examples of key reactions investigated in this field

Reaction	Energy consumption commonly reported	TRL
CO_2 splitting $2CO_2 \rightarrow 2CO + O_2$ $\Delta H = 283$ kJ·mol^{-1}	0.48–33 MJ (per mol CO_2 converted)	3–4
CO_2 hydrogenation $CO_2 + 4H_2 \rightarrow CH_4 + 2H_2O$ $\Delta H = -165$ kJ·mol^{-1}	0.96–57 MJ (per mol CO_2 converted)	2–3
$CO_2 + 3H_2 \rightarrow CH_3OH + H_2O$ $\Delta H = -40.9$ kJ·mol^{-1}	11–50 MJ (per mol CH_3OH produced)	1–2
DRM $CO_2 + CH_4 \rightarrow 2CO + 2H_2$ $\Delta H = 247$ kJ·mol^{-1}	1.9–65 MJ (per mol CO_2 converted)	3–4
Nitrogen fixation $N_2 + 2O_2 \rightarrow 2NO$ $\Delta H = 180.4$ kJ·mol^{-1}	2.5–20 MJ (per mol N fixed)	3–5
$N_2 + 3H_2 \rightarrow 2NH_3$ $\Delta H = -92.4$ kJ·mol^{-1}	34–150 MJ (per mol NH_3 produced)	1–2

The TRLs listed are based on the overview from Ref. [22], with adaptations reflecting the status as of 2024.

2 Experimental systems

2.1 Experimental set-up

Over the years, numerous experimental set-ups have been developed for plasma-based gas conversion research. These systems are tailored to meet specific research objectives and experimental designs, incorporating a variety of equipment configurations. Despite this variation, most laboratory-scale experiments share common components, which can be broadly categorized into three major parts, as illustrated in Fig. 2.

2.1.1 Gas handling and condition control

Gas reactants are typically fed to the reactor continuously

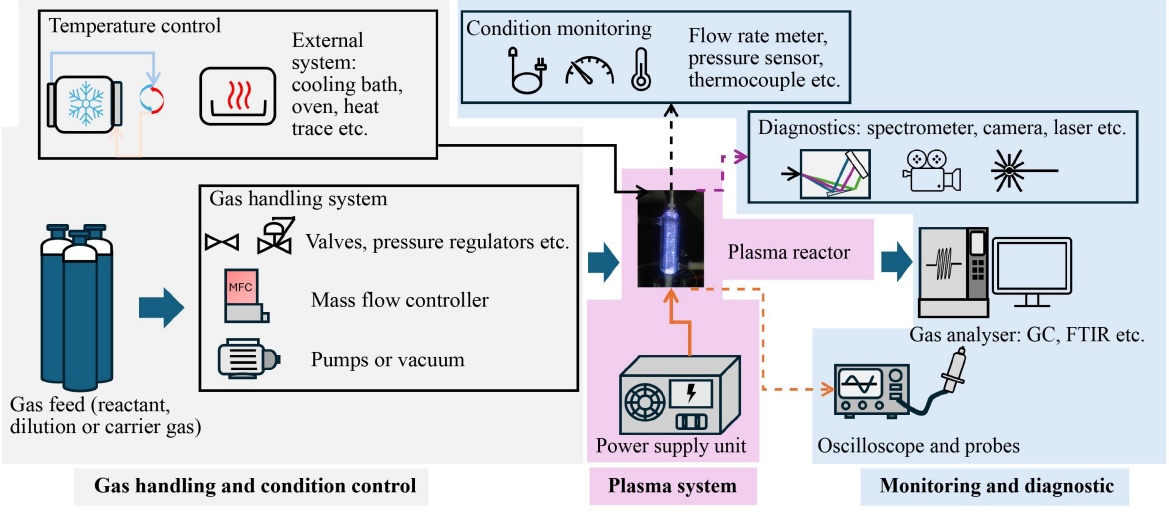

Fig. 2 Generic summary of experimental set-up which contains three parts: gas handling and condition control, plasma system, and monitoring and diagnostic system (GC: gas chromatography, FTIR: Fourier-transform infrared spectroscopy).

at a constant flow rate and desired concentration. Mass flow controllers are widely used to regulate flow rates, and these devices require calibration prior to experiments and periodic recalibration for accuracy. Gas pressure within the system, especially in the plasma reactor, is critical as it directly affects plasma properties and chemical performance. Most plasma experiments are conducted at or near atmospheric pressure, leveraging a key advantage of plasma chemistry over conventional methods through reduced costs and simplified process complexity. In some cases where plasma is operated at higher pressure, additional components like pressure control valves, back-pressure regulators, and pressure relief valves for safety need to be installed in the system. Conversely, in microwave plasma reactors, sub-atmospheric pressures are often employed, necessitating vacuum systems with pumps, control valves, pressure gauges, and sometimes a dedicated chamber. It needs to be noted that stable pressure, flow rate, and a compatible temperature profile are essential to ensure accurate measurements by downstream analytical equipment such as FTIR or GC. Additional devices such as diaphragm pumps can be utilized as needed.

Temperature control is another crucial factor in experimental system design. Unlike conventional thermal catalysis, the role of temperature in plasma or plasma-catalysis is more complex. Temperature variations can influence both plasma characteristics and catalyst activities, while the plasma itself generates heat, raising gas and catalyst temperatures. To address these effects, systems with various temperature control strategies have been established. Biset-Peiró et al. [23] categorized plasma reactors based on heat management strategies into three types: isothermal, adiabatic, and pseudo-adiabatic. Figure 3 compares experimental systems reported in the literature for these categories. In isothermal systems, comparisons with thermal catalysis at equivalent temperatures are often made to isolate plasma effects. However, it should be noted that the set temperature from external heating, or the measured average temperature does not reflect the practical temperature profile due to the plasma heating which may cause localized temperature increases.

Pseudo-adiabatic systems are widely used, particularly in plasma reactors without catalysts. External heating or cooling should be considered alongside reactor design to achieve optimal outcomes. An example is the water-electrode dielectric barrier discharge (DBD) reactor, which integrates cooling and plasma generation, although external water/coolant circulation is still required [24,25]. The impact of cooling has also been studied in microwave plasma reactors. For instance, Fuente's study on a surface wave microwave plasma reactor demonstrated a significant impact of cooling rates on CO_2 conversion, underscoring the importance of cooling system design for process optimization [26]. In warm plasmas like microwave [27] and gliding arc (GA) [28], external cooling is often essential to prevent overheating and maintain stable plasma operation.

Apart from the reactor, thermal management can also be applied to inlet and outlet gas streams, influencing experimental results. For example, Paulussen et al. [29] showed that preheating inlet gases to achieve temperatures between 30 and 170 °C led to a modest increase in CO_2 conversion from 26% to 28.5%. In addition, for reactions such as CO_2 hydrogenation, DRM, where water or liquid products may form, heating the pipelines and connectors is necessary to prevent condensation.

2.1.2 Plasma system

The fundamentals of non-thermal plasma generation including discharge mechanism, criteria and sources follow the general principles which have been described in many papers and textbooks [30,31]. However, establishing a plasma system requires practical considerations and cross-disciplinary knowledge. The two major components in a plasma system are the reactors and the power supply unit (PSU). To date, various reactor designs have been studied, and the design of reactors itself remains a significant research topic in this field. The design of plasma reactors is reviewed in Section 2.2.

The development of an efficient power supply for plasma systems is also a topic worth exploring, especially in the case of large-scale applications in which the overall energy consumption and cost of the entire process should be emphasized. This area intersects with electrical engineering, particularly with research on transformer systems and power electronics, including materials,

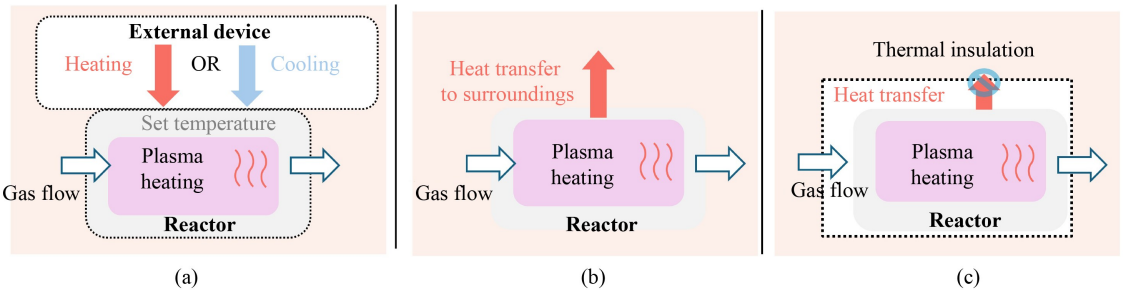

Fig. 3 Types of plasma reactor based on heat management: (a) isothermal, (b) pseudo-adiabatic and (c) adiabatic.

design, and topologies, as mentioned in several studies [32−34]. As for laboratory-scale experimental studies, the power supplies used vary widely, ranging from simple homemade devices with readily available components to high-precision commercial products. Output power can range from a few watts to kilowatts, with voltage signals in various forms, including constant (direct current (DC) power supply), sinusoidal (alternating current (AC) power supply), or pulsed, depending on the discharge type and reactor design. Most studies involving AC power supply use a single-phase output with adjustable power and a frequency range in kHz. While 50 Hz or three-phase systems which are closer to the industrial standard, have only been studied in a few cases [35−37]. The PSU plays a crucial role in experimental studies, particularly in enabling precise control and variation of key parameters during operation. This typically includes the modulation of output voltage, power, and frequency, all of which can significantly affect the performance of the plasma reactor. Commercially available PSUs often come equipped with built-in features for adjusting these parameters, as well as advanced functions such as feedback control and pulsed operation modes. In contrast, customized or home-made PSUs may require circuit modifications to achieve similar functionalities, which can be more complex.

Pulsed power supplies can be employed for plasma generation in various reactors, including DBD, corona, and plasma jets. In recent years, there has been growing interest in direct-driven nanosecond plasma discharge. The use of nanosecond pulsed power excitation provides a higher instantaneous power density and reduces the electric field, enhancing energy efficiency for reactions and preventing gas and reactor overheating that typically occurs with continuous operation [38]. It is important to mention that generating high-voltage (HV) nanosecond pulses and managing source-plasma interactions are critical to the system's overall energy efficiency [39]. However, these factors are often not considered in reported research, particularly in plasma-based CO_2 conversion, as they may fall outside the primary scope of plasma chemistry, plasma-catalysts or reactor development. Nonetheless, key parameters have been investigated in a few studies. For example, Montesano et al. studied the effect of different pulse patterns on the reduction of CO_2, and their results highlighted the importance of inter-pulse duration [40]. They also observed a delay of CO_2 dissociation after breakdown, and proposed a possible way to improve energy efficiency by shortening the interpulse period [41].

An essential point to consider is that the plasma discharge reactor is typically viewed as an unconventional load connected to the power supply, which influences the circuit's characteristics. For instance, a GA reactor behaves as a dynamic load with nonlinear and fast-changing V-I characteristics [42], while a DBD reactor is often considered a capacitive component with a distorted current profile that cannot function with a steady-state DC power source. Additionally, other components may be connected to the circuit for protection, monitoring, or plasma modulation. These components include but are not limited to, ballast resistors to limit current, resistive shunts to monitor current, and capacitors in series with DBD reactors to generate Lissajous figures.

In addition to conventional electrical power supplies, a new type of system based on triboelectric nanogenerators (TENGs) has recently been applied in the field of plasma-based gas conversion. Triboelectric plasma systems are relatively simple and can directly utilize various types of mechanical energy to generate plasma using TENGs characterized by HVs. Several studies have reported plasma generation using TENG-based systems [43,44], and explored their potential applications, such as nitrogen fixation [45,46], and CO_2 conversion [47,48]. However, the current TENG systems operate at very low power levels and may only be suitable for microplasma applications.

2.1.3 Monitoring and diagnostic systems

Equipment and devices used for monitoring and diagnostic purposes in plasma-based gas conversion experiments generally operate within two types of systems: operando and offline/ex-situ. Devices for monitoring experimental conditions, such as pressure and temperature, are usually part of the gas handling and control system. These include flow meters, pressure gauges, and thermocouples. Electrical diagnostics for plasma discharges are typically integrated into the plasma system and include equipment such as HV probes, Rogowski coils, oscilloscopes, and measuring capacitors or resistors. Proper selection of these devices is crucial, depending on the type of plasma discharge and measurement objectives. For instance, an oscilloscope with a high sampling rate is essential for capturing fine details of fast discharge phenomenon. Separately, an online gas analyzer is a key component of the monitoring and diagnostic system, often installed downstream of the reactor. Common gas analysis equipment includes GC, FTIR, and mass spectrometry (MS) for identifying and quantifying reaction products. Proper calibration of these instruments, particularly using internal standards based on specific experimental conditions, is crucial for obtaining accurate results. Furthermore, practical consideration needs to be taken during system integration. For instance, GA reactors typically operate at flow rates (several to tens of $L \cdot min^{-1}$) that may be too high for direct GC sampling or could cause pressure drop in infrared (IR) gas cell [49]. In such cases, an online measurement with a gas bypass line or additional components like flow controllers may be required. Conversely, in some cases with DBD

reactors operating at very low flow rates, a significant measurement delay may occur due to the extended travel time for the gas to reach the sampling point.

Optical diagnostic methods are commonly employed to study plasma properties, with systems such as optical emission spectroscopy (OES) and laser absorption spectroscopy in use. The complexity of these systems varies from simple spectrometers to integrated laser set-ups. It is often critical to use reactors, gas cells, and lenses tailored for specific measurement purposes. Examples of advanced *in situ* diagnostics for plasma-catalytic reactors are discussed in Section 5.

Offline/*ex-situ* diagnostic tools focus primarily on studying material properties, particularly catalysts and electrodes used in plasma-based experiments. Equipment commonly used such as X-ray diffraction, scanning electron microscopy, transmission electron microscopy, and Brunauer-Emmett-Teller analysis are similar to those used in conventional catalysis research. Although these devices are not directly integrated into the experimental set-up, it is essential to consider them during experimental planning. For example, the preparation and transfer of catalyst samples from the plasma reactor can be critical to maintaining material integrity for accurate analysis.

2.2 The design of plasma reactors

The plasma reactors used in this field are predominantly custom-designed, with materials and configurations tailored to meet specific experimental goals and laboratory conditions. Typically, the reactor dimensions reported in the literature range from a few to several tens of centimeters, although larger reactors, reaching up to meters in scale, have been documented in limited cases. These larger designs are less common, as most studies focus on laboratory-scale reactors with low TRL. The fundamental requirements for reactor development are ensuring stable and safe plasma operation. However, advanced reactor design also aims to enhance performance, particularly by improving energy efficiency and conversion. This calls for research on optimizing plasma properties and distribution, minimizing gas bypass around the plasma zone, and facilitating beneficial interactions between plasma and catalysts. Achieving these improvements often requires detailed study of plasma operation, electrode configuration, gas flow patterns, as well as heat and mass transfer within the reactor. The fundamentals of various reactor types for plasma-based gas conversion have been reviewed in several previous studies [30,50,51], to which we refer for background information. This section provides an overview focused specifically on the design and development of these reactors.

2.2.1 Non-catalytic reactors

Although reactor designs vary widely, they typically adhere to a few fundamental configurations. The most commonly studied types include DBD, GA, corona, microwave, and radiofrequency (RF) plasma reactors.

2.2.1.1 DBD reactors

DBD is one of the most studied plasma discharge types which has a history that could date back to 1857 when the first experimental study by Siemens was reported [52]. The configuration of a DBD reactor consists of two electrodes, a gas gap and at least one dielectric barrier. With the HV supply connected to the electrodes, a strong electric field is created to generate plasma in the gap, while the existence of the dielectric barrier prevents the formation of sparks, hence keeping the plasma with non-thermal equilibrium characteristics. There have been many different designs of DBD reactors which can be found in the review of Brandenburg [53]. In the case of gas conversion, DBD reactors are often manufactured as planar or coaxial configuration, as shown in Figs. 4(a) and 4(b). There are also designs of plasma jet reactors which are based on the DBD concept as shown in Fig. 4(c). The coaxial configuration provides better performance due to more uniform gas velocity distribution across the discharge zone. The key reactor parameters include gap size and discharge length, which determine the discharge volume and, consequently, the residence time of the reactants. The thickness and material properties of the dielectric barrier (e.g., dielectric constant), as well as the choice of electrode material, can influence reactor performance. This has been reported in several papers including the one from Wu et al. [54] who

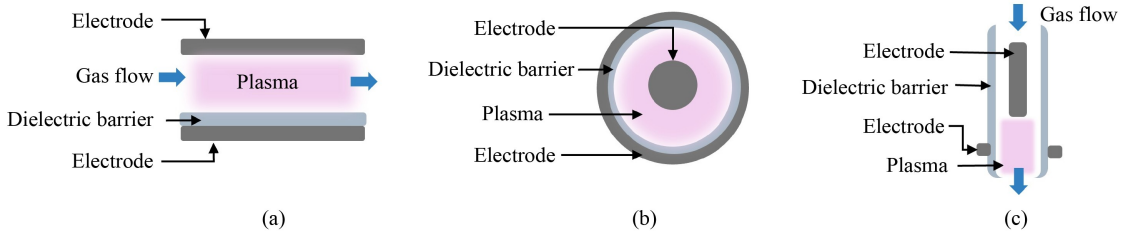

Fig. 4 The schematic of commonly used DBD reactors with (a) planar configuration, (b) coaxial configuration and (c) "jet" type configuration.

observed a better performance using an aluminum rod as the inner electrode than a copper or stainless-steel rod in their study of CO_2 conversion with a coaxial DBD reactor. The author believes that aluminum is preferred due to its moderate thermal conductivity and electrical conductivity, while copper works better as an external electrode due to its high electrical conductivity.

Several attempts have been made to investigate different designs of a DBD reactor to enhance the conversion of CO_2. For example, Belov et al. [55] studied the influence of the conductive carbonaceous coating on the electrical properties and CO_2 conversion; Wang et al. [56] studied the design with segmented outer electrode; and Niu et al. [57] reported their reactor design with multi-electrode system. Although it is possible to improve the conversion or energy efficiency through the design of the DBD reactor, such improvement is not significant. Based on the reported literature so far, DBD reactor alone shows a low energy efficiency in general, making it less suitable for industrial conversion of relatively stable molecules such as CO_2 and N_2 [50].

2.2.1.2 GA reactors

The GA discharge is a promising type of "warm" plasma which has attracted much attention in the field of gas conversion during the past 30 years. In fact, this type of discharge phenomenon has been observed and studied for an even longer period, such as the typical example of the "Jacob's ladder" [58]. A key advantage of GA reactors is their potential to achieve high energy efficiency in chemical conversion. This efficiency primarily arises from the electron temperature (e.g., 0.4–3.4 eV as reported in literature [59]), which is optimal for the vibrational excitation of molecules such as CO_2 and N_2, while the high arc temperature also facilitates the thermal activation of inert molecules. Additionally, GA reactors are characterized by robust designs and the ability to operate at atmospheric pressure. The fundamental physics and chemical properties of GA reactors, along with their applications, have been described by Fridman et al. [60]. Additionally, Liu et al. [59] provide a specific review of CO_2 conversion using GA technology. For further details, we direct readers to these publications.

In principle, the classic GA reactor design is based on a pair of divergent electrodes as shown in Fig. 5(a). The arc ignites at the narrowest gap and then propagates to a wider gap due to the buoyant force and the gas flow. The arc elongates during the process until it reaches its maximum and becomes extinct, then a new cycle starts with ignition at the narrowest gap again. This classic GA reactor design is often referred to as the "2D" GA (2D: two-dimensional), primarily due to its nearly 2D arc propagation. Numerous studies have investigated various design factors of 2D GA reactors, including configurations, materials, and operational parameters, to enhance performance in chemical conversion. For example, Sun et al. [61] investigated the influence of

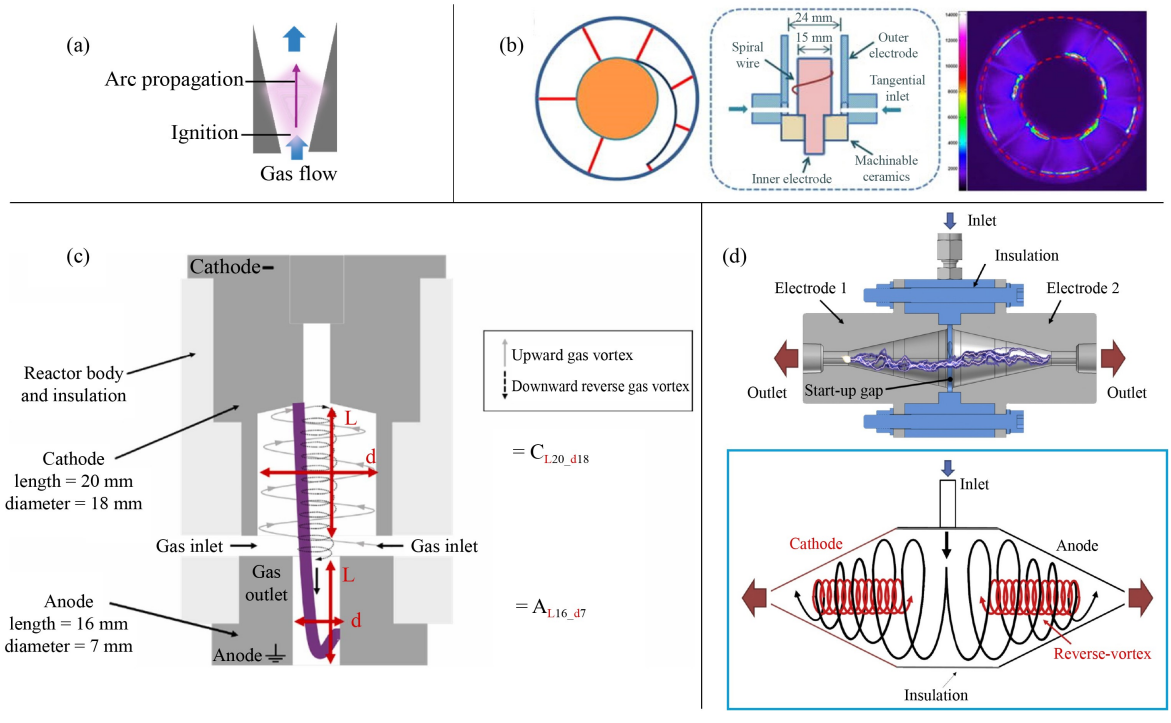

Fig. 5 (a) GA discharge reactor with classic 2D configuration; (b) forward vortex GA reactor. Reprinted with permission from Ref. [65], copyright 2014, AIP Publishing. (c) Reverse vortex GA plasmatron. Reprinted with permission from Ref. [66], copyright 2023, Elsevier. (d) Dual-vortex plasmatron. Reprinted with permission from Ref. [67], copyright 2020, Elsevier.

different electrode materials and graphite outperformed iron, stainless steel, and brass regarding energy efficiency. The author linked these results with the motion characteristics of GA when different material was used. In the study of Li et al. [62], the effect of the flow rate, diameter of the injector nozzle and its distance to the electrodes as well as the structure of the quartz cover have been investigated, providing insight into the optimization of the reactor design parameters for better performance in CO_2 dissociation. Another study from the same group reported an enhancement effect achieved by applying an external magnetic field [63]. This enhancement was attributed to the expanded plasma region, particularly at low gas flow rates. The Lorentz force can influence the arc, thereby increasing processing capacity, as also noted by Chen et al. [64]. However, it is important to consider the direction of the external electric field and operational parameters, especially the flow rate. Ivanov et al. [28] investigated the use of a magnetic field in different orientations to accelerate or stabilize the GA for CO_2 conversion. They found no improvement when attempting to accelerate the arc; however, good performance was observed at low flow rates when stabilizing the arc, after which conversion dropped drastically with increasing flow rates.

It is important to note several drawbacks that need to be addressed in classical 2D GA reactors. A major issue is that only a limited fraction of the gas is exposed to plasma, as some gas bypasses the arc within the reactor. Additionally, conventional GA reactors face other challenges, including the need for high gas velocity, significant convective heat loss, and electrode degradation over time [67]. These issues are critical focus areas for further research in reactor design.

Apart from the 2D GA, more sophisticated three-dimensional (3D) or rotating GA reactor designs have been developed by many groups. Two pioneer examples can be found are designs of plasmatron by Bromberg et al. [68,69] from Massachusetts Institute of Technology and Fridman et al. [70,71] from Drexel University. In principle, the rotating motion of arc in 3D GA reactors can be created in different ways, including using magnetic field to drive the arc such as in the study by Liu et al. [72], or mechanical rotation similar to the plasma-shade reactor reported in literature [73]. However, the most common way is to implement the gas flow, often with gas inlets in the tangential direction, to create a forward or reversed vortex. Several designs of forward vortex GA reactors have been reported [74,65], and an example is shown in Fig. 5(b). Two electrodes are located coaxially, and the gas can be introduced to the reactor via tangential inlets at the bottom of the reactor. The outer electrode is normally cylindrical while the inner electrode can be a corn-shaped rod, or a spiral wire as shown in the figure to guide the arc propagation along the electrode under the effect of the gas flow. In the case of reverse vortex GA, an example of reactor design is shown in Fig. 5(c). When the arc ignites between the electrodes, it moves to the center of the reactor and is stabilized under the effect of the reverse vortex flow. The motion of the arc is associated with strong convective cooling and thermal insulation from the reactor wall, hence providing better thermal efficiency [59]. The study of Ramakers et al. [75] revealed the arc dynamics and its correlation with CO_2 conversion in a reverse vortex GA reactor.

Research efforts have been made to explore the design of 3D GA reactors for improved CO_2 conversion. A study by Trenchev et al. [67] highlighted their design of a dual vortex plasmatron reactor as shown in Fig. 5(d). This design with a novel electrode configuration can elongate the arc in two directions to increase the residence time, hence improving the conversion of CO_2. The results showed that 41% energy efficiency with 9% conversion can be achieved by this reactor. At the same time, the gas convection and the rotation of the arc can also prevent electrode degradation by cooling the cathode spot. Vertongen et al. [66] evaluated several new electrode configurations in a GA plasmatron and observed the influence of different designs, but the improvement in CO_2 conversion was limited. This indicates a performance limit of this reactor design, and the author recommended modification on the post-plasma region for possible further improvement. This recommendation is in line with the research of Dinh et al. [76] who investigated the effect of attaching a nozzle downstream of the GA in the reactor. In their study on DRM, 75% higher CO_2 conversion and 47% higher energy efficiency were achieved with the nozzle which enhanced heat transfer from the arc to the reactant and reduced the heat loss to the wall. There is also another study by Kwon et al. [77] who modified the downstream of the GA but with a quenching device. In their case, the selectively of H_2 was increased by preventing its consumption via suppression of the reverse water gas shift reaction. Besides, new ideas and innovative designs in this research direction could be highly beneficial for further exploration and the reactor design as well as creating new opportunities. Nagasou et al. [78] reported an interesting design which combines a solar receiver and a GA reactor. This solar-plasma reactor is aimed to decompose CO_2 by using both concentrated solar energy and plasma driven by renewable energy. Their results demonstrated the interaction between plasma and solar radiation under different configurations.

2.2.1.3 RF and microwave plasma reactors

In the case of RF plasma, RF power is applied to plasma reactors via either inductive or capacitive coupling as in Figs. 6(a) and 6(b). An impedance matching unit/matching box as one important component, is connected in the circuit with the external RF generator

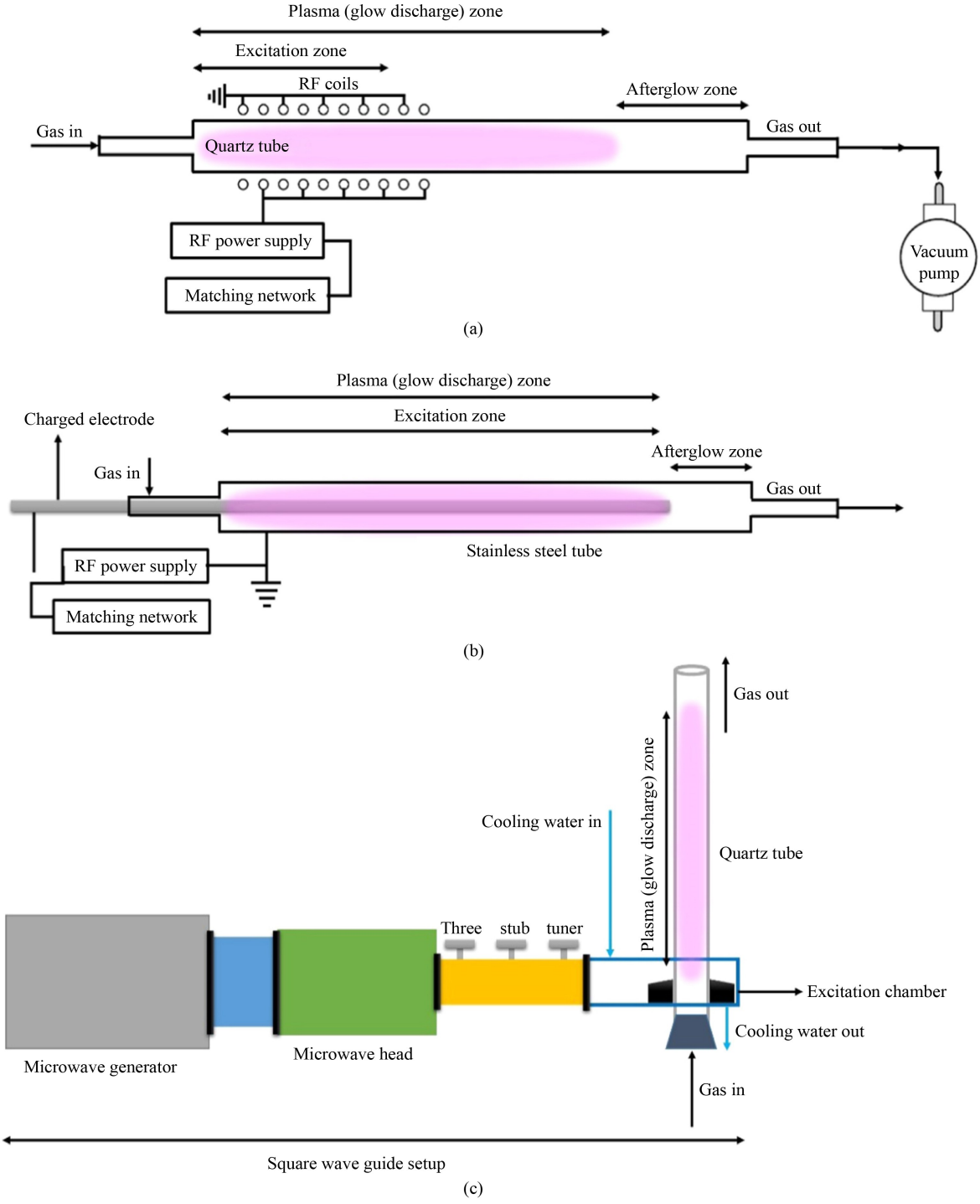

Fig. 6 (a) Inductive coupled RF plasma reactor; (b) capacitive coupled RF plasma reactor; (c) microwave plasma reactor. Reprinted with permission from Ref. [86], copyright 2019, IOP Publishing Ltd.

and the reactor for stable plasma operation and reduced power loss. While a typical microwave plasma system consists of several more components as indicated in Fig. 6(c). HV power supply is used to drive the magnetron to produce microwave power, and the microwave-to-plasma applicator transfers microwave energy to plasma. Other components in the system such as the isolator (e.g., circulator) and matching circuit maintain the necessary practical function including preventing the damage from reflected power and matching the impedance of the magnetron with that of the load [79]. Recently reported studies on CO_2 conversion by microwave plasma have been reviewed in Refs. [80] and [81]. In reactor design and optimization research, efforts have focused on enhancing quenching, which is crucial for improving CO_2 conversion. Rapidly reducing

gas temperature in the post-plasma region helps prevent CO from reacting with oxygen species, such as O or O_2, which would otherwise reform CO_2 [82,83]. Hecimovic et al. [84] demonstrated this approach by using a downstream nozzle, testing various nozzle diameters and distances at pressures from 100 to 900 mbar. The results demonstrated an enhancement at a pressure close to atmospheric with the conversion and energy efficiency comparable to the values achieved at 200 mbar. Another study by Mercer et al. [85] developed a converging-diverging nozzle attached to a microwave plasma reactor. Such nozzle design resulted in a 21% and 71% increase in energy efficiency and CO_2 conversion at 700 and 300 mbar, respectively.

2.2.1.4 Other types of reactors

There are also studies on CO_2 conversion with plasma reactors based on other types of discharges such as corona, spark or atmospheric glow. Corona discharge reactors have one or more electrodes with sharp edges or points that could create a highly divergent electric field. Due to this feature, the plasma generated is not uniform and often limited in volume, which is not preferred considering the limited fraction of gas treated which leads to a low conversion. Therefore, despite relevant research prior to 2010, only a limited number of cases have been reported in recent years [87]. The spark discharge reactor operates with a pair of electrodes between which streamers develop into spark channels that periodically extinguish and reignite. Various electrode configurations, such as plate-to-plate, point-to-plate, or sphere-to-sphere, can be used at different distances. While limited research has focused on CO_2 splitting using spark discharge reactors [71], there has been more emphasis on DRM [88−90], with studies reporting high conversion efficiencies and low energy consumption (e.g., CO_2 conversion > 84% with energy consumption of 0.218 $MJ \cdot mol^{-1}$ [75]).

Glow discharge reactors also present a promising option, and their reactor design can be similar to corona or spark, often using point-plate electrode configurations. Traditionally, glow discharge experiments were conducted at pressures below atmospheric, and some recent studies continue to operate at low pressure [91,92]. However, there is growing interest in atmospheric-pressure glow discharge (APGD) due to the operational advantages at atmospheric conditions. A critical consideration for APGD is preventing the transition from glow to arc discharge at high pressures, which can be managed through circuit and power supply design. An example can be found in the study of Renninger et al. who reported APGD driven by appropriate power supply with low complexity, high efficiency above 70%, and a maximum overall system efficiency of 22% has been achieved [93]. Also, in this study, they used a magnetic field to expand the discharge volume which could lead to a higher fraction of gas treated. A different approach was made by Wanten et al. [94] and Trenchev et al. [95] by confining the reactor volume to maximize the fraction of gas treated by plasma, and improved reactor performance was achieved in this way. The operation parameters could further enhance the performance of APGD reactors for CO_2 conversion. This has been demonstrated by Meng et al. [96] who conducted a relevant study and concluded that key parameters including gap distance, power and flow rate play synergistic roles in improving the conversion and energy efficiency.

2.2.2 Plasma-catalyst integration

The core of plasma-catalytic reactor design lies in optimizing plasma-catalyst integration to achieve maximum synergy. Two primary configurations exist: in-plasma catalysis (IPC) and post-plasma catalysis (PPC). In IPC, also known as a one-stage configuration, catalysts are placed directly within the plasma zone, allowing intense interactions between plasma-generated species (both short- and long-lived) and the catalyst. However, the presence of catalysts in the plasma zone also impacts plasma properties. Conversely, in PPC (or two-stage configuration), the catalysts are located downstream of the plasma zone, where only long-lived species interact with the catalyst surface. Building on these two configurations, multi-stage designs have been explored, allowing for different catalysts or plasma treatments at each stage for optimized performance [97].

Applying the IPC configuration is not always straightforward in plasma reactors; for example, in “warm” plasmas with high temperatures, a two-stage configuration is often a more practical choice. Examples can be seen in studies on GA [98], microwave [99] and glow discharges [100].

Zhang et al. [101] investigated CO_2 splitting using a GA reactor packed with photocatalyst TiO_2 located downstream of the discharge gap. By varying the distance of the catalyst bed, both IPC and PPC configurations were tested. The presence of catalysts led to enhancements of 138% in CO_2 conversion and 133% in energy efficiency for the IPC configuration, while the improvement was negligible in the PPC configuration. Interestingly, the presence of the catalyst container downstream reduced reactor performance at low flow rates but significantly improved performance at higher flow rates. This effect is attributed to backflow introduced by the container, which increases the fraction of gas treated. This example also illustrates the potential influence of PPC beyond mere catalytic effects.

To date, most studies have employed IPC configurations due to the critical role of short-lived species in plasma-induced reactions, particularly for surface reactions. For instance, vibrationally excited

species at atmospheric pressure have lifetimes on the order of nanoseconds, which is too short for effective utilization in PPC [3]. Different reactor set-ups, such as packed bed, structured bed, and fluidized bed, have been explored for IPC, and will be discussed in this section.

2.2.2.1 Packed bed

Directly packing catalysts (in the form of pellets or spheres) into a DBD reactor is the most used approach so far due to the simplicity and convenience of experimental tests. Very often comparisons between a DBD reactor with or without catalysts packing were made in many studies to reveal the effect of the catalysts or packing materials. The purpose of packing catalysts is to create more surface and introduce catalytic surface reaction in DBD reaction. At the same time, there are other important factors that need to be considered which make the reactor packed with catalysts very different from an empty reactor. When packing material is introduced into the reactor, the gas channel volume decreases, forcing gas to flow only through the voids of the packaging. This results in shorter residence time at the same flow rate and could cause pressure drop, especially at high flow rates. Additionally, the effective gas gap is reduced by packing, which lowers the voltage range required for plasma generation and generally reduces the power delivered compared to an empty reactor under similar conditions. More importantly, the discharge mode is modified, resulting in a combination of discharges within the void spaces and surface discharges on the packing material [53]. The existence of packing (mainly dielectric material) enhances the electric field, especially near the contact points between pellets, leading to plasma generation and increased electron energy which is normally referred to as packed-bed effect [102]. The physical properties of the packing material, including size, shape, surface area, and dielectric constant, play a crucial role and can impact chemical conversion even without considering the catalytic surface reactions introduced. These factors should be carefully considered when selecting catalysts, designing reactors, or comparing results obtained from different experimental set-ups or reported literature. Nevertheless, these influences have already been the focus of several studies, with investigations through both experimental work [103−105] and modeling [106]. Readers are encouraged to refer to these sources for more comprehensive insights.

In addition to fully packed DBD reactors, where catalysts fill the entire discharge zone and significantly alter the discharge mode, partially packed reactors have also been explored in the literature. Unlike full packing, which changes the discharge characteristics considerably, partial packing can preserve strong filamentary discharges while enabling effective plasma-catalyst interactions. This effect was demonstrated by Tu et al. [107] in their study of DRM using Ni/γ-Al_2O_3 catalysts, where enhanced physical and chemical interactions were observed. Gadkari et al. [108] further examined the influence of partial packing in a DBD reactor through a 2D numerical fluid model. They found that, compared to an empty DBD reactor, partial packing enhanced the electric field at the top surface of the packing and at contact points between the packing and dielectric layer, resulting in increased power density and electron energy. Apart from partial packing, mixed or sectioned packing configurations have also shown an impact on reactor performance. Wang et al. [109] investigated CO_2 hydrogenation using a packed DBD reactor with Co catalysts. They tested four different packing arrangements: fully and partially packed catalysts, a mixture of catalysts with Al_2O_3, and separate sections for catalysts and Al_2O_3. The latter configuration achieved a significant increase in C_2 hydrocarbon selectivity, highlighting the importance of packing arrangement, particularly when multiple materials are involved.

2.2.2.2 Structured bed

Instead of using packed pellets or spheres, structured materials can also be utilized in plasma reactors. A common example is the honeycomb discharge, which can feature various configurations, as illustrated in Figs. 7(a–c). In this type of reactor, the fixed gas channels within the catalyst bed allow for high throughput, enabling the processing of gas at large flow rates with minimal pressure drop, an advantage that has made honeycomb structures popular in commercial systems such as the case of car exhaust catalysts. However, key challenges include achieving stable, uniform plasma

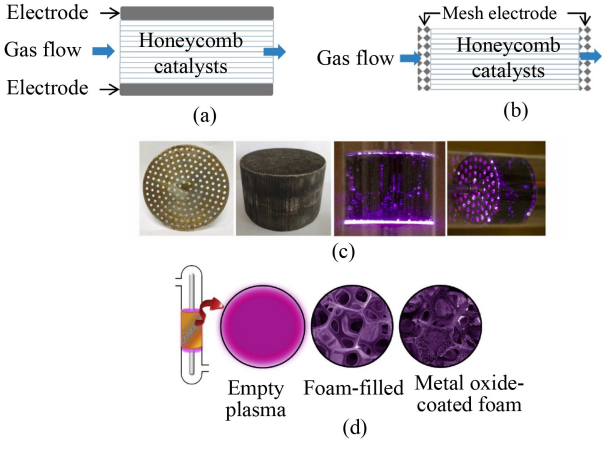

Fig. 7 (a) DBD-based honeycomb discharge reactor. (b) honeycomb discharge reactor with mesh-to-mesh configuration. (c) images of electrodes, honeycomb catalysts and plasma discharge in the reactor. Reprinted with permission from Ref. [115], copyright 2022, Elsevier. (d) DBD based reactor with polyurethane foam. Reprinted with permission from Ref. [116], copyright 2021, Elsevier.

generation within the reactor and ensuring optimal interaction between plasma species and the catalytic surface. Depending on the reactor design, charge particle loss can occur due to interactions with the channel walls, often requiring higher voltages; in some cases, sparking between electrodes through the channels can lead to damage to the catalyst bed [110]. This necessitates careful design of the catalyst structure and the electrode configuration to balance these challenges. There are different designs of honeycomb discharge reactors reported during the last 20 years, including wires-to-wires [111], mesh-to-mesh [112,113], sliding discharge-based designs [114] and many others.

Similarly, foam-type materials can also be utilized in plasma reactors. For instance, Taghvaei et al. [116] demonstrated CO_2 decomposition using a DBD reactor packed with polyurethane foam, as illustrated in Fig. 7(d). This foam-filled arrangement enabled uniform distribution of packing materials, with the foam serving as a support for different metal oxides to compare their effects on conversion and energy efficiency. $BaTiO_3$-coated foam achieved a 124% increase in conversion compared to foam-only reactors, and a 203% improvement over empty reactors. However, research on plasma-catalytic conversion of gas with structured catalyst beds remains limited. Current studies focus more on catalyst development than on reactor design. At laboratory scale, where large flow rates are not typically required, structured bed reactors receive less attention. However, structured beds are more frequently applied in plasma reactors for volatile organic compound (VOC) removal, where low concentrations of reactants necessitate high flow rates. Nevertheless, structured beds remain a promising area for exploration, especially considering the development of plasma-catalytic reactors for large-scale applications.

2.2.2.3 Fluidized bed

The combination of plasma technology with fluidized bed reactors represents a promising approach that leverages the benefits of both plasma chemistry and fluidization, particularly in enhancing gas-solid processing through improved mass and heat transfer. Numerous studies have focused on plasma-fluidized bed reactors primarily in the realm of material processing, including catalyst treatment [117,118], polymer processing [119], and surface modification of nanoparticles [120] and powders [121]. While there has been substantial research on thermal plasma-based fluidized bed reactors for material applications, as reviewed by Du et al. [122], comparatively fewer studies have explored in the case of non-thermal plasma and their potential for gas conversion, despite the significant advantages this configuration could offer in enhancing the interaction between plasma and catalysts. A notable contribution by Chen et al. [9] has highlighted the use of fluidized bed plasma reactors for the conversion of CH_4 and CO_2 in their review paper along with the fundamental principles and recent developments in the field.

In a fluidized bed reactor, the motion of catalyst particles is a crucial factor, especially under plasma conditions. The fluidization behavior of particles within the reactor is primarily governed by the superficial gas velocity, which is determined by the reactor geometry and gas flow rate. At low gas flow rates, the pressure drop across the bed is much smaller than the gravitational force acting on the particles, resulting in a fixed bed where particles remain stationary. When the gas flow rate exceeds the minimum fluidization velocity, particles begin to move randomly, achieving a state known as incipient fluidization. As the gas flow rate is further increased, the fluidization becomes homogeneous. With even higher flow rates, the system transitions into inhomogeneous fluidization patterns, such as bubbling. When the gas flow rate reaches the terminal settling velocity of the particles, the gravitational force and the upward hydrodynamic force are balanced. If the gas flow rate continues to increase beyond this point, particles will be carried out of the reactor due to pneumatic transport. Generally, the terminal settling velocity (U_t) can be estimated using the following equation [123]:

$$U_t = \left(\frac{4 d_s (\rho_s - \rho_g) g}{3 \rho_g C_D} \right)^{\frac{1}{2}}, \tag{1}$$

where ρ_s and ρ_g are the density of the particle and gas media, d_s is the particle size, C_D is the drag coefficient and g is the gravitational acceleration. This equation highlights the importance of particle properties in achieving effective fluidization, and it can be used to guide the selection of both operating parameters and particle characteristics to ensure proper fluidization. However, it is important to note that fluidized bed plasma reactors offer less flexibility than fixed-bed reactors, as they require careful control of gas flow to maintain fluidization. Consequently, reactor design and selection of catalysts need to be made to couple optimal plasma conditions with fluidization.

In addition, it should be noted that Eq. (1) only considers conventional fluidized bed conditions whereas the existence of plasma could introduce more complexity to the particles' motion via possible effects such as the enhanced Coulomb force between charged particles or due to external electric field. It is not a surprise that precipitation could occur on the reactor wall or electrode since the electrostatic precipitator was developed based on such a principle. Increasing the particle size can be a way to solve this issue [110]. On the other hand, it is also possible that the existence of plasma facilitates the fluidization of the particles inside the reactor. A study on acetaldehyde removal using a fluidized bed DBD reactor

was conducted by Jia et al. [124]. In their study, 6.5 g catalysts in the form of pellets with a mass of 20 mg per pellet were inserted into a co-axial DBD reactor which has a 2 cm radius. The flow rate tested was 100 mL·min^{-1} which is not enough to cause fluidization. While plasma with a low frequency (1–50 Hz) was applied, the pellets were charged and moved alternatively between electrodes, leading to an electrically enhanced fluidization which is very different from the conventional gas-dominated fluidization. The authors also noted that this electrically enhanced fluidization effect was absent at higher frequencies, as the rapid alternation of the electric field does not allow sufficient time for the particles to move and achieve fluidization.

In addition, catalysts in plasma fluidized bed reactors can significantly impact discharge behavior. Pou et al. investigated a plasma fluidized bed reactor with multiple electrodes for CO_2 decomposition [125]. In this study, copper powder mixed with aluminum oxide was used, serving not only as a catalyst for the reaction but also to improve the uniformity of discharge distribution within the fluidized bed. This setup resulted in more randomized discharge points, reducing the formation of primary discharge channels and "hot spots". The authors suggested that the increased randomness of discharges, achieved by adjusting voltage, frequency, and anode positioning in fluidized bed plasma reactors, could enhance CO_2 conversion efficiency.

So far, fluidized/spouted bed plasma reactor designs based on DBD and GA have been reported, two reported examples of the reactor design are shown in Figs. 8(a) and 8(b). In the case of DBD, a comparison between fluidized bed and fixed bed has been made by Wang et al. [126] in their study on DRM. Using Ni/γ-Al_2O_3 catalytic particles, the conversion of methane with and without plasma under different temperatures was compared along with the synergy effect which is indicated by the synergetic factor I_{SE} (Eq. (16) in Section 3.3). Although higher conversion of CO_2 and CH_4 were observed in the case of a packed bed, a higher synergetic factor was achieved with a fluidized bed reactor in the temperature range from 673 to 798 K. Higher I_{SE} of CO_2 was also achieved with an increased discharge power. In another study conducted by Bouchoul et al. [127], the comparison was made for DBD reactor with γ-Al_2O_3. When a fluidized bed was used, an increase in the conversion was obtained from 8.5% to 12.1% and from 3.4% to 6.2% for CH_4 and CO_2, respectively, along with the increase of surface area of alumina from 260 to 312 m^2·g^{-1}. The opposite trend was observed in the case of packed bed reactors. This discrepancy is attributed to the enhanced surface reaction in fluidized bed plasma reactors. In packed bed configurations, plasma is generated near the contact point of catalysts due to the packed-bed effect, limiting the plasma-catalysts interaction. In contrast, fluidized bed reactors allow catalysts to be dispersed throughout the plasma zone, making more catalyst surface sites available for reactions and thus achieving higher conversions. This distinction underscores the unique advantages of fluidized bed designs for plasma-catalytic processes, particularly in enhancing gas conversion. Chen et al. [128] reported their design of a FB DBD reactor and conducted a detailed study on DRM with La-Ni/Al_2O_3 as catalysts. The reactor uses a coaxial structure with a hollow internal electrode to feed gas in, creating a jet to sustain fluidization for the power in a reversed direction. The authors demonstrated that the reaction was promoted by combining DBD with a fluidized bed due to the extended surface area of powder catalysts, interaction with reactive species generated by plasma, enhanced heat and mass transport as long as long residence time. Without plasma, such promotion is limited, indicating the crucial role of plasma in breaking the C–H bond which is considered as the rate-limiting step. In addition, the power and mean discharge current in the case of a fluidized bed DBD reactor is 1/3 of that in a packed bed reactor at fixed sustain voltage and frequency. The doubled pressure also caused a reduction in E/N.

Regarding the case with GA, the reactor design in combination with the spouted bed offers the advantage of inserting catalyst particles inside the discharge zone which is difficult to achieve with a packed bed of IPC configuration due to the discharge behavior (arc path, high temperature etc.), and it led to more intensive plasma-catalysts interaction than a PPC configuration. A typical spouted bed consists of a central region where gas entrains solid particles, causing them to move upwards, and an outer region where solids move in a slower, counter-current flow. Particles rise in the central spout and descend in the outer region, and then move toward the center at lower parts of the reactor to be accelerated again, hence the circulation of particles can be achieved [122]. For such functions, cone shape or other designs rather than flat bottoms are used to avoid dead zones. This could match the divergent electrode geometry of the classical GA reactor. The high gas velocity required for spouted bed operation aligns well with the characteristics of a GA reactor. Several studies have already reported the conversion of methane with catalysts [129−131], and the conversion of CO_2 with biochar as a co-reactant [132], in spouted-bed GA reactors. In the study of Schmidt-Szalowski et al. [131], the effect of a spouted bed on the electrical characteristics of GA discharge has been observed. A much smoother voltage and current waveforms with decreased periods between active parts of discharge were observed when the spouted bed was applied. The authors stated that the recombination of ions and electrons on the particle surface could be a reason, and the influence of charged particles on the breakdown voltage should be considered as well. Notably, the existence of catalyst particles may not always be beneficial. This has been evidenced in the research of

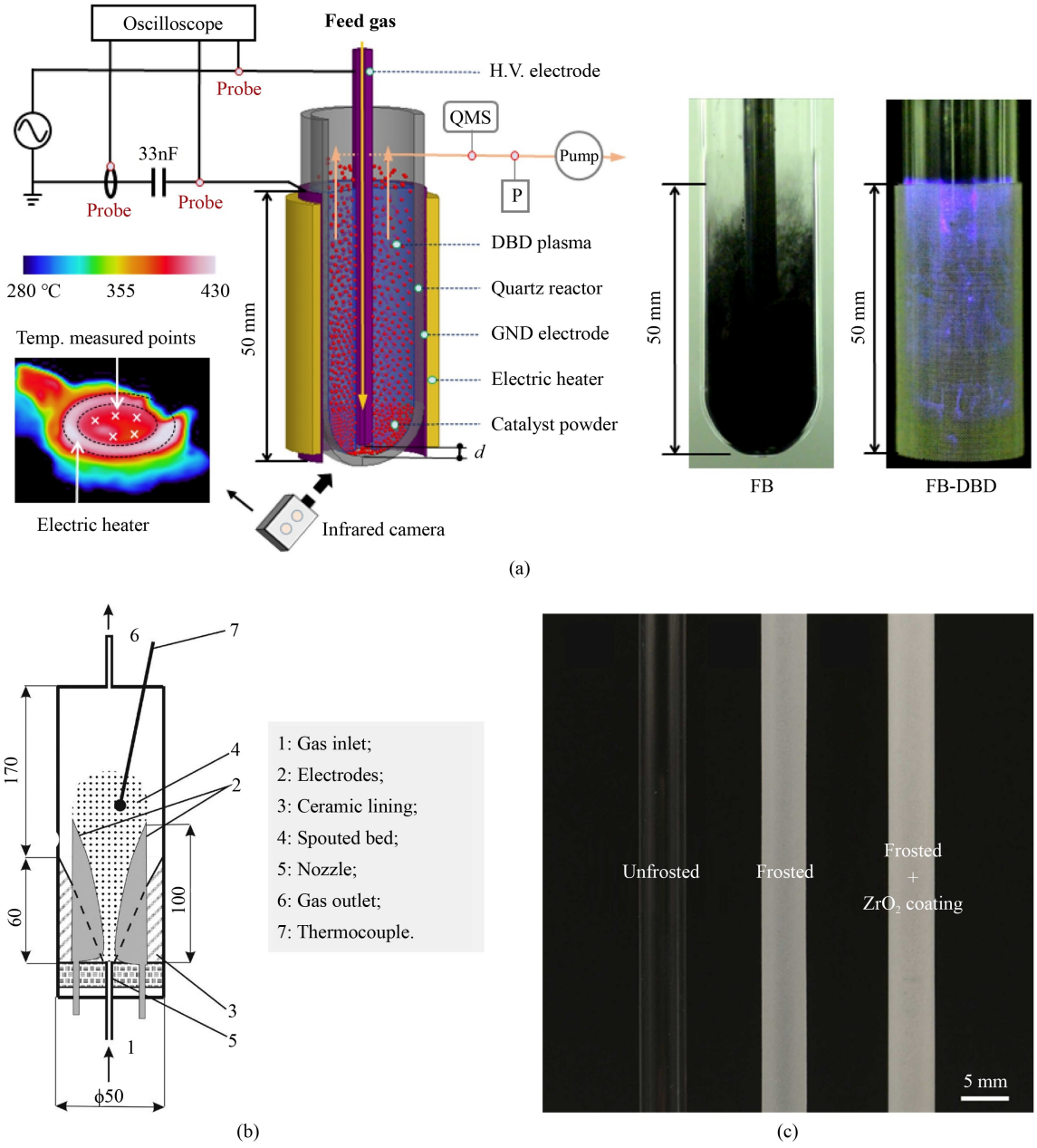

Fig. 8 (a) FB DBD reactor. Reprinted with permission from Ref. [128], copyright 2021, Elsevier. (b) Spouted-bed GA reactor. Reprinted with permission from Ref. [131], copyright 2007, John Wiley & Sons. (c) Frosted dielectric surface with ZrO_2 coating in a DBD reactor. Reprinted with permission from Ref. [134], copyright 2022, Elsevier.

Martin-Del-Campo et al. [133] who used a rotating GA reactor in combination with a spouted bed using Ni-supported catalysts for DRM. The results from their experiments showed a decrease in the conversion of CO_2 and CH_4 due to the catalysts interfering with the arc formation, including reduced volume accessible and altering the arc itself, which limits the production of active species. However, they also observed an increase in selectivity of H_2 and CO, and a reduction of carbon deposition on the electrode. Moreover, they compared two support materials in the reactor and achieved more stable plasma operation with Al_2O_3 over SiO_2 due to a higher melting point. This leads to a discussion about the effect of exposure to high-temperature arc on the catalysts in spouted bed GA reactor, which is a general situation that should be considered when designing such plasma-catalysts system.

2.2.2.4 Other types of arrangement

Coating provides an effective approach to introducing catalysts onto the walls of plasma reactors. With a thickness of only a few micrometers—significantly thinner than the discharge gap, typically in the millimeter

or centimeter range—these coatings do not substantially alter the reactor geometry, residence time, or the distribution of the electric field. However, this may be different when a microgap or microplasma is considered. Coating offers practical advantages, such as reducing pressure drop and avoiding the packed-bed effect. The material properties (e.g., dielectric constant, conductivity) and surface characteristics (e.g., surface area, pore size) of the coating are critical factors. Xia et al. [135] used a frosted quartz tube coated with CeO_2 as reactor wall of a DBD reactor for the decomposition of CO_2, as shown in Fig. 8(c). The conversion and energy efficiency obtained was 23.3% and 8%, which indicated an enhancement compared to an uncoated reactor with 16.3% conversion and 6% energy efficiency. The author stated that this enhancement is not mainly caused by the strong CO_2 adsorption ability of CeO_2, but more intensive microdischarges which are reflected by the current waveform measured. In another study, Ding et al. [134] demonstrated that applying a ZrO_2 coating to the reactor wall improved CO_2 conversion and energy efficiency. This enhancement was primarily attributed to the high dielectric constant of ZrO_2, which increased the reactor's effective capacitance, promoted more frequent micro-discharges, and elevated the mean electron energy.

Another method to introduce catalysts is through catalytic electrodes, achieved by coating, depositing catalysts on electrodes, or using catalytic materials directly as electrodes. Subrahmanyam et al. [136−138] demonstrated this in early studies on VOC decomposition using a DBD reactor with a sintered metal fiber electrode impregnated with Mn and Co oxides. Although limited research has explored catalytic coatings or electrodes specifically for CO_2 conversion, these approaches represent promising avenues for advancing reactor design.

3 Experimental approaches

3.1 Operation schemes

The operation of experimental systems in plasma-catalysis research is typically straightforward, with most studies employing plasma reactors at atmospheric pressure, and reactants are continuously flowing through the reactor, where they are exposed to plasma to initiate chemical reactions. Tests with variations of feed gas flow rate and electrical parameters such as voltage and power are often performed. This general setup is effective for testing reactors and catalyst performance under standard conditions. However, the operation can also be more flexible, with different parameters to form operation schemes that can be tailored to specific research objectives. There are different options can be selected, as shown in Fig. 9. In this section, three key factors are discussed.

3.1.1 Pressure condition

Operating plasma reactors at atmospheric pressure has significant advantages, such as reducing overall process complexity and costs by eliminating the need for pressure modulation equipment. As a result, atmospheric-pressure operation is the primary focus in most experimental studies. However, pressure is a critical factor that influences plasma properties and, consequently, reactor performance. For this reason, studies on modulated pressure conditions have also been explored, particularly for certain types of plasma sources like microwave plasma, where low-pressure conditions are frequently investigated. Belov et al. [139] studied CO_2 dissociation in microwave plasma across a wide range of pressures, from 200 mbar to 1 bar, and observed a general decline in both conversion and energy efficiency as pressure increased. As the pressure increases toward the atmospheric pressure, the rotational and vibration temperature tends to reach equilibrium, leading to increased temperatures and reduced efficiency in CO_2 dissociation due to depletion of vibrational excited CO_2 via V-T relaxation. Additionally, the recombination reaction which oxidizes the produced CO to CO_2 becomes more important at higher pressure. Besides, increased pressure can result in a transition of microwave discharge from the diffusive regime to the contracted regime, leading to changes in plasma properties, mass and heat transfer which ultimately impacts reactor performance [81,140].

There are a few examples of pressure modulation in the case of DBD, GA and corona discharge reactors. Rad

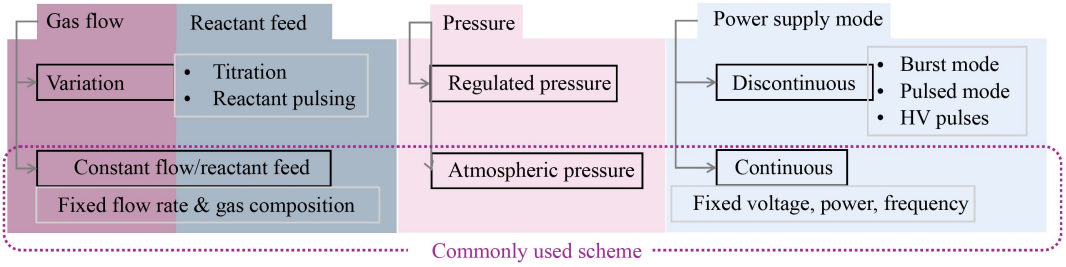

Fig. 9 Different options for parameters to form operation schemes.

et al. [141] conducted a study on CO_2 splitting in a DBD reactor under increased pressure, showing a threefold improvement in CO_2 conversion and energy efficiency from 1 to 2 bar. Considering the general laboratory-scale reactor with a discharge gap in mm to cm range, higher pressure operation above atmospheric requires higher breakdown voltage for plasma generation according to Paschen's law, and it is also associated with instability of discharges. Hence in their study, Argon dilution was used to stabilize the plasma at moderate voltages of up to 13.5 kV. In another example, Yong et al. [142] examined CO_2 dissociation using nanosecond pulsed discharges at pressures from 5 to 12 bar. The author indicated that the motivation of such tests is to understand how pressure-dependent reactions are coupled with the non-equilibrium electron energy transfer and plasma chemistry, which is relevant to large-scale carbon capture, utilization, and storage applications. Despite the demonstrated benefits of low- or higher-pressure operation for enhancing CO_2 conversion and energy efficiency, atmospheric pressure operation remains the main research focus for practical applications. Nonetheless, pressure modulation is a valuable approach for exploring both fundamental reaction mechanisms and practical reaction conditions.

3.1.2 Reactant feed

The majority of plasma-based gas conversion studies utilize flow reactors, where a continuous feed gas stream with fixed flow rates and compositions is used. This setup allows for a straightforward assessment of reactor and catalyst performance under consistent flow conditions. However, modulating the reactant feed during plasma operation has been considered a technique for specific purposes, such as investigating surface reactions in plasma-catalyst systems. One example of feed modulation is in the study by van Raak et al. [143], who explored ammonia synthesis using a DBD reactor packed with Ru/CeO_2 and $Ru/Ti\text{-}CeO_2$ catalysts. A titration technique named "unimolecular plasma operation scheme" was used to understand the surface reaction mechanism. This scheme involved alternating the feed gas to generate H_2 plasma and N_2 plasma in different sequences within the catalytic reactor, as shown in Fig. 10(a). A significant increase in ammonia production was observed with the $Ru/Ti\text{-}CeO_2$ catalyst, which yielded 2.8 times more ammonia when using N_2 plasma compared to the maximum yield of Ru/CeO_2 under H_2 plasma. In a study by Barboun et al. [144], ammonia synthesis was investigated using Ni/Al_2O_3 catalysts under sequential N_2 and H_2 plasma or thermal treatment, as shown in Fig. 10(b). This experimental approach enabled a clear distinction between plasma-phase and plasma-catalytic reactions. The results revealed that surface nitrogen species generated by plasma actively participate in subsequent hydrogenation reactions, which are driven either thermally or through H_2 plasma exposure.

When liquid reactants, such as water, are involved in plasma processes, they can be introduced in batch mode while the gas phase continuously flows through the plasma zone. This semi-batch reactor configuration is more commonly observed in water treatment experiments rather than gas conversion studies. Another frequently used approach is feeding H_2O into the reactor via controlled evaporation, typically achieved using an evaporator or mixer. The vaporized water is mixed with a carrier gas, often another reactant gas or dilution gas such as Ar. Examples of this method can be found in the literature [145]. Additionally, a noteworthy case is sorption-based gas conversion using plasma, which operates in batch mode. For instance, plasma-assisted CO_2 capture and conversion was demonstrated in our previous study on carbon capture and conversion using a plasma-sorbent system [146]. In this study, the sorbent was first saturated with a CO_2-containing stream, allowing CO_2 adsorption over a set period. Subsequently, the CO_2-saturated sorbent was flushed and exposed to plasma, enabling simultaneous desorption and conversion. A detailed discussion of this concept will be provided in Section 4.2.

3.1.3 Power supply mode

Depending on the power supply configuration, plasma reactors can operate in either continuous or discontinuous modes. In most studies, a continuous power supply is employed, with AC or DC power set to generate plasma discharges at fixed levels of power, voltage or frequency. Discontinuous operation is primarily represented by pulsed power discharges, in which power is delivered as voltage pulses in the microsecond or nanosecond range, as discussed in Section 2.1(b). The duty cycle, defined as the fraction of the period during which the power is on, indicates the degree of discontinuity in the plasma discharge and is an important parameter that influences the performance of the plasma reactor.

Apart from pulsed power discharges, other discontinuous modes have been explored in several research. For example, Ozkan et al. [147] investigated the AC burst mode operation of a DBD reactor for the conversion of CO_2. This method involves switching the power supply on and off periodically. Compared to continuous AC operation under the same total power input, burst mode offers higher instantaneous power and electric fields, resulting in more energetic electrons and hence improved the conversion of CO_2. A similar mode was applied in the study of Rohit et al. [148] who studied reverse water gas shift reaction, as shown in Fig. 11(a). In their study, millisecond periodic switching reduced the temperature and offered a better microdischarge distribution, which has been considered an additional advantage.

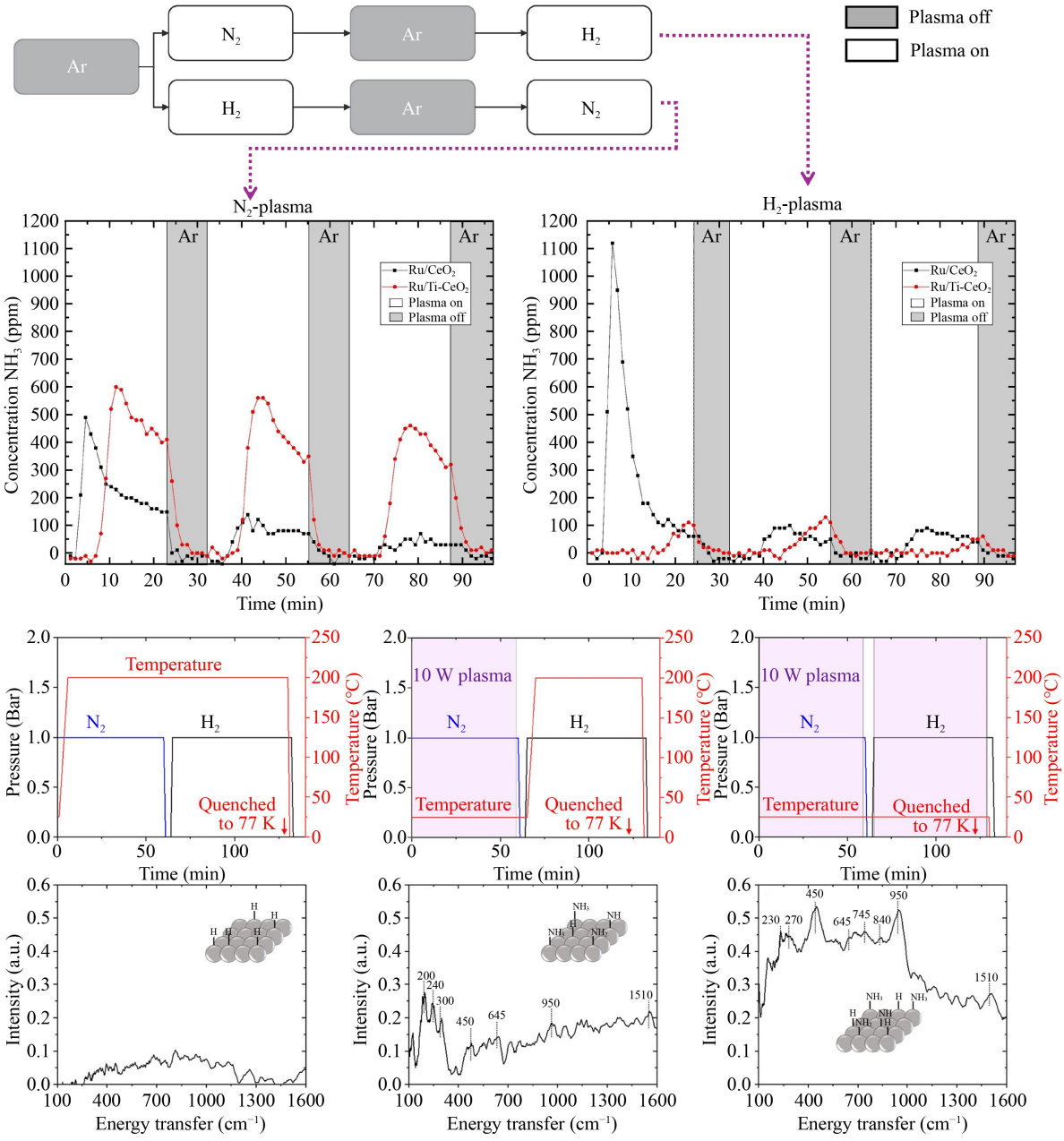

Fig. 10 (a) Unimolecular plasma exposure in the study of van Raak et al. and tested and the concentration of NH_3 measured. Reprinted with permission from Ref. [143], copyright 2022, Elsevier. (b) Sequential exposure of N_2 and H_2 plasma and thermal treatment applied in the study of Barboun et al., along with their corresponding inelastic neutron scattering spectra. Reprinted with permission from Ref. [144], copyright 2021, American Chemical Society.

In the case of GA reactor, a study by Li et al. [149] has used periodic switching of AC power supply, namely AC pulsed mode, to investigate the spatial profile of classical 2D GA reactor, as shown in Fig. 11(b). This method couples the periodic operation with the natural periodic behaviors of the GA discharges. By adjusting the duty cycle, the plasma volume can be controlled, and the spatial profile of the reactor's performance can be deduced. These studies highlight that discontinuous operation can serve as an effective research technique for investigating the reactor design and operation. Moreover, beyond simply adjusting operational parameters, selecting an appropriate power supply mode is essential for optimizing reactor performance.

3.2 Diagnostic approaches

Various diagnostic methods can be applied to the study of plasma-based gas conversion, and a generic presentation of targeted parameters/phenomena is demonstrated in Fig. 12. As mentioned in 2.1(c), both operando and offline/*ex-situ* approaches can be applied. Offline/*ex-situ*

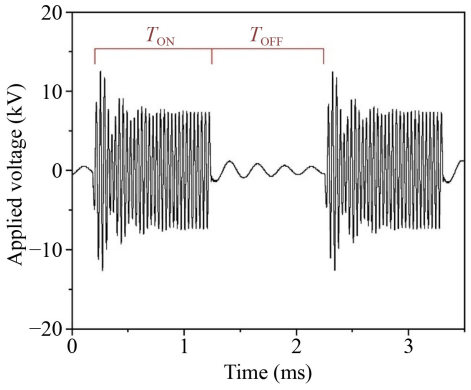

Power supply mode	Flow rate/ (mL·min^{-1})	CO_2 conversion (%)	Selectivity (%)		Energy efficiency for CO (mmol·kWh^{-1})
			CO	CH_4	
Continuous AC	40	49.4	93.4	6.6	156.2
	80	28.4	96.0	3.8	184.9
	100	24.6	96.0	3.9	199.8
	200	14.7	97.0	3.0	240.7
Burst mode	40	30.1	96.0	3.9	195.9
	80	20.3	97.6	2.4	268.4
	100	17.1	97.9	2.1	283.7
	200	9.7	98.5	1.4	324.9

(a)

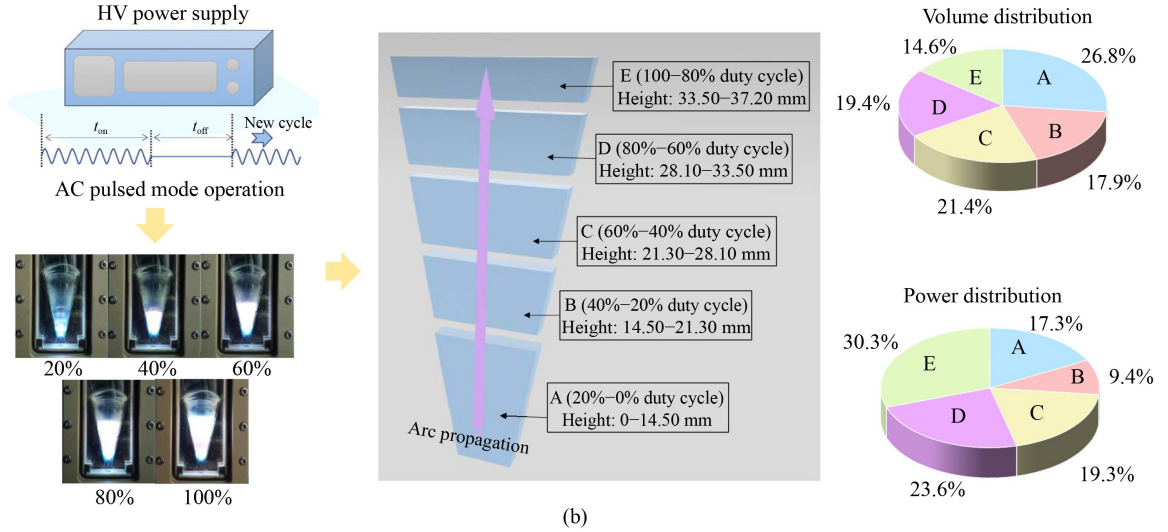

(b)

Fig. 11 (a) Burst mode operation applied in the study of Rohit et al., results are compared with the case of continuous operation under the same conditions. Reprinted with permission from Ref. [148], copyright 2020, Elsevier. (b) AC pulsed mode operation for controlled GA plasma volume, and deduced spatial profile of the reactor for NO_x synthesis. Reprinted with permission from Ref. [149], copyright 2023, American Chemical Society.

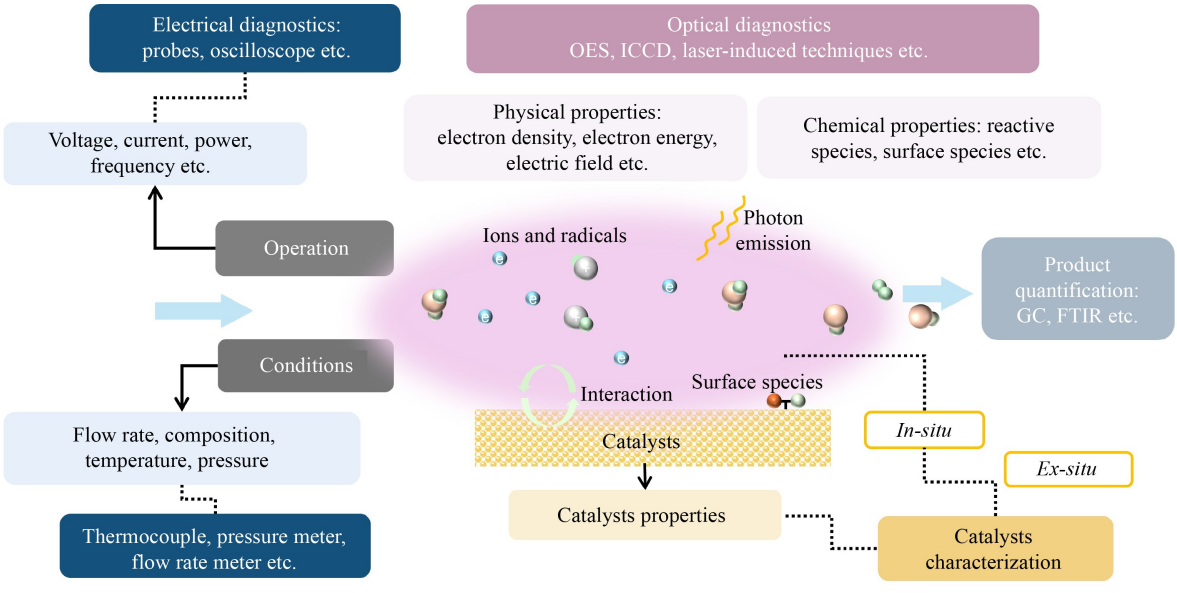

Fig. 12 Brief summary of the application of diagnostic techniques in plasma-based gas conversion experiments.

diagnostics primarily involve the characterization of catalysts, typically by measuring changes in physical and chemical properties before and after plasma exposure. This helps verify the effect of plasma on the catalysts. For operando diagnostics, two commonly used methods are optical and electrical diagnostics.

3.2.1 Electrical diagnostics

3.2.1.1 Equipment

For laboratory-scale reactors with mm- to cm-sized discharge gaps operating at atmospheric pressure, the voltage typically falls within the kV range. This necessitates the use of HV probes to ensure safe and accurate measurements. A HV probe is a device based on a voltage dividing circuit, which scales down the target voltage to a measurable range suitable for measurement devices, such as an oscilloscope. When selecting an appropriate HV probe, three key parameters must be considered: the measurement range (voltage ratio), bandwidth, and input impedance. A high bandwidth allows for the accurate measurement of fast-changing voltage signals, while a high input impedance minimizes loading effects, thereby improving measurement accuracy.

For discharge current measurement, two common methods are widely employed. The simplest method involves installing a shunt resistor, also known as a current viewing resistor, in series with the reactor and measuring the voltage across this resistor. The discharge current is then calculated using Ohm's law. This technique can be applied to both AC and DC discharges. To minimize energy losses and ensure the voltage drop remains within the measurable range, the resistor's value should be low. The second method involves using a current probe, such as a Rogowski coil, which converts the AC current signal into a voltage signal by detecting the magnetic field generated by the current changes. When selecting a current probe, its sensitivity (e.g., the A-to-V ratio), bandwidth, and measurement range must be carefully considered.

To record and analyze the measured signals, an oscilloscope is required, and its specifications—sampling rate, bandwidth, and resolution (ADC bits)—should be taken into account. A higher sampling rate allows for more data points to be captured per unit of time, resulting in higher precision. However, this comes at the cost of generating larger data sets, which may require additional storage space or longer processing times. Resolution, which determines the smallest step size in the signal that the oscilloscope can display, is calculated using Eq. (2). Typically, an 8-bit oscilloscope is sufficient for most discharge experiments. However, for transient discharges where current can vary significantly, such as GA discharges, an oscilloscope with 10-bit or higher resolution is preferred to ensure better accuracy.

$$Step\ size = \frac{V_{max} - V_{min}}{2^m}. \tag{2}$$

It is worth mentioning that when considering the bandwidth of the devices, including both the probe and the oscilloscope, the overall bandwidth of the system must be taken into account. This overall bandwidth is lower than that of any individual device and can be calculated using the following equation:

$$System\ bandwidth = \frac{1}{\sqrt{\frac{1}{probe\ band\ width^2} + \frac{1}{scope\ bandwith^2}}}. \tag{3}$$

To accurately measure the amplitude and capture necessary details (third and fifth harmonics) of the signal, the bandwidth of the oscilloscope and the probe should be at least 3–5 times the frequency of the measured signal. Additionally, for plasma discharges, particularly nanosecond pulse discharges, which exhibit highly transient characteristics, the rise time (T_r) and its corresponding frequency (f_r) or equivalent bandwidth, must be considered instead of solely relying on the signal frequency. f_r can be calculated from $f_r = C/T_r$. Here, C is a constant that depends on the type of system response, with values of 0.35 for Gaussian-type responses and 0.4–0.45 for maximally flat responses. Most oscilloscopes with a bandwidth of 1 GHz or below typically exhibit a Gaussian-type response.

3.2.1.2 Discharge characteristics and analysis

The discharge characteristics are commonly revealed through the analysis of electrical properties, as indicated by the measured voltage and current waveforms. These waveforms vary depending on the discharge types, with the observed differences reflecting underlying physical phenomena, as explained in literature [30,150]. Figure 13 provides a general overview of the discharge regimes, represented through their voltage-current (V-I) characteristics.

DBD is one of the most extensively studied discharge types, and its electrical characteristics have been thoroughly investigated and systematically summarized by many researchers [152,153]. The ideal voltage and current waveforms of a DBD reactor operated under an AC sinusoidal voltage are shown in Fig. 14(a). Plasma is periodically ignited and terminated (the period indicated from circled i to t), which is reflected by the many current peaks superimposed on the AC components of the current waveforms. The magnitude and number of these peaks can serve as a qualitative indication of the intensity of the plasma discharges. However, it is important to clarify that each current peak does not directly correspond to individual microdischarges in the DBD reactor.

Figure 14(b) illustrates a classic equivalent circuit for a

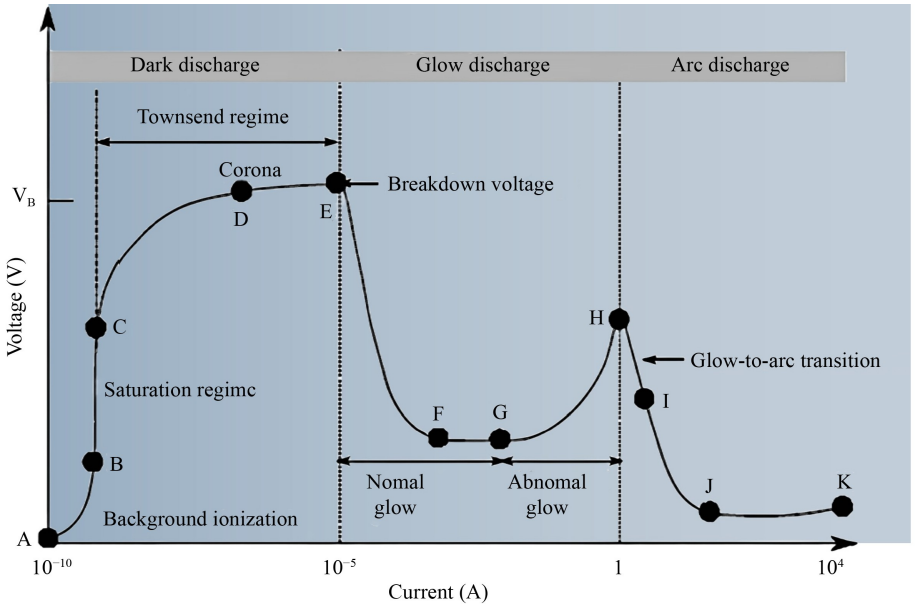

Fig. 13 Discharge regimes represented as V-I characteristics based on DC electric discharge. The voltage values are indicative of trends and not explicitly quantified. Reprinted with permission from Ref. [151], copyright 2016, Springer Nature.

DBD reactor. The reactor is represented by two capacitors, C_g and C_d, connected in series, corresponding to the gas gap and the dielectric barrier, respectively. During the discharge period, the plasma generated acts as a conductive medium, allowing charge transfer across the gap. This behavior is modeled by a variable resistor $R(t)$, connected in parallel with C_g. In practical scenarios, discharges often do not cover the entire electrode area due to factors such as uneven gaps or non-uniform surfaces of the barrier or electrodes. For these partially discharged DBD reactors, Peeters et al. [154] proposed an equivalent circuit. In this model, the capacitances C_g and C_d are further divided into discharging (β) and non-discharging (α) fractions. Additionally, most experimental set-ups include parasitic capacitances, which can influence the analysis of electrical characteristics but are often omitted from the classic equivalent circuit. For packed-bed DBD reactors, which are widely used in plasma-catalysis studies, the reactor's capacitance becomes more complex. In the study by Rad et al. [141], the equivalent circuit of a packed-bed DBD reactor replaced the gap capacitance C_g with the packed-bed capacitance C_{pb}. C_{pb} represents the overall capacitance of the packed zone, which includes contributions from the gas phase, the packing material, and surface discharges. However, the individual contributions of these components to the electrical characteristics cannot be distinguished. The equivalent circuit approach for diagnosing DBD reactors has been extensively studied and documented in the literature, where further details and examples can be explored [155].

The *Q-V* Lissajous plot is a widely used tool for analyzing the electrical properties of DBD reactors. In this method, a measurement capacitor with a known capacitance (C_m) is connected in series with the reactor, and the voltage across the capacitor (V_m) is measured. To ensure accurate results, the capacitance of the measurement capacitor should be significantly larger than that of the DBD reactor, typically around 1000 times larger as a general rule of thumb [53]. If C_m is too small, it could lead to a high V_m value that exceeds the voltage measurement range of the oscilloscope. Key parameters, such as the capacitance of the reactor (C_{cell}), the effective capacitance of the dielectric barrier, and the self-sustaining voltage (U_{min}), can be extracted from the *Q-V* Lissajous diagram. Figure 14(c) illustrates an ideal *Q-V* Lissajous figure with these parameters clearly indicated.

While the approach is well-established, certain challenges can arise in non-ideal scenarios. For instance, the shape of the diagram may deviate from the ideal parallelogram to an elliptical shape due to charge residues during the plasma-off phase or may become noisy due to measurement inaccuracy. These issues are discussed in detail in [153], which provides further insights. One notable variant of the typical *Q-V* parallelogram is the almond-shaped diagram, often observed in packed-bed reactors and surface discharge reactors. This shape arises from the gradual expansion of the plasma volume across the packing material or dielectric surface during the discharge phase, resulting in an increased effective capacitance. The curved slope of the *Q/V* relationship produces the characteristic almond shape [157]. Other cases that exhibit deformation of the Lissajous figure include pulsed-driven DBDs and reactors with asymmetric configurations. In these cases, the *V-Q* plot deviates significantly from the standard parallelogram, making the interpretation less straightforward, and the typical analysis methods for standard parallelograms are often not applicable. However, specific methods have

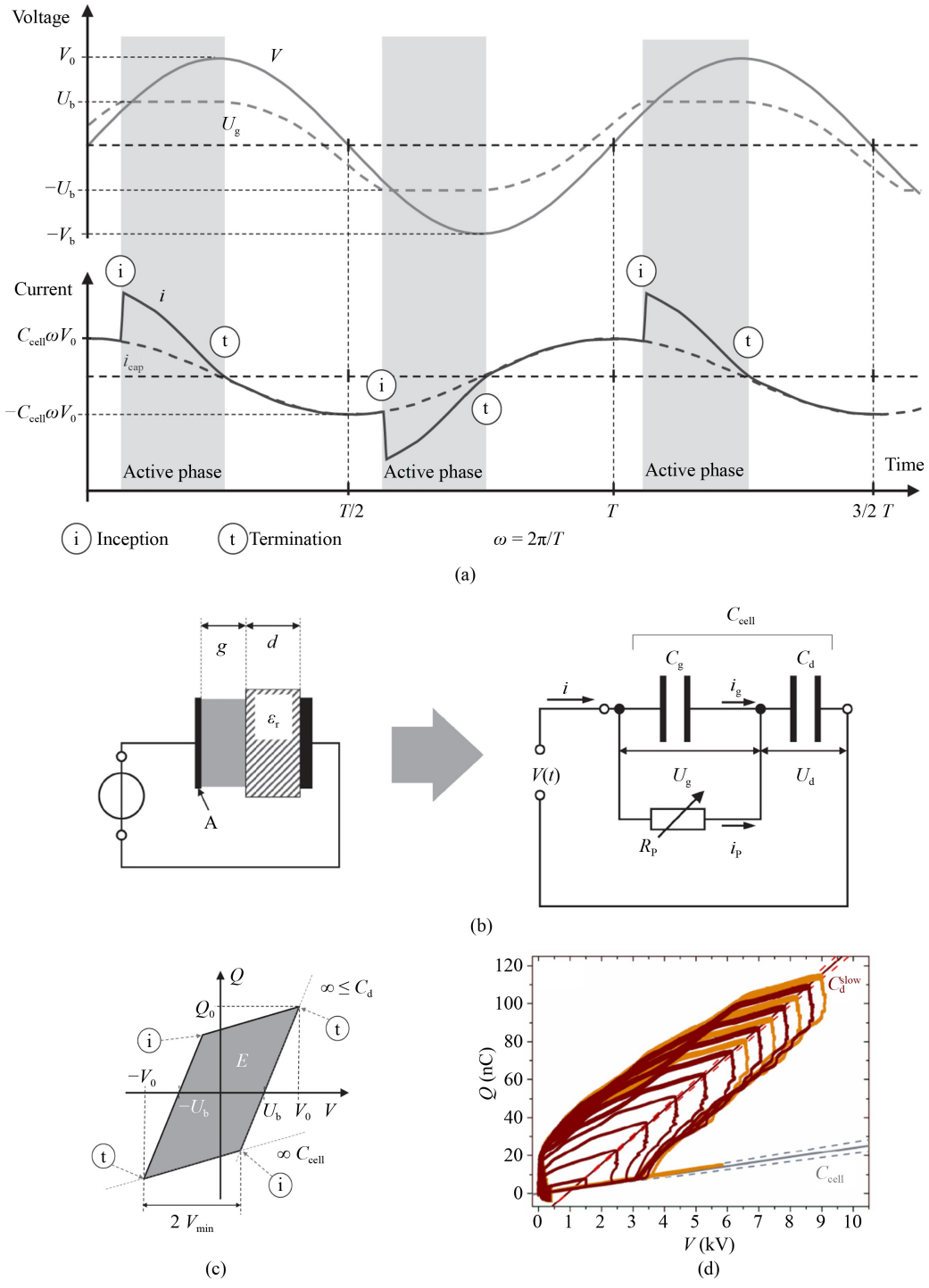

Fig. 14 (a) Schematic waveform of applied voltage $V(t)$, gap voltage U_g, burning voltage U_b, mean current i and its capacitive component i_{cap}; (b) classic equivalent circuit of DBD reactor; and (c) Q-V Lissajous figure. Reprinted with permission from Ref. [53], copyright 2017, IOP Publishing Ltd. (d) Determination of dielectric barrier capacitance C_d for pulsed driven DBD reactor using Q_{max} at given V_{max}. Reprinted with permission from Ref. [156], copyright 2013, John Wiley and Sons.

been developed for the analysis of pulsed-driven DBDs [158,159]. Figure 14(d) provides an example from a study [156], where the reactor capacitance (C_{cell}) and the capacitance of the dielectric barrier (C_d) can be determined. This is achieved by analyzing the slopes formed by the maximal points (Q_{max}-V_{max}) obtained under different applied voltages, with and without plasma ignition respectively.

In the case of typical GA discharges, the discharge characteristics span a broad range of time scales, from nanoseconds to seconds. Taking an AC GA discharge in a classical 2D reactor as an example, the voltage and

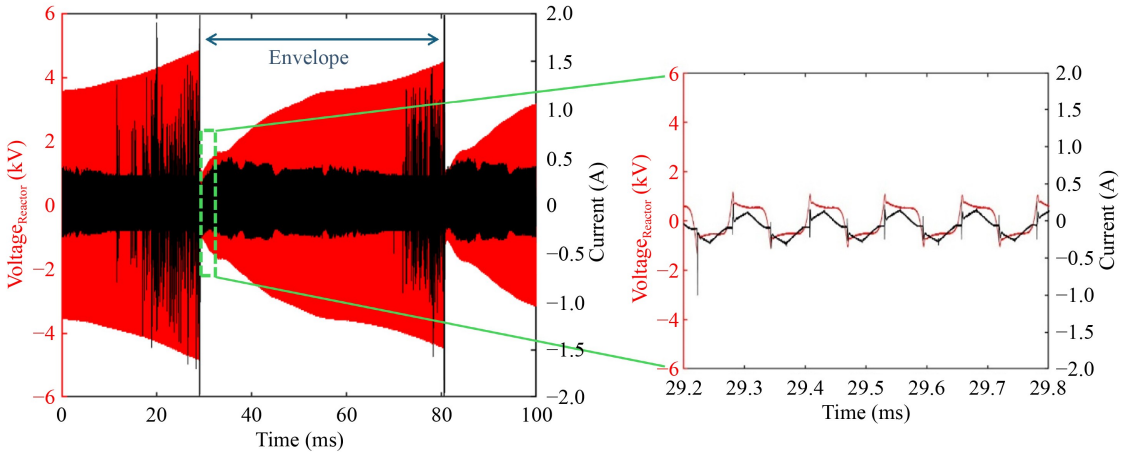

Fig. 15 Voltage and current waveforms of a classic 2D GA reactor. Reprinted with permission from Ref. [160], copyright 2025.

current waveforms are shown in Fig. 15 [160]. The individual discharges are characterized by pulses in nanosecond scale, while the collective behavior of these discharges, which corresponds to the dynamics of the GA development, spans milliseconds or even seconds per cycle. This collective behavior is typically represented as an "envelope" in the voltage waveform. The envelope time corresponds to the full propagation of the GA—from its ignition at the narrowest gap of the reactor to its cut-off at the widest gap. A high sampling rate is required to capture the fine details of individual voltage and current pulses, while measurements over a larger time scale are also essential to register the characteristics of the entire GA cycle. This dual requirement imposes significant demands on equipment, such as oscilloscopes, and necessitates the processing of large volumes of data for analysis.

In practical experiments, the variation of the GA cycle from ignition to cut-off exhibits a degree of randomness, leading to non-identical electrical characteristics, such as variations in envelope length. These variations become especially prominent in systems with high gas velocities or large reactor sizes. As a result, analysis must often be performed over multiple cycles, averaging the data to draw reliable conclusions. Furthermore, due to the transitional nature of the GA as a "warm plasma", a wide range of current variations is typically observed within a single GA cycle. This can include a "glow-like" mode with currents in the milliampere range and a "spark-like" mode where currents can reach tens of amps or even hundreds of amperes. These two modes correspond to different plasma properties, which significantly influence the chemical performance of the plasma reactor. This large range of current variation poses significant challenges for measurement, requiring high-resolution equipment, such as an oscilloscope with a high ADC bit depth, to capture both ends of the spectrum accurately in a single measurement. If such equipment is unavailable, separate measurements at different current ranges need to be conducted. These measurements must then be combined, and multiple measurements are required to obtain an average value, ensuring reliability and accuracy in the analysis.

3.2.1.3 Power calculation

In principle, the reactor power can be calculated by multiplying the measured voltage by the discharge current, and the energy consumed can be determined by integrating the calculated power over the plasma operation period. While this approach is straightforward in most cases, special attention is required in practice to avoid inaccuracies. For instance, there can be a measurement delay between the voltage and current signals, which can lead to a miscalculation of the discharge power. This issue is particularly significant in cases with highly transient discharge characteristics, such as nanosecond pulsed discharges, where precise synchronization is critical. The delay may be caused by various factors, including the influence of measurement probes (e.g., compensation circuits), the physical distance between voltage and current probes, and different lengths of signal cables. Accurate power calculation demands that such delays be accounted for. For example, in a study of nanosecond discharges by Montesano et al. [40], this delay was quantified by superimposing the first derivative of the voltage and the current before breakdown, during which the current primarily exhibited a capacitive nature.

Another scenario requiring special attention during power calculation is the GA discharge. The challenges here stem from measurement difficulties associated with the nature of the discharges, including wide variations in current (ranging from milliamperes to tens of amperes) and their periodic behavior due to arc propagation. Achieving accurate power analysis in such systems often necessitates multiple measurements taken at carefully selected time intervals, processing large amounts of data, and the use of high-performance equipment as discussed in the previous section.

For experiments involving DBD, a widely adopted

method for power calculation is the Lissajous method, originally proposed by Manley [161]. Based on the product of instantaneous voltage and current, the derivation of this method is expressed in Eq. (4) [153]. The area enclosed by the Q-V Lissajous plot, calculated as $\oint V(t)\mathrm{d}Q(t)$, corresponds to the average energy per operational cycle. By incorporating the applied frequency f, the power can then be determined.

$$P = \frac{1}{T}\int_0^T V(t)\cdot i(t)\,\mathrm{d}t = \frac{1}{T}\int_0^T V(t)\cdot C_\mathrm{m}\mathrm{d}V_\mathrm{m}(t) = f\oint V(t)\,\mathrm{d}Q(t). \quad (4)$$

In the case of discontinuous operation, such as burst mode or pulsed operation as mentioned in Section 3.1.3, the voltage and current signals measured are discontinuous. The calculation of power typically begins by determining the "instantaneous power" during the "plasma-on" period. This is then averaged over the entire operation period, including the "plasma-off" phase, by accounting for the duty cycle. In such scenarios, the instantaneous power provides insights directly related to plasma properties, whereas the average power reflects the overall performance profile of the reactor. By comparing both calculated power values with those of continuously operated plasma reactors at the same total power, valuable insights can be gained, such as the effects of high instantaneous power, or potential phenomena like plasma quenching and re-ignition.

Apart from ensuring the accuracy of measurements and calculations, it is crucial to use the correct terminology for power to enhance clarity, accuracy, and comparability. Unfortunately, confusion and incorrect conclusions are evident in some literature due to a lack of proper clarification. There are several power definitions: reactor power, PSU output power, plug power, and process power. The power calculated from the voltage across the reactor and the discharge current only considers the reactor itself and is therefore referred to as "reactor power", which is often the focus of plasma studies. On the other hand, the PSU output power, sometimes directly displayed on commercial power supplies, represents the total power of all components connected to the PSU. This includes reactor power, line consumption, and the power drawn by other electrical components such as ballast resistors. The "plug power", which reflects the total power consumption of the entire plasma system, includes the reactor power, the standalone power of the PSU, and the power consumption of all other components in the circuit. Plug power can often be directly measured using a power meter. However, while the plug power provides an overview of the entire plasma system, it is not ideal for comparing data across the literature since electrical systems differ significantly among experimental set-ups used by various researchers. Therefore, both plug power and PSU output power should not be confused with reactor power when evaluating reactor performance. Instead, accurate measurement of the voltage and current, and subsequent calculations based on these, remain the most reliable approach. Additionally, it is important to recognize that the plasma system is not the only component consuming power in chemical conversion processes. Auxiliary units, such as external heating or cooling systems, also contribute to overall energy consumption and must be accounted for when evaluating the energy efficiency of the entire process. This comprehensive approach ensures that the energy efficiency of plasma-based processes is not overstated or overclaimed.

3.2.2 Optical diagnostics

Optical diagnostics play a crucial role in advancing our understanding of plasma chemistry and plasma catalysis. Numerous methods, originally developed in plasma physics research, are well-established for studying plasma-based gas conversion. In general, optical diagnostics fall into two main categories: imaging and spectroscopic methods. Time-resolved imaging has been used to study the characteristics and spatial and temporal development of plasma discharges. Many previous studies have reported the use of ICCD cameras with high sensitivity and fast gating to visually trace the microdischarges [162]. In the case of plasma-catalytic reactors, the distribution and dynamics of discharges on the catalyst surface can be investigated [163,164]. Furthermore, it could help to study the influence of different catalyst packings on the plasma, providing vital information to reveal the plasma-catalyst interaction [165]. The results can also be studied in combination of results from modeling [166] or other techniques for validation or compensation, including integration with a spectrometer for enhanced measurement of emission spectra [167]. While imaging techniques are relatively straightforward, they require careful attention to several factors in practice, such as a good optical path, particularly in the case of plasma-catalytic reactors. Additionally, the temporal and spatial characteristics of the fast discharge phenomenon need to be synchronized with the acquisition of the ICCD camera, with a certain resolution that is feasible for analysis. These considerations emphasize the need for careful equipment setting and reactor design in laboratory studies.

Spectroscopic techniques, including OES, laser-induced fluorescence, scattering, and absorption spectroscopy, provide valuable data on key plasma parameters such as gas temperature, electron density, electric field, and active species concentrations. This information is essential for understanding reaction mechanisms and plasma properties. These spectroscopic methods are well-established and have been reviewed extensively in the literature [168−175]; interested readers are encouraged to

consult these sources for further details. In recent years, *in situ*/operando spectroscopic characterization of catalysts under plasma conditions has become increasingly important in plasma-catalysis research. Techniques such as *in situ* IR, Raman, and X-ray absorption fine structure (XAFS) spectroscopy have been applied to gain insights into the dynamic behavior of catalysts in a reactive plasma environment. Due to the highly reactive environment and complex plasma-catalyst interactions, measurement and analysis in this context present significant challenges, often requiring custom experimental set-ups. For instance, conventional plasma-catalytic reactors like coaxial DBD reactors with dense packing are frequently avoided in *in situ* IR studies due to limited optical access and difficulties in integrating optical components due to reactor size and operating conditions. Instead, custom-designed cells with small sample volumes and reduced electrode dimensions are used to focus measurements specifically on areas of plasma-catalyst interaction. Since these designs prioritize optical access and measurement control over reactor performance factors (such as plasma uniformity and gas residence time), the chemical performance of these *in situ* cells is not always comparable to that of reactors optimized for conversion and energy efficiency. However, connecting microscopic insights from *in situ* diagnostics with macroscopic chemical performance remains an important goal, and future efforts in reactor design are needed to achieve this.

In *in situ* set-ups, DBD and plasma jet sources are often used because they can operate at atmospheric pressure and relatively low temperatures. High-temperature sources like GA and microwave plasmas are less common due to the challenges of controlling temperature and preventing damage to cell windows and other sensitive components [171]. Moreover, the sampling methods for optical measurement influence the design of cell configuration, especially the arrangement of the electrodes. For example, IR absorption spectroscopy set-ups may vary between transmission IR (TIR), diffuse-reflectance IR Fourier transform spectroscopy (DRIFTS), and attenuated total reflection modes, each requiring different cell configurations. Figure 16 presents examples of two different plasma cells for *in situ* IR study. To ensure reliable measurements, custom cells must meet three criteria: (1) provide an unobstructed optical path across the catalyst-plasma interaction region; (2) enable effective plasma-catalyst contact, ensuring that plasma species can interact with the catalyst surface; (3) allow stable plasma operation with minimal interference to measurements, avoiding issues such as window overheating or electromagnetic noise affecting the measurement.

Other practical considerations include aligning the cell

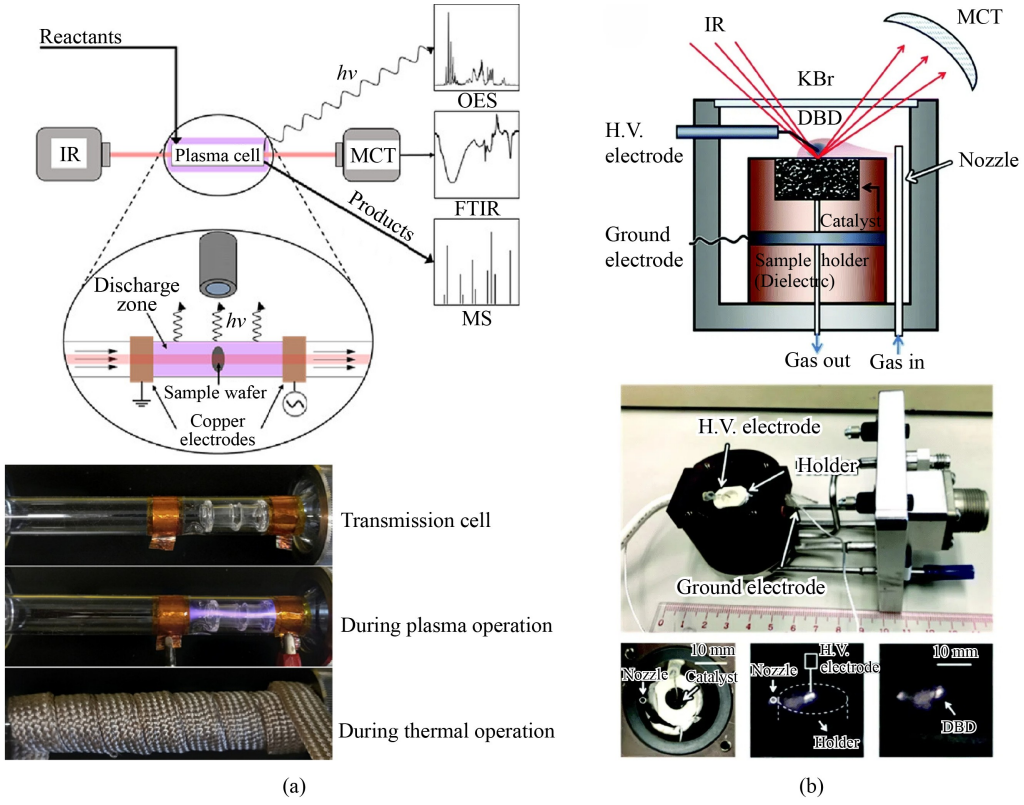

Fig. 16 (a) *In situ* TIR cell used along with OES and MS (MCT: mercury-cadmium-telluride). Reprinted with permission from Ref. [177], copyright 2022, American Chemical Society. (b) *In situ* plasma DRIFTS cell. Reprinted with permission from Ref. [178], copyright 2020, Royal Society of Chemistry.

and light path precisely, focusing the beam at the plasma-catalyst interface, and adjusting beam intensity to optimize measurement sensitivity. Weak IR signals, a common challenge due to low transmission through catalyst samples, are often addressed by using KBr as a sample carrier due to its minimal IR absorption. Moreover, for DRIFTS or TIR, the gas species which are sensitive to IR, could introduce interference to the measurement of IR signals from the surface species. Hence it is beneficial to consider surface-specific techniques such as polarization-modulation IR reflection-absorption spectroscopy (PM-IRAS). PM-IRAS can differentiate IR absorption between the s- and p-linearly polarized light for surface species, providing a high surface sensitivity. Lee et al. [176] have demonstrated the use of PM-IRAS in their study of plasma-catalytic conversion of CH_4. The author developed a multimodal spectroscopic diagnostic system which combines PM-IRAS, OES and MS to correlate reactions in both gas phase and on the surface with the products. While interesting results have been achieved for the analysis of reaction mechanisms, the authors also stated the limitations of their diagnostic system, such as suitability only for low-surface-area materials and the requirement that surface species have a perpendicular dipole moment. Nonetheless, this approach offers valuable insights and could inspire future multimodal systems for deeper study of plasma-catalyst interactions.

Raman spectroscopy is often considered as a complementary to IR for catalyst characterization. Common catalyst supports like alumina and silica are not Raman active, facilitating the detection of active species adsorbed on their surfaces [175]. Till now, there is limited research using *in situ*/operando Raman spectroscopy in plasma-catalysis studies. However, an example can be found in the study of Saito et al. [179] who investigated the CO_2 reduction with CH_4 and H_2 in a DBD reactor with copper nanoparticles supported on zinc oxide as the catalysts. The raman peaks measured were compared with literature and results from density function theory calculations. Important information was gained to analyze the surface species and their reaction pathways including CH_3CHO and CH_3COO formation, and the role of activated H_2 and H_2O. Besides, results from *in situ* Raman could also assist the study of possible structural changes of the catalysts during reaction under plasma exposure. This has been demonstrated by the work of Sun et al. [180] who studied the reaction-driven transformation of Pd-ZnO interface during plasma-catalytic conversion of CO_2 via reverse water gas shift reaction.

The change of structure can also be monitored by *in situ* XAFS. This was demonstrated in the study by Gibson et al. [181]. In their work of plasma-catalytic oxidation of CH_4, significant structural changes of the catalysts used (Pd/Al_2O_3) did not occur during the plasma exposure, but the temperature increase of Pd nanoparticles was observed, although the temperature was insufficient for thermal reaction to occur. The temperature of surface Pd was estimated from the changes in mean squared thermal disorder parameter based on premade calibration data. The authors also noted that the XAFS provides bulk averaging results which may not indicate possible minor changes below the detection level.

3.2.3 Other methods and techniques

In addition to the diagnostic and analytical methods mentioned above, there are other approaches reported in literature. A notable example is isotope tracing, which is a well-established technique in chemical reaction studies that has been effectively adapted to investigate reaction mechanisms within plasma environments. For example, isotopes of carbon and oxygen can be used in plasma reactors to trace the behavior of reactants such as CO_2. Among carbon isotopes, ^{12}C and ^{13}C are stable, while ^{14}C is used primarily for radiolabelling; for oxygen, the stable isotopes are ^{16}O, ^{17}O, and ^{18}O. Navascués et al. [182] applied isotope tracing in a DBD reactor for DRM using $^{13}CO_2$ and $^{12}CH_4$ as reactants. Their analysis of reaction products revealed that C_2 and C_3 hydrocarbons contained only ^{12}C, while carbon monoxide included both ^{12}C and ^{13}C, suggesting parallel reaction pathways for CO_2 and CH_4 with minimal interaction between the two reactants in plasma conditions. Morillo-Candas et al. [183] investigated fast oxygen atom exchange in CO_2-CO-O_2 mixture with RF plasma. Isotopic tracing using $^{18}O_2$ was performed and the author developed a fitting algorithm for 12 isotopologues of CO_2 and 6 of CO in gas mixtures. They observed the incorporation of ^{18}O into CO and CO_2 and analyzed the mechanism with an emphasis on excited oxygen atoms O (1D). Besides the gas phase reaction, examples of isotope tracing can be found in reported studies on plasma-based surface processing [184,185], and surface reaction in plasma-catalytic CO_2 conversion [186]. This method shows significant promise for uncovering detailed reaction pathways and mechanisms, offering a valuable avenue for future research in plasma catalysis.

Another example is the work by Parastaev et al. [186], who developed a technique called temperature-programmed plasma surface reaction (TPPSR) to investigate the plasma-catalytic hydrogenation of CO_2. This method consists of four key steps: (1) adsorbing the reactant, CO_2 in this case, onto the catalyst surface at ambient temperature; (2) flushing the reactor to remove any gas-phase CO_2; (3) exposing the catalyst to plasma at ambient temperature to eliminate weakly adsorbed species; (4) ramp the temperature by gradually heating the catalyst at a constant rate in the presence of plasma while monitoring the gas-phase products. According to the authors, the TPPSR method enables the study of

reactions primarily occurring on the catalyst surface, with minimal interference from gas-phase reactions. This approach helps to decouple surface reactions from gas-phase processes, addressing a fundamental challenge in understanding reaction mechanisms within plasma-catalyst systems. However, the authors also acknowledge certain limitations of the TPPSR technique. These include the need to avoid extensive gas-phase conversion of the reactant, the necessity for at least one reactant to exhibit reasonable adsorption on the catalyst surface, and the unclear effects of plasma-induced heating on reaction dynamics.

3.3 Key performance indicators

The testing of various process parameters in experiments forms a fundamental approach for examining the influence of these variables and comparing the performance of different reactors and systems. Beyond directly controlled parameters such as flow rate, gas composition, and discharge power, a key process parameter frequently used in the analysis is the specific energy input (SEI, sometimes referred to as SIE). SEI represents the amount of energy delivered per mole or per unit volume of gas treated by plasma. In the case of a flow reactor, SEI is calculated as a ratio of the plasma power to the total feed gas flow rate, as shown in Eq. (5). Typically, it is expressed in units such as $J \cdot L^{-1}$ or $eV \cdot molecule^{-1}$ by considering the volume at specific temperature and pressure with Avogadro number. SEI is a critical factor which has been extensively used in analysis in many reported studies. However, it cannot be adjusted directly, but through changing the power or flow rate. As the same SEI can be achieved under different conditions (e.g., high power with high flow rate or low power with low flow rate), discussions regarding the effect of SEI should be done carefully.

Given the broad diversity and interdisciplinary nature of research in plasma, establishing a standard for results reporting and validation poses a significant challenge. Alves et al. addressed this challenge in their review paper, focusing on laying the foundation for plasma standards to enhance reproducibility, transparency, and collaboration [187]. In the case of gas conversion, taking CO_2 as an example, terms and key performance indicators such as conversion, selectivity, and energy efficiency are frequently discussed. Previous review papers have provided detailed descriptions, such as relevant equations referenced in [50,59]. Table 3 contains examples of equations used in the case of plasma-based CO_2 conversion.

These energy-related metrics are calculated based on power, necessitating particular attention to accurate power measurement. As discussed in Section 3.2.1(b), it is crucial to determine which power measurement should be utilized—whether it is the reactor power, the plug power, or the total power consumption of the entire process, including other process units. When calculating energy efficiency, Eqs. (4), (5) and (7), based on the reaction enthalpy and the SEI, serves as a fundamental

Table 3 Examples of key performance indicators for plasma-based CO_2 conversion

SEI	$SEI\left(\mathrm{J \cdot mL^{-1}}\right) = \frac{Energy\,(\mathrm{J})}{Treated\ gas\ volume\,(\mathrm{mL})} = \frac{Power\,(\mathrm{W})}{Flow\ rate\left(\mathrm{mL \cdot s^{-1}}\right)}$,	(5)
Absolute conversion	$\chi_{CO_2} = \frac{\dot{n}_{CO_2,in} - \dot{n}_{CO_2,out}}{\dot{n}_{CO_2,in}}$,	(6)
Effective conversion	$\chi_{eff,CO_2} = \chi_{CO_2} \times \frac{\dot{n}_{CO_2,in}}{\dot{n}_{CO_2,in} + \sum \dot{n}_{other\ reactant,in}}$,	(7)
Total conversion	$\chi_{total} = \sum_i \chi_{eff,reactant}$,	(8)
Selectivity (carbon-based)	$S^{c}_{C_xH_yO_z} = \frac{x\dot{n}_{C_xH_yO_z}}{\dot{n}_{CO_2 converted} + \dot{n}_{CH_4 converted}}$,	(9)
Carbon balance	$CB = \sum S^{c}_{C_xH_yO_z}$,	(10)
Energy efficiency	$\eta = \frac{\chi_{total} \times \Delta H^{\circ}_{298K}}{SEI}$,	(11)
	$\eta = \frac{\sum(\dot{n}_{product} \times LHV_{product})}{E_{applied} + \sum(\chi_{eff,reactant} \times \dot{n}_{reactant} \times LHV_{reactant})}$,	(12)
Energy consumption/cost	$EC_{converted\ CO_2} = \frac{SEI \times V_m}{\chi_{eff,co_2}}$,	(13)
	$EC_{converted\ reactant} = \frac{SEI \times V_m}{\chi_{total}}$,	(14)
	$EC_{product} = \frac{Power}{\dot{n}_{product_i}}$,	(15)
Synergetic factor	$I_{SE} = \frac{\chi_{plasma\ and\ catalyst}}{\chi_{plasma\ only} + \chi_{catalyst\ only}}$,	(16)

V_m is the molar volume of gas, and 24.5 $L \cdot mol^{-1}$ is often evaluated at 298 K and 1.013×10^5 Pa.

principle and can be easily applied to cases such as CO_2 splitting. However, in more intricate scenarios like DRM and CO_2 hydrogenation, this approach becomes impractical. Consequently, an alternative method utilizing the lower heating value, outlined in Eqs. (4), (5) and (8), is often employed. The definition of energy consumption or cost varies in literature depending on the process's focal point. Equations (4), (5) and (9), and (4), (5) and (10) are utilized if the cost pertains to the energy required per unit of CO_2 conversion or total reactants, whereas Eqs. (4), (5) and (11) quantifies the energy necessary to produce per unit of product.

It is crucial for these aspects to be clearly defined to ensure accurate analysis and reporting of relevant performance indicators. Bart et al. [49] conducted a critical review that summarized correct terms and definitions while highlighting common errors in the literature. The authors addressed the change in volumetric flow rate as a prevalent issue leading to inaccurate analysis, and they discussed corrected methods to improve data comparability, such as the use of a flux ratio as a potential solution. The flux ratio can be determined using a stoichiometrically derived expression in straightforward cases, such as CO_2 splitting. However, in more complex scenarios, like DRM, this approach becomes impractical due to the formation of by-products. In such cases, alternative methods are required, such as utilizing a flow meter or introducing a standard reference component at the reactor outlet.

In the exploration of the synergy between plasma and catalysts, prior research by Wang et al. introduced the "synergetic factor". This factor is calculated as the ratio between the conversion achieved using the plasma-catalyst system and the sum of conversions achieved separately using plasma alone and catalysts alone [126]. It is essential to carefully maintain consistent reaction conditions when discussing this factor. The mutual influence of plasma on catalysts and vice versa may lead to variations in conditions, such as discharge properties and catalyst bed temperature, under which these conversions are attained.

4 Trends and new opportunities

Research in plasma-based gas conversion is expected to grow continuously, with current directions, such as exploring reaction mechanisms and plasma-catalyst interactions, remaining key focal areas. Significant advancements can also be anticipated in innovative catalyst material development and reactor design. Beyond these established approaches and topics, there are emerging opportunities and new trends which hold great potential to further advance the technology and broaden the scope of research in this field.

4.1 AI as a research tool

AI is rapidly emerging as a transformative tool in scientific research, revolutionizing methodologies, strategies, and the perspectives of researchers across various disciplines, including plasma science. With a strong focus on machine learning, AI offers new possibilities in modeling, simulation, and process control, with applications spanning from low-temperature plasmas to fusion research. In areas such as plasma physics, plasma chemistry, and plasma-surface interactions, AI has been utilized to accelerate simulations, enhance predictive capabilities, and reduce the need for costly experimental work. Comprehensive reviews in literature provide insights into the fundamentals of machine learning, its applications, as well as its strengths, limitations, and challenges [188−192]. In the context of plasma-based gas conversion, the integration of AI is still in its early stages. However, several pioneering studies have begun exploring its potential, demonstrating promising results.

4.1.1 Machine learning for analysis, prediction and optimization

There are already published works which demonstrated the application of machine learning to analyze, predict the experimental results and optimize the process [193−197]. Most of those cases use feed-forward artificial neural networks (ANNs) to predict macroscopic properties such as conversion, energy efficiency or selectivity as the output. The input can be the operational parameters such as discharge power, flow rate or gas composition, and reactor or catalyst properties such as the size and geometry. A general structure of an ANN is shown in Fig. 17(a), it typically consists of minimally 3 layers: an input layer, one or more hidden layers and an output layer, each containing several neurons. Each neuron in the input layer (n^{IL}) represents an input variable of the ANN model, such as electrode spacing or input potential. The neurons in the output layer (n^{OL}) represent output parameters such as energy efficiency or conversion. The input neurons are multiplied by a weight ($w_{i,n}^{\mathrm{IL}}$) and incremented with a bias (b_i^{IL}). The result is modified by a transfer function (F_i^{IL}) and values for all the input neurons are summed. The result is a neuron in the hidden layer (n^x), which has no relevant physical meaning on its own. A hidden layer can have multiple neurons, each with its own weights and biases. This process can be repeated multiple times, with the neurons of the hidden layer becoming the input for the next hidden layer until the output layer is reached. The number of hidden layers, the number of neurons per hidden layer and the type of transfer function are design choices when setting up the ANN. In the evaluated works most often, a single hidden layer is used containing around 10 neurons.

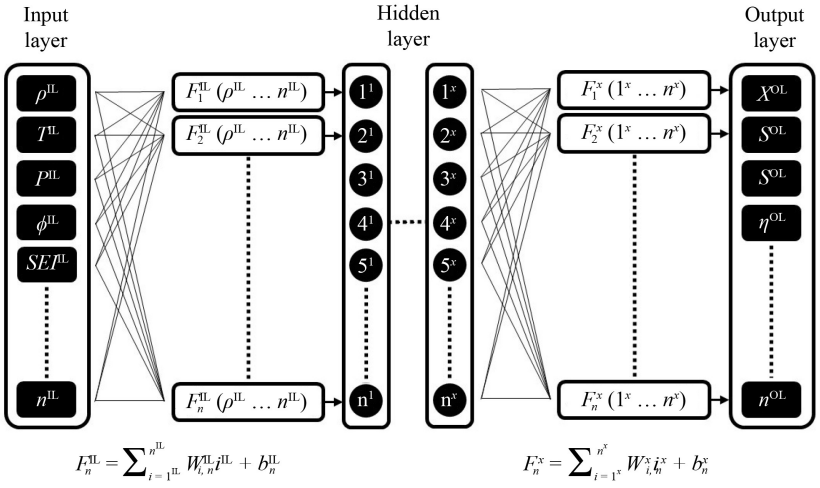

(a)

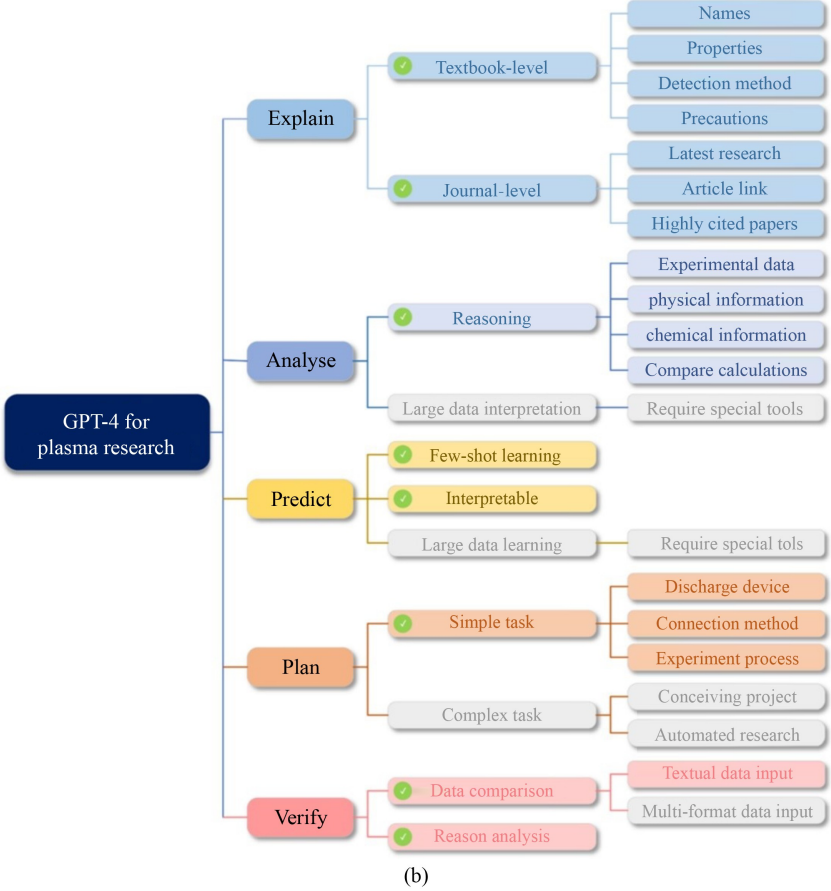

(b)

Fig. 17 (a) The general structure of an ANN; (b) GTP-4 can be used for plasma research in different stages. Reprinted with permission from Ref. [200], copyright 2024, John Wiley & Sons.

For the training of an ANN, a large data set is required. This data set is divided into at least two subsets: a training set and a validation set. To obtain the values of the weights and biases, the training set is used. A loss function describes the difference between the solution of the neural network and the experimental data from the training set. This error can be expressed for example as the mean squared error or the R^2 value. During training, the value of the loss function is reduced by adjusting the values of the weights and biases via algorithms such as the Levenberg-Marquardt, Broyden-Fletcher-Goldfarb-Shanno Bound or the backpropagation algorithm. After training, the validation data set is used to determine the reliability of the ANN.

In the study of Cai et al. [194], prediction and optimization of the plasma catalytic DRM process were

conducted with a hybrid model combining ANN, support vector regression, and regression trees to handle limited data sets and complex parameter interactions. The model provided insights into the relative significance of different parameters, revealing that the total flow rate had the most significant impact on CO_2 and CH_4 conversion, while Ni loading on the catalyst had a relatively minor effect on the overall plasma process performance. Another study by Chen et al. [198] used an ANN to screen for an optimal catalyst for NO_x reduction. They compiled a data set from literature and their own experimental measurements to predict NO_x conversion consisting of information about catalyst elemental composition, catalyst structure and morphology, the catalyst synthesis method and the NO_x reduction conditions. The authors succeeded in developing a low-cost catalyst with a broad temperature operation window. In plasma catalyst design, ANNs can accelerate catalyst development compared to traditional trial-and-error methods. Additionally, multiple synthesis conditions can be optimized simultaneously, offering a more efficient pathway to improved catalyst performance.

It is important to note that ANN models are data-driven and can produce predictions that violate physical laws. The performance of ANNs relies heavily on the quality and diversity of their training data sets, necessitating caution when extrapolating results to scenarios that significantly deviate from the training data. For example, an ANN trained on data from a single plasma gas conversion set-up is unlikely to accurately predict performance for different set-ups. Developing robust and broadly applicable ANNs requires large, diverse data sets that encompass various reactor geometries and operational parameters. However, such comprehensive data sets remain scarce in plasma gas conversion research. A 2022 report highlighted this gap, attributing it to inconsistent definitions, unstructured metadata, and a lack of standardized formats [192]. To address these limitations and fully integrate machine learning techniques into plasma system modeling, the plasma research community must adopt standardized reporting practices aligned with the FAIR data principles (Findable, Accessible, Interoperable, and Reusable) [199]. A current debate concerns that if large data sets are necessary to build predictive models, how machine learning can still contribute to reducing practical experimental efforts. This remains a question to be answered by further exploration.

4.1.2 Large language models (LLMs)

The recent heat on LLMs has had a profound impact on both daily life and scientific research. Tools like ChatGPT, which garnered significant attention following its release in November 2022, have introduced transformative changes across various fields, including plasma-relevant research. As von Keudell discussed [201], these tools bring both substantial benefits and challenges to scientific workflows.

At their core, LLMs like ChatGPT operate by analyzing vast amounts of text data and generating responses based on the statistical likelihood of word sequences.

Owing to its sophisticated deep learning algorithm known as the transformer, and training with massive text data from various sources, LLMs can provide answers with a certain degree of accuracy for common questions and recurring topics. They also excel in simplifying explanations and summarizing conclusions. In research, LLMs can assist in multiple ways, such as conducting literature reviews, analyzing and visualizing data, designing experiments, and supporting scientific writing. For instance, Bai et al. [200] demonstrated the use of GPT-4 throughout various stages of their research on plasma-based nitrogen fixation (see Fig. 17(b)). In their work, GPT-4 went beyond merely retrieving information for literature analysis—it also analyzed data, explained observed phenomena, provided insights, and suggested strategies. Additionally, LLMs can support programming by aiding in coding tasks, which could be especially useful for modeling and simulation in plasma and chemical processes.

However, as with any new research tool, LLMs come with limitations and challenges that require careful consideration. Three key issues are particularly relevant:

(1) LLMs do not inherently understand physical and chemical phenomena. As a result, they may generate incorrect or misleading statements. Furthermore, correct answers are often oversimplified, which is problematic in interdisciplinary fields like plasma-based gas conversion, where nuanced and highly specialized information is critical.

(2) While LLMs can perform well with general queries, they struggle with complex mathematical, physical, or chemical problems, especially those at the cutting edge of research. This limitation underscores the need for expert validation of their output.

(3) Since LLMs are trained on pre-existing data and have limited capacity to incorporate recent developments, they may not capture the latest advancements, especially in the field like plasma-based gas conversion which has been evolving rapidly in recent years.

These limitations highlight the importance of human oversight when integrating LLMs into research workflows. Additionally, concerns about data security and integrity must be addressed, as well as risks related to plagiarism, originality, and reliability in scientific writing. Adhering to ethical guidelines and maintaining transparency are essential when using such tools. In summary, LLMs serve as valuable assistants with extensive general knowledge and rapid response capabilities, but they are not replacements for your experienced colleagues, supervisors, or collaborators.

4.2 Plasma-material systems

Beyond plasma-catalyst interactions, which have been extensively studied, recent years have seen growing interest in exploring other plasma-material systems. A prominent example is the plasma-sorbent system, which has shown promise in applications of CO_2 conversion and ammonia synthesis. For instance, Rouwenhorst et al. [202] demonstrated the use of zeolite 4A to enhance the energy yield of plasma-based ammonia synthesis. In their study, the *in situ* adsorption of synthesized ammonia on zeolite effectively suppressed ammonia decomposition by the plasma, resulting in a twofold improvement in energy yield. Furthermore, Li et al. [146] highlighted the potential of plasma-sorbent systems for CO_2 capture and conversion within a single reactor. Using a DBD reactor packed with hydrotalcite, the authors implemented a cyclic operation in which CO_2 was first captured from air or flue gas by the sorbent material, followed by plasma-induced desorption and conversion, as illustrated in Fig. 18. During plasma exposure, CO_2 desorption occurs due to electron-stimulated desorption, plasma-induced heating, or interactions with reactive plasma species. Simultaneously, CO_2 undergoes splitting, either in the gas phase or on the sorbent surface. This dual function of plasma—driving chemical reactions and inducing desorption—addresses one of the most energy-intensive steps in conventional CO_2 capture processes. Furthermore, this plasma-sorbent system can be extended to reactions involving CO_2, such as hydrogenation or DRM, as demonstrated by Vertongen et al. [203]. Apart from solid sorbents, a similar concept has also been demonstrated in systems that combine plasma with ionic liquids. For example, Attri et al. [204,205] reported a system using the ionic liquid 1-butyl-3-methylimidazolium chloride ([Bmim]Cl) to capture CO_2, followed by plasma treatment to convert it into CO. Although research in this field is still in an early stage, the potential for such systems to enable efficient process integration has garnered significant attention.

Another emerging area of research in plasma-material systems is the integration of plasma with membranes in a single reactor. Two distinct approaches have been explored: (1) employing membranes as reactant distributors or as supports for catalysts within the reactor; (2) using membranes to separate products from plasma-induced reactions, thereby minimizing back-reactions and shifting the reaction equilibrium.

For the first approach, an example is the study by Veng et al. [206], who developed a membrane-DBD reactor for ammonia synthesis. The reactor design, illustrated in Fig. 19(a), utilized an alumina membrane as both the dielectric barrier and a distributor for H_2. This innovative design allowed hydrogen to be transported radially while N_2 flowed axially, increasing the residence time of N_2 in the plasma zone to promote the production of atomic nitrogen. Simultaneously, H_2 which requires less energy for dissociation, was evenly distributed. This configuration achieved an energy yield of 0.25 g-NH_3·kWh^{-1}, which is three times higher than conventional DBD operation. The authors also demonstrated that both ammonia production and power consumption were inversely proportional to the product of membrane pore size and porosity.

In the second approach, the *in situ* separation of products significantly enhances reactor performance and facilitates process integration. For instance, Hayakawa et al. [207] investigated hydrogen production from ammonia decomposition in a plasma-membrane reactor combining a DBD plasma with a Pd-Cu alloy membrane. By integrating the membrane, the maximum hydrogen production rate increased from 13% to 24.4%, compared to a conventional plasma reactor. The authors proposed a plasma-driven permeation mechanism, as depicted in Fig. 19(b). Ammonia was decomposed in plasma to produce H radicals, which were adsorbed on the membrane surface. These radicals diffused through the membrane and recombined on the opposite side to form H_2. This study highlighted the synergy between plasma and membranes, where plasma not only drives the reaction but also facilitates permeation. The contribution of plasma can occur through the generation of excited species or heat, which improves membrane performance

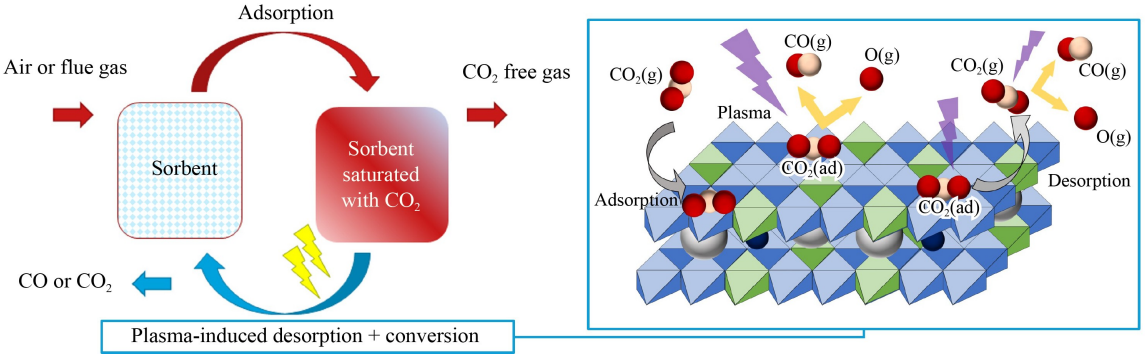

Fig. 18 Plasma-sorbent system for capture and conversion of CO_2. Reprinted with permission from Ref. [146], copyright 2021, Elsevier.

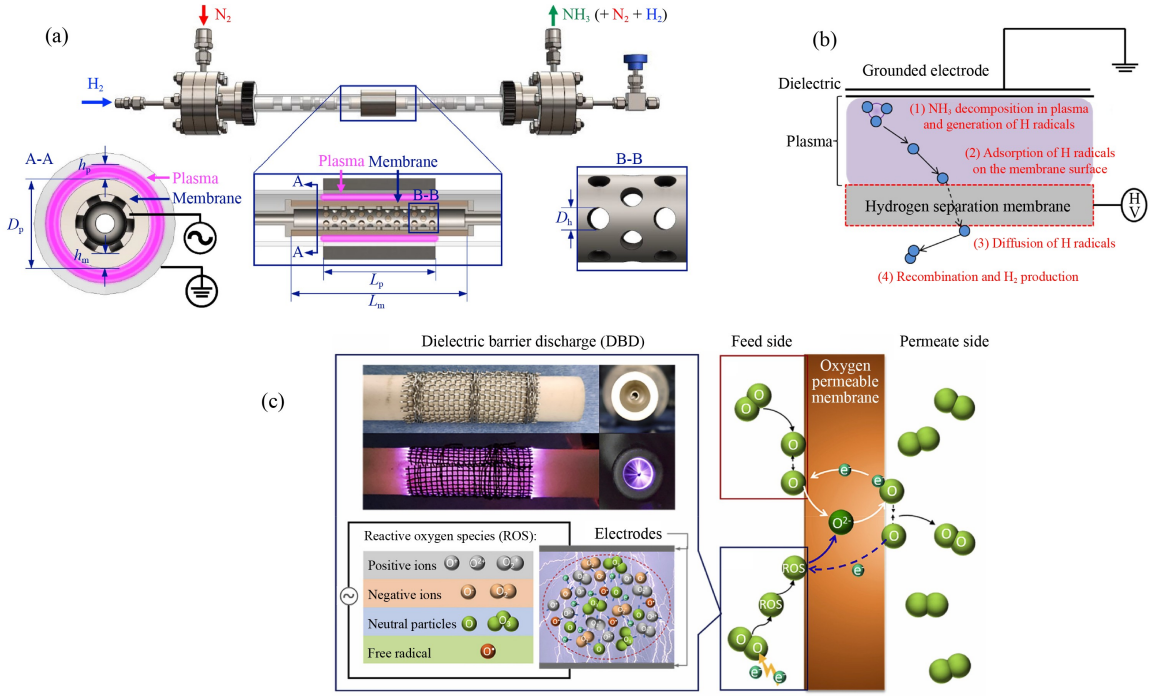

Fig. 19 (a) Membrane-DBD reactor for ammonia synthesis. Reprinted with permission from Ref. [206], copyright 2023, Springer Nature. (b) Plasma-driven permeation mechanism proposed for *in situ* H_2 separation from ammonia decomposition, Reprinted with permission from Ref. [207], copyright 2020, Elsevier. (c) Mechanism of *in situ* O_2 separation in the plasma-membrane reactor. Reprinted with permission from Ref. [208], copyright 2022, Elsevier.

by enhancing separation or enabling operation under milder conditions. For example, Zheng et al. [208] studied oxygen permeation in a plasma-membrane reactor composed of an oxygen-permeable membrane ($La_{0.6}Sr_{0.4}Co_{0.2}Fe_{0.8}O_{3-\delta}$) and a DBD plasma. The proposed permeation mechanism, shown in Fig. 19(c), demonstrated the role of plasma in activating O_2, which enhanced the dissociation of O_2 and the ionization of O that reached the membrane surface, facilitating permeation. Their results showed a remarkable 30-fold increase in oxygen flux at 600 °C with the application of plasma with 15 W power. Since high temperatures are favorable for the optimal performance of perovskite membranes, it may be beneficial to consider the use of warm plasma in this context. A study conducted by Chen et al. [209] implemented microwave plasma in combination with an $La_{0.6}Ca_{0.4}Co_{0.2}Fe_{0.8}O_{3-\delta}$ hollow fiber membrane, achieving an oxygen permeation rate of up to 4 $mL \cdot min^{-1} \cdot cm^{-2}$). The membrane also demonstrated excellent chemical resistance toward CO_2 and CO_2 plasma. Such a dual-function membrane reactor represents a novel approach, with several promising research directions worth exploring, including membrane material development and plasma–membrane reactor design [210].

In summary, the development of novel plasma-material systems presents exciting opportunities for process intensification and integration. However, further studies are essential to understand the interaction mechanisms, design or select optimal combinations of materials and plasma, and develop tailored materials or plasma reactors for such applications. Additionally, the operation of these systems and their experimental methodologies may need to be adapted. For instance, plasma-sorbent systems often employ cyclic operations involving adsorption and desorption steps, which differ from the continuous operations commonly used in plasma-based gas conversion studies. Furthermore, plasma–membrane systems often require careful coupling of operating conditions, as optimal temperature and pressure differences across the membrane are typically necessary for effective permeation. This may necessitate operating the plasma under modified conditions to ensure compatibility with membrane performance requirements.

4.3 Process level considerations

Research on the process development of non-thermal plasma technology for the conversion of N_2, CO_2, and CH_4 remains relatively scarce, primarily due to the low TRL of this field. Naturally, there is significant uncertainty which needs to be clarified for process development. However, process-level consideration at this stage could provide a critical understanding of the requirements and guide further research toward practical applications. In our previous work, several critical gaps were identified in the process development required to transition this technology from laboratory research to industrial implementation [211]. A key point that needs attention is the unique characteristics of plasma technology, which must be factored into process design

and conceptualization. For instance, in the discussion of centralized versus modular process concepts, plasma technology could offer distinct advantages for modular systems. Its inherent flexibility and compatibility with distributed renewable electricity make it particularly suitable for decentralized set-ups. This contrasts with the centralized processes commonly used in conventional chemical production, offering an opportunity for innovative deployment in distributed systems. Similarly, the integration of plasma reactors with other process units requires careful consideration of plasma technology's unique operational features. A widely touted advantage of plasma reactors is their instant response to intermittent renewable electricity, enabling dynamic operation with "turnkey" functionality. However, other process units that work with plasma reactors may not operate as efficiently under such fluctuating conditions. This discrepancy necessitates special attention to ensure compatibility and efficiency in the overall process design.

4.3.1 Scaling up of the non-thermal plasma system

Scaling up is a critical step in advancing the TRL of plasma technology. For thermal plasma reactors, upscaling is relatively straightforward and can be achieved through sizing up the reactor. This is largely due to the ionization-overheating stability of thermal plasmas, which remain stable despite fluctuations in temperature, density, and the reduced electric field [212]. However, in non-thermal plasma reactors, the instability of plasma properties becomes a limiting factor, particularly in terms of power density and pressure conditions. As a result, the numbering-up approach, which involves deploying multiple reactors in parallel, is often more suitable.

Nonetheless, even with numbering-up, laboratory-scale reactors (typically with discharge gaps in the millimeter range or a few centimeters) need to be scaled to a larger size (e.g., tens of centimeters) before considering parallel operation. Practical examples of scaling up plasma reactors for environmental and energy applications have been reviewed in the work of Okubo [213]. Industrial ozone production, which employs hundreds of DBD reactor tubes operating in parallel, is frequently cited as a classic example of scaling up non-thermal plasma reactors. However, while this provides a useful reference, the energy efficiency of DBD reactors remains generally too low for CO_2, N_2 and CH_4 conversions, hence significant improvement is required before upscaling.

On the other hand, warm plasma reactors, such as GA systems, exhibit favorable energy efficiency and robustness, making them strong candidates for industrial applications. The transitional nature of warm plasmas, which exhibit characteristics of both thermal and non-thermal plasmas, presents unique opportunities and challenges for scaling up. Specifically, achieving high energy efficiency in warm plasma reactors hinges on maintaining operation within the "warm" plasma regime, as transitioning to the thermal regime often results in reduced performance. Additionally, the heat management required for thermal plasmas—such as active cooling—can increase maintenance requirements and overall costs. Therefore, retaining the warm plasma regime during scale-up is crucial. Directly increasing the size and power input of GA reactors can inadvertently push the system into the thermal plasma regime, requiring careful attention during the scaling-up process. Rabinovich et al. [212] demonstrated the scaling-up of a GA reactor operating at a power level of 2–3 kW. Their analysis indicated maximum current and power per unit length for non-equilibrium GAs at 1–2 A and 0.15 $kW \cdot cm^{-1}$, respectively. Furthermore, their findings suggested a physical limit, with the maximum expected power per unit length at approximately 0.5 $kW \cdot cm^{-1}$—nearly 20 times lower than for thermal arc discharges. Tsonev et al. [214] investigated the geometric effects on scaling up GA reactors for nitrogen fixation. Their study compared two reactors with different sizes but identical pin-to-pin configurations. Results showed that increasing reactor size and flow rate without proportionally increasing plasma volume significantly reduced reactor performance. This issue stems from the contracted nature of plasma discharges, which limits the gas flow's interaction with plasma, thereby diminishing overall efficiency. To address this, the authors implemented a torch configuration, which created a longer plasma volume and enhanced gas flow coverage. This design achieved higher production rates and reduced energy consumption compared to the pin-to-pin configuration, underscoring the importance of reactor design in scaling-up efforts.

When scaling beyond the limitations of size increases, the numbering-up approach becomes essential for systems such as GA reactors. O'Modhrain et al. demonstrated the parallelization of GA plasmatron reactors housed within a single unit, as in Fig. 20(a) [215]. Their design preserved the performance observed at the laboratory scale with a single reactor while significantly increasing CO_2 conversion rates, demonstrating the feasibility of numbering up. Further improvements can be achieved by increasing the number of reactors and the flow rate while maintaining optimal SEI.

For multi-reactor systems, the connection strategy of individual reactors is critical to overall performance. Van Raak et al. [216] investigated series and parallel connection methods (as shown in Fig. 20(b)) in their study on NO_x synthesis. Their results showed that the series connection of two reactors enhanced both NO_x production and energy efficiency compared to other configurations, including parallel reactor connections and a single reactor with a doubled discharge gap. This enhancement was attributed to longer residence times, altered discharge behavior, and only a moderate increase in power.

The power supply system is a crucial component of numbering-up strategies for plasma reactors. Van Raak et al.'s study [216] utilized reactors electrically connected in series and powered by a single power PSU. However, because GA reactors behave as dynamic loads, their interconnected operation affects discharge characteristics and increases the complexity of the overall electrical system. This is reflected by the different voltage and current characteristics observed as shown in Fig. 20(c). By contrast, O'Modhrain et al. [215] employed individual PSUs for each reactor in their numbering-up approach. The authors believe this strategy avoided issues such as power division in centralized PSUs and allowed for optimized individual PSU performance, leading to cost advantages over centralized systems, where a single, larger PSU distributes power to all reactors. To further scale plasma systems to power outputs ranging from hundreds of kilowatts to megawatts, future research should also focus on optimizing PSU designs for stability, durability, and safety. Moreover, it needs to be noted that the cost of power supplies is often a significant factor influencing the capital expenditure of the entire system and, ultimately, the economic feasibility of plasma processes. Hence, cost-efficiency is a key consideration in

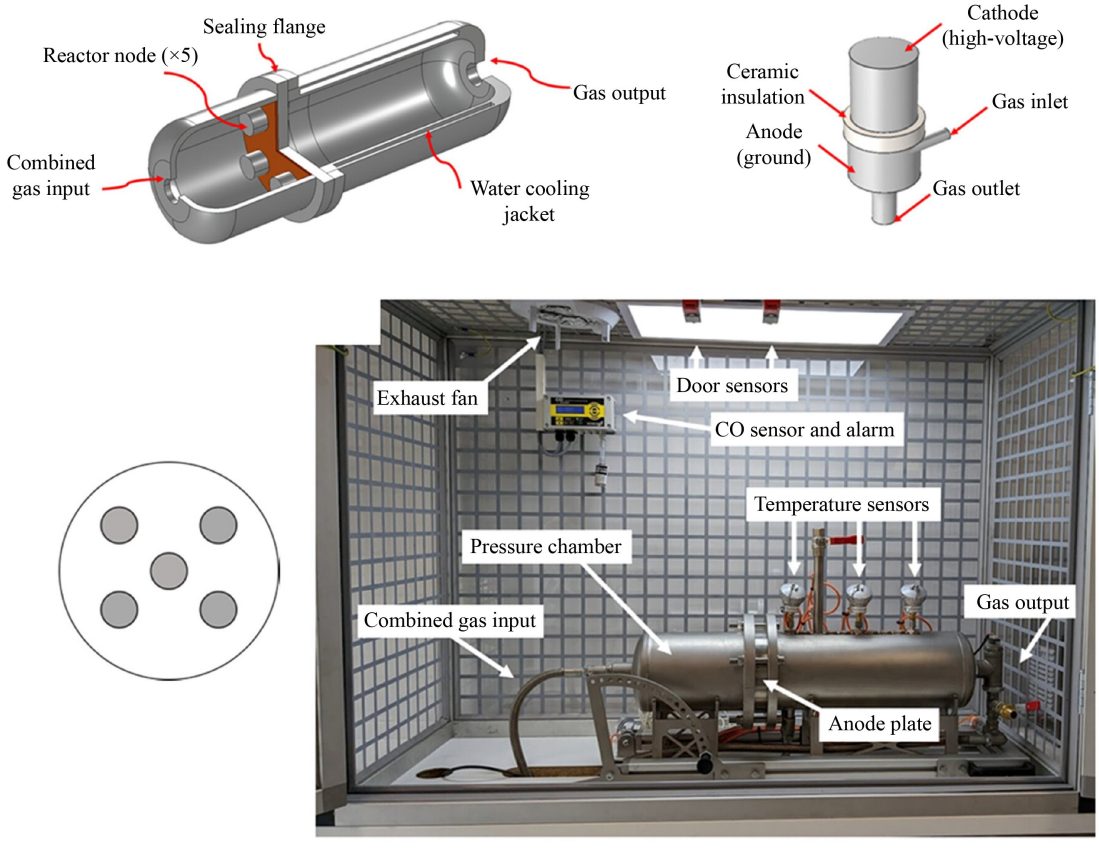

(a)

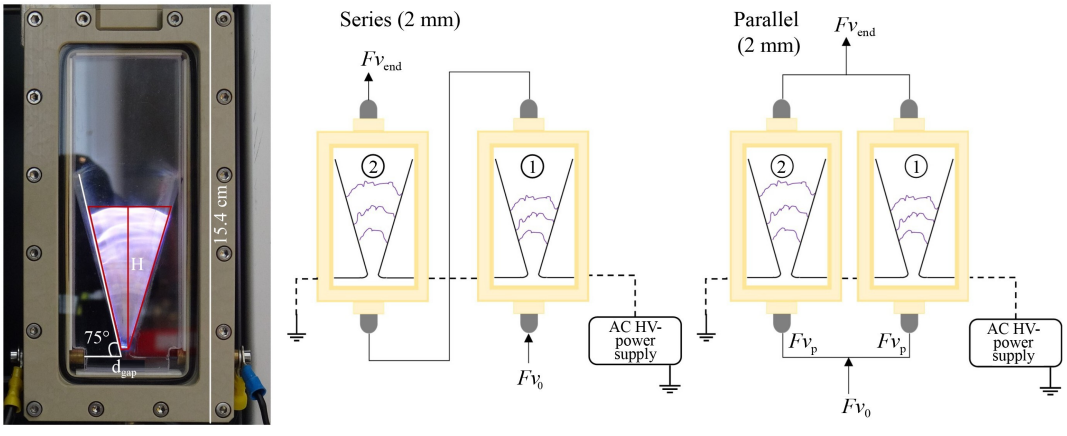

(b)

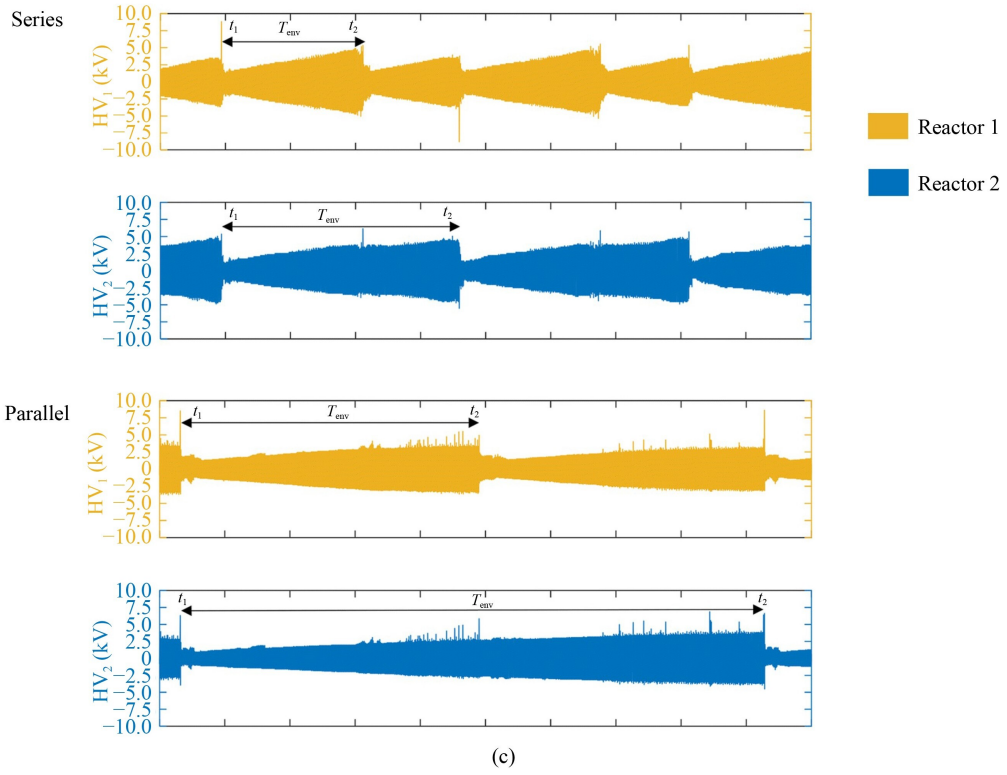

Fig. 20 (a) Multi-reactor GA plasmatron reported by O'Modhrain et al. Reprinted with permission from Ref. [215], copyright 2024, American Chemical Society. (b) Series and parallel connection of GA reactor and (c) the corresponding voltage waveforms. Reprinted with permission from Ref. [216], copyright 2024, Royal Society of Chemistry.

the design of the PSU.

4.3.2 Process evaluation

Apart from technological development, another significant challenge is understanding the economic feasibility and environmental impact of plasma-based processes. To address this, TEA and life cycle assessment (LCA) are crucial for evaluating the potential of plasma technologies. Currently, there are limited publications on the TEA and LCA of plasma processes, mainly due to the low technological maturity and the scarcity of data for comprehensive analysis. Nevertheless, perspective assessments can guide the advancement of plasma technology in its early stages and assist in the practical development and optimization of plasma processes. This includes three major benefits of such assessments:

(1) Establishing performance targets: By comparing plasma technologies with conventional methods or other innovative approaches, a clear understanding of the current status of plasma-based processes can be developed. This comparison helps define technological performance targets for future research. For example, Winter et al. [217] analyzed the economic and environmental competitiveness of plasma-assisted ammonia synthesis. They found that for modular ammonia production powered by renewable energy, plasma processes would need a 6-fold improvement in energy efficiency to become competitive. Furthermore, they highlighted that if hydrogen (H_2) is produced via steam methane reforming and powered by natural gas, the plasma process would emit more CO_2 than the Haber-Bosch process unless its energy efficiency improves by a factor of 28.5.

(2) Understanding process integration: Exploring potential process designs provides valuable insights into the overall plasma process, particularly its integration with other process units. Van Rooij et al. [218] evaluated a microwave plasma process for CO production from CO_2, integrating CO_2 removal, recycling via the Benfield process, and purification through pressure swing adsorption. Their analysis showed that separation costs were the dominant expense, underscoring the need for better plasma conversion efficiency to reduce costs. Similarly, Kaufmann et al. [219] studied power-to-liquid plants that integrate plasma CO_2 splitting with oxygen separation through gas diffusion electrodes (GDE), along with hydrogen production and Fischer-Tropsch synthesis. Their study found that GDE performance significantly impacted production costs, accounting for 30%–70% of capital expenditures. Both studies emphasize the importance of a holistic view and process integration for plasma-based processes.

(3) Identifying viable application scenarios: Assessing different application scenarios helps identify the windows of opportunity for deploying plasma-based processes. For

example, Delikonstantis et al. [220] conducted a study on plasma-assisted ethylene production from methane. Their analysis indicated that under current industrial electricity prices (ranging from 50 to 120 USD·MWh^{-1}), the process was not economically viable. To achieve break-even, electricity prices would need to drop to 23–35 USD·MWh^{-1}.

In summary, the exploration of plasma-based chemical production continues to uncover new opportunities and challenges. The success of this technology hinges on bridging existing knowledge gaps, responsibly leveraging advanced methodologies, and designing processes that align with industrial and environmental demands. Future research is expected to focus on these critical areas, striving for higher energy efficiency and yield while facilitating the transition from laboratory-scale innovations to impactful industrial solutions

Acknowledgements The authors gratefully acknowledge the support of the PLACHEM project and the sponsorship provided by Casale. Special thanks are extended to Ludovica Villantieri, Pierdomenico Biasi, Chris Emmery and Daniel Emmery for their assistance.

Competing interests The authors declare that they have no competing interests.

References

1. Kim H H, Teramoto Y, Ogata A, Takagi H, Nanba T. Plasma catalysis for environmental treatment and energy applications. Plasma Chemistry and Plasma Processing, 2016, 36(1): 45–72
2. Bogaerts A, Centi G. Plasma technology for CO_2 conversion: a personal perspective on prospects and gaps. Frontiers in Energy Research, 2020, 8: 1–23
3. George A, Shen B, Craven M, Wang Y, Kang D, Wu C, Tu X. A review of non-thermal plasma technology: a novel solution for CO_2 conversion and utilization. Renewable & Sustainable Energy Reviews, 2021, 135: 109702
4. Chen G, Snyders R, Britun N. CO_2 conversion using catalyst-free and catalyst-assisted plasma-processes: recent progress and understanding. Journal of CO_2 Utilization, 2021, 49: 101557
5. Xu S, Chen H, Hardacre C, Fan X. Non-thermal plasma catalysis for CO_2 conversion and catalyst design for the process. Journal of Physics D: Applied Physics, 2021, 54(23): 233001
6. Anoop N, Sundaramurthy S, Jha J M, Chandrabalan S, Singh N, Verma J, Parvatalu D, Katti S. Plasma catalysis: a feasible solution for carbon dioxide valorization? Clean Technologies and Environmental Policy, 2021, 23(10): 2789–2811
7. Salden A, Budde M, Garcia-Soto C A, Biondo O, Barauna J, Faedda M, Musig B, Fromentin C, Nguyen-Quang M, Philpott H, et al. Meta-analysis of CO_2 conversion, energy efficiency, and other performance data of plasma-catalysis reactors with the open access PIONEER database. Journal of Energy Chemistry, 2023, 86: 318–342
8. Ullah S, Gao Y, Dou L, Liu Y, Shao T, Yang Y, Murphy A B. Recent trends in plasma-assisted CO_2 methanation: a critical review of recent studies. Plasma Chemistry and Plasma Processing, 2023, 43(6): 1335–1383
9. Chen X, Kim H H, Nozaki T. Plasma catalytic technology for CH_4 and CO_2 conversion: a review highlighting fluidized-bed plasma reactor. Plasma Processes and Polymers, 2023, 21(1): 2200207
10. Bogaerts A, Tu X, Nozaki T. Plasma-Based CO_2 Conversion. In: Zhang G, Bogaerts A, Ye J, Liu C, eds. Advances in CO_2 Utilization. Singapore: Springer, 2024, 209–243
11. Maitre P A, Bieniek M S, Kechagiopoulos P N. Plasma-enhanced catalysis for the upgrading of methane: a review of modelling and simulation methods. Reaction Chemistry & Engineering, 2020, 5(5): 814–837
12. Li S, Ahmed R, Yi Y, Bogaerts A. Methane to methanol through heterogeneous catalysis and plasma catalysis. Catalysts, 2021, 11(5): 590
13. Maslova V, Nastase R, Veryasov G, Nesterenko N, Fourré E, Batiot-Dupeyrat C. Current status and challenges of plasma and plasma-catalysis for methane coupling: a review. Progress in Energy and Combustion Science, 2024, 101(1): 101096
14. Wang N, Otor H O, Rivera-Castro G, Hicks J C. Plasma catalysis for hydrogen production: a bright future for decarbonization. ACS Catalysis, 2024, 14(9): 6749–6798
15. Baig S, Sajjadi B. Non-thermal plasma enhanced catalytic conversion of methane into value added chemicals and fuels. Journal of Energy Chemistry, 2024, 97: 265–301
16. Rouwenhorst K H R, Engelmann Y, van 't Veer K, Postma R S, Bogaerts A, Lefferts L. Plasma-driven catalysis: green ammonia synthesis with intermittent electricity. Green Chemistry, 2020, 22(19): 6258–6287
17. Zhou D, Zhou R, Zhou R, Liu B, Zhang T, Xian Y, Cullen P J, Lu X, Ostrikov K. Sustainable ammonia production by non-thermal plasmas: status, mechanisms, and opportunities. Chemical Engineering Journal, 2021, 421(P1): 129544
18. Zeng X, Zhang S, Hu X, Zhang C, Ostrikov K, Shao T. Recent advances in plasma-enabled ammonia synthesis: state-of-the-art, challenges, and outlook. Faraday Discussions, 2023, 243: 473–491
19. Rouwenhorst K H R, Jardali F, Bogaerts A, Lefferts L. From the Birkeland-Eyde process towards energy-efficient plasma-based NO_x synthesis: a techno-economic analysis. Energy & Environmental Science, 2021, 14(5): 2520–2534
20. Abdelaziz A A, Komuro A, Teramoto Y, Schiorlin M, Kim D Y, Nozaki T, Kim H H. Atmospheric-pressure plasmas for NO_x production: short review on current status. Current Opinion in

Green and Sustainable Chemistry, 2024, 50: 100977
21. Zhang Y, Niu J, Chen S, Chen Y, Chen H, Fan X. Ammonia synthesis by nonthermal plasma catalysis: a review on recent research progress. Journal of Physics D: Applied Physics, 2024, 57(32): 323001
22. Bogaerts A, Tu X, Whitehead J C, Centi G, Lefferts L, Guaitella O, Azzolina-Jury F, Kim H H, Murphy A B, Schneider W F, et al. The 2020 plasma catalysis roadmap. Journal of Physics D: Applied Physics, 2020, 53(443001)
23. Biset-Peiró M, Mey R, Guilera J, Andreu T. Adiabatic plasma-catalytic reactor configuration: energy efficiency enhancement by plasma and thermal synergies on CO_2 methanation. Chemical Engineering Journal, 2020, 393: 124786
24. Wang L, Yi Y, Guo H, Tu X. Atmospheric pressure and room temperature synthesis of methanol through plasma-catalytic hydrogenation of CO_2. ACS Catalysis, 2018, 8(1): 90–100
25. Lisi N, Pasqual Laverdura U, Chierchia R, Luisetto I, Stendardo S. A water cooled, high power, dielectric barrier discharge reactor for CO_2 plasma dissociation and valorization studies. Scientific Reports, 2023, 13(1): 1–12
26. De la Fuente J F, Moreno S H, Stankiewicz A I, Stefanidis G D. On the improvement of chemical conversion in a surface-wave microwave plasma reactor for CO_2 reduction with hydrogen (The Reverse Water-Gas Shift reaction). International Journal of Hydrogen Energy, 2017, 42(18): 12943–12955
27. Mohsenian S, Nagassou D, Elahi R, Yu P, Nallar M, Wong H-W, Trelles J P. Carbon dioxide conversion by solar-enhanced microwave plasma: effect of specific power and argon/nitrogen carrier gases. Journal of CO_2 Utilization, 2019, 34: 725–732
28. Ivanov V, Paunska T, Lazarova S, Bogaerts A, Kolev S. Gliding arc/glow discharge for CO_2 conversion: comparing the performance of different discharge configurations. Journal of CO_2 Utilization, 2023, 67: 102300
29. Paulussen S, Verheyde B, Tu X, De Bie C, Martens T, Petrovic D, Bogaerts A, Sels B. Conversion of carbon dioxide to value-added chemicals in atmospheric pressure dielectric barrier discharges. Plasma Sources Science & Technology, 2010, 19(3): 034015
30. Fridman A, Chirokov A, Gutsol A. Non-thermal atmospheric pressure discharges. Journal of Physics D: Applied Physics, 2005, 38(2): R1–R24
31. Conrads H, Schmidt M. Plasma sources science and technology plasma generation and plasma sources related content plasma generation and plasma sources. Plasma Sources Science & Technology, 2000, 9(4): 441–454
32. Kołek J, Hołub M. Practical design of a high-voltage pulsed power supply implementing SiC technology for atmospheric pressure plasma reactors. Applied Sciences (Basel, Switzerland), 2019, 9(7): 1451
33. Stryczewska H D. Supply systems of non-thermal plasma reactors. Construction review with examples of applications. Applied Sciences (Basel, Switzerland), 2020, 10(9): 3242
34. Stryczewska H D, Jakubowski T, Kalisiak S, Gizewski T, Pawlat J. Power systems of plasma reactors for non-thermal plasma generation. Journal of Advanced Oxidation Technologies, 2013, 16(1): 52–62
35. Ray D, Saha R, Ch S. DBD plasma assisted CO_2 decomposition: influence of diluent gases. Catalysts, 2017, 7(9): 244
36. Rutberg P G, Nakonechny G V, Pavlov A V, Popov S D, Serba E O, Surov A V. AC plasma torch with a $H_2O/CO_2/CH_4$ mix as the working gas for methane reforming. Journal of Physics D: Applied Physics, 2015, 48(24): 245204
37. Kim S C, Chun Y N. Development of a gliding arc plasma reactor for CO_2 destruction. Environmental Technology, 2014, 35(23): 2940–2946
38. Shao T, Wang R, Zhang C, Yan P. Atmospheric-pressure pulsed discharges and plasmas: mechanism, characteristics and applications. High Voltage, 2018, 3(1): 14–20
39. Huiskamp T. Nanosecond pulsed streamer discharges Part I: generation, source-plasma interaction and energy-efficiency optimization. Plasma Sources Science & Technology, 2020, 29(2): 023002
40. Montesano C, Quercetti S, Martini L M, Dilecce G, Tosi P. The effect of different pulse patterns on the plasma reduction of CO_2 for a nanosecond discharge. Journal of CO_2 Utilization, 2020, 39: 101157
41. Montesano C, Salden T P W, Martini L M, Dilecce G, Tosi P. CO_2 reduction by nanosecond-plasma discharges: revealing the dissociation's time scale and the importance of pulse sequence. Journal of Physical Chemistry C, 2023, 127(21): 10045–10050
42. Komarzyniec G, Stryczewska H D, Krupski P. The Influence of the architecture of the power system on the operational parameters of the glidarc plasma reactor. IEEE International Pulsed Power & Plasma Science, 2019
43. Cheng J, Ding W, Zi Y, Lu Y, Ji L, Liu F, Wu C, Wang Z L. Triboelectric microplasma powered by mechanical stimuli. Nature Communications, 2018, 9(1): 3733
44. Liu F, Liu Y, Lu Y, Wang Z, Shi Y, Ji L, Cheng J. Electrical analysis of triboelectric nanogenerator for high voltage applications exampled by DBD microplasma. Nano Energy, 2019, 56: 482–493
45. Wong M C, Xu W, Hao J. Microplasma-discharge-based nitrogen fixation driven by triboelectric nanogenerator toward self-powered mechano-nitrogenous fertilizer supplier. Advanced Functional Materials, 2019, 29(44): 1904090
46. Han K, Luo J, Feng Y, Xu L, Tang W, Wang Z L. Self-powered electrocatalytic ammonia synthesis directly from air as driven by dual triboelectric nanogenerators. Energy & Environmental Science, 2020, 13(8): 2450–2458
47. Li S, Zhang B, Gu G, Xiang X, Zhang W, Shi X, Zhao K, Zhu Y, Guo J, Cui P, et al. Triboelectric plasma decomposition of CO_2 at room temperature driven by mechanical energy. Nano Energy, 2021, 88: 106287
48. Zhang B, Ru Q, Liu L, Wang J, Zhang Y, Zhao K, Gu G, Xiang X, Li S, Zhu Y, et al. Overcoming energy mismatch of metal oxide semiconductor catalysts for CO_2 reduction with triboelectric plasma. Journal of Catalysis, 2023, 419: 1–8
49. Wanten B, Vertongen R, De Meyer R, Bogaerts A. Plasma-based CO_2 conversion: how to correctly analyze the performance? Journal of Energy Chemistry, 2023, 86: 180–196
50. Snoeckx R, Bogaerts A. Plasma technology-a novel solution for CO_2 conversion? Chemical Society Reviews, 2017, 46(19):

5805–5863
51. Bogaerts A, Neyts E, Gijbels R, van der Mullen J. Gas discharge plasmas and their applications. Spectrochimica Acta, Part B: Atomic Spectroscopy, 2002, 57(4): 609–658
52. Siemens W. Ueber die elektrostatische induction und die Verzögerung des stroms in Flaschendrähten. Annalen der Physik, 1857, 178(9): 66–122
53. Brandenburg R. Dielectric barrier discharges: progress on plasma sources and on the understanding of regimes and single filaments. Plasma Sources Science & Technology, 2017, 26(5): 53001
54. Wu P, Li X, Ullah N, Li Z. Synergistic effect of catalyst and plasma on CO_2 decomposition in a dielectric barrier discharge plasma reactor. Molecular Catalysis, 2021, 499: 111304
55. Belov I, Paulussen S, Bogaerts A. Appearance of a conductive carbonaceous coating in a CO_2 dielectric barrier discharge and its influence on the electrical properties and the conversion efficiency. Plasma Sources Science & Technology, 2016, 25(1): 015023
56. Wang B, Wang X, Zhang B. Dielectric barrier micro-plasma reactor with segmented outer electrode for decomposition of pure CO_2. Frontiers of Chemical Science and Engineering, 2020, 15(3): 687–697
57. Niu G, Qin Y, Li W, Duan Y. Investigation of CO_2 splitting process under atmospheric pressure using multi-electrode cylindrical DBD plasma reactor. Plasma Chemistry and Plasma Processing, 2019, 39(4): 809–824
58. Almazova K I, Belonogov A N, Borovkov V V, Gorelov E V, Dubinov A E, Klyushin D S, Morozov I V. Dynamics of gliding arc climbing in a unipolar Jacob's ladder. Technical Physics, 2020, 65(7): 1032–1035
59. Liu J, Wang X, Li X, Likozar B, Zhu A. CO_2 conversion, utilisation and valorisation in gliding arc plasma. Journal of Physics D: Applied Physics, 2020, 53(25): 253001
60. Fridman A, Nester S, Kennedy L A, Saveliev A, Mutaf-Yardimci O. Gliding arc gas discharge. Progress in Energy and Combustion Science, 1999, 25(2): 211–231
61. Sun H, Chen Z, Chen J, Long H, Wu Y, Zhou W. The influence of back-breakdown on the CO_2 conversion in gliding arc plasma: based on experiments of different materials and improved structures. Journal of Physics D: Applied Physics, 2021, 54(49): 495203
62. Li L, Zhang H, Li X, Kong X, Xu R, Tay K, Tu X. Plasma-assisted CO_2 conversion in a gliding arc discharge: improving performance by optimizing the reactor design. Journal of CO_2 Utilization, 2019, 29: 296–303
63. Li LL, Zhang H, Li X, Huang J, Kong X, Xu R, Tu X. Magnetically enhanced gliding arc discharge for CO_2 activation. Journal of CO_2 Utilization, 2020, 35: 28–37
64. Chen Z, Sun H, Wu W, Chen B, Wu Y, Jiang X, Guo Y. Better CO_2 utilization under comprehensive control of airflow and electromagnetic field. Physica Scripta, 2023, 98(9): 095605
65. Zhao T L, Liu J L, Li X S, Liu J B, Song Y H, Xu Y, Zhu A M. Temporal evolution characteristics of an annular-mode gliding arc discharge in a vortex flow. Physics of Plasmas, 2014, 21(5): 053507
66. Vertongen R, Bogaerts A. How important is reactor design for CO_2 conversion in warm plasmas? Journal of CO_2 Utilization, 2023, 72: 102510
67. Trenchev G, Bogaerts A. Dual-vortex plasmatron: a novel plasma source for CO_2 conversion. Journal of CO_2 Utilization, 2020, 39: 101152
68. Bromberg L, Cohn D R, Rabinovich A. Plasma reformer-fuel cell system for decentralized power applications. International Journal of Hydrogen Energy, 1997, 22(1): 83–94
69. Bromberg L, Cohn D R, Rabinovich A, Heywood J. Emissions reductions using hydrogen from plasmatron fuel converters. International Journal of Hydrogen Energy, 2001, 26(10): 1115–1121
70. Kalra C S, Gutsol A F, Fridman A A. Gliding arc discharges as a source of intermediate plasma for methane partial oxidation. IEEE Transacation on Plasma Science, 2005, 33(1 I): 32–41
71. Nunnally T, Gutsol K, Rabinovich A, Fridman A, Gutsol A, Kemoun A. Dissociation of CO_2 in a low current gliding arc plasmatron. Journal of Physics D: Applied Physics, 2011, 44(27): 274009
72. Liu J L, Li X S, Liu J L, Zhu A M. Insight into gliding arc (GA) plasma reduction of CO_2 with H_2: GA characteristics and reaction mechanism. Journal of Physics D: Applied Physics, 2019, 52(28): 284001
73. Liu J, Zhu X, Li X, Li K, Shi C, Zhu A. Effect of O_2/CH_4 ratio on the optimal specific-energy-input (SEI) for oxidative reforming of biogas in a plasma-shade reactor. Journal of Energy Chemistry, 2013, 22(5): 681–684
74. Lee D H, Kim K T, Kang H S, Jo S, Song Y H. Optimization of NH_3 decomposition by control of discharge mode in a rotating arc. Plasma Chemistry and Plasma Processing, 2014, 34(1): 111–124
75. Ramakers M, Medrano J A, Trenchev G, Gallucci F, Bogaerts A. Revealing the arc dynamics in a gliding arc plasmatron: a better insight to improve CO_2 conversion. Plasma Sources Science & Technology, 2017, 26(12): 125002
76. Dinh D K, Trenchev G, Lee D H, Bogaerts A. Arc plasma reactor modification for enhancing performance of dry reforming of methane. Journal of CO_2 Utilization, 2020, 42: 101352
77. Kwon H, Kim T, Song S. Dry reforming of methane in a rotating gliding arc plasma: improving efficiency and syngas cost by quenching product gas. Journal of CO_2 Utilization, 2023, 70: 102448
78. Nagassou D, Mohsenian S, Bhatta S, Elahi R, Trelles J P. Solar-gliding arc plasma reactor for carbon dioxide decomposition: design and characterization. Solar Energy, 2019, 180: 678–689
79. Lebedev Y A. Microwave discharges: generation and diagnostics. Journal of Physics: Conference Series, 2010, 257: 012016
80. Chen G, Britun N, Godfroid T, Georgieva V, Snyders R, Delplancke-Ogletree M P. An overview of CO_2 conversion in a microwave discharge: the role of plasma-catalysis. Journal of Physics D: Applied Physics, 2017, 50(8): 084001
81. Qin Y, Niu G, Wang X, Luo D, Duan Y. Status of CO_2 conversion using microwave plasma. Journal of CO_2 Utilization,

2018, 28: 283–291
82. Vermeiren V, Bogaerts A. Plasma-based CO_2 conversion: to quench or not to quench? Journal of Physical Chemistry C, 2020, 124(34): 18401–18415
83. Li J, Zhang X, Shen J, Ran T, Chen P, Yin Y. Dissociation of CO_2 by thermal plasma with contracting nozzle quenching. Journal of CO_2 Utilization, 2017, 21: 72–76
84. Hecimovic A, D'Isa F A, Carbone E, Fantz U. Enhancement of CO_2 conversion in microwave plasmas using a nozzle in the effluent. Journal of CO_2 Utilization, 2022, 57: 101870
85. Mercer E R, Van Alphen S, van Deursen C F A M, Righart T W H, Bongers W A, Snyders R, Bogaerts A, van de Sanden M C M, Peeters F J J. Post-plasma quenching to improve conversion and energy efficiency in a CO_2 microwave plasma. Fuel, 2023, 334(P2): 126734
86. Carreon M L. Plasma catalysis: a brief tutorial. Plasma Research Express, 2019, 1(4): 043001
87. Babaeva N Y, Naidis G V. On the efficiency of CO_2 conversion in corona and dielectric-barrier discharges. Plasma Sources Science & Technology, 2021, 30(3): 03LT03
88. Mierczyński P, Mierczynska-Vasilev A, Szynkowska-Jóźwik M I, Ostrikov K, Vasilev K. (Ken), Vasilev K. Plasma-assisted catalysis for CH_4 and CO_2 conversion. Catalysis Communications, 2023, 180: 106709
89. Moshrefi M M, Rashidi F, Bozorgzadeh H R, Ehtemam Haghighi M. Dry reforming of methane by DC spark discharge with a rotating electrode. Plasma Chemistry and Plasma Processing, 2013, 33(2): 453–466
90. Lašič Jurković D, Liu J L, Pohar A, Likozar B. Methane dry reforming over Ni/Al_2O_3 catalyst in spark plasma reactor: linking computational fluid dynamics (CFD) with reaction kinetic modelling. Catalysis Today, 2021, 362: 11–21
91. Ma T, Wang H X, Shi Q, Li S N, Sun S R, Murphy A B. Experimental study of CO_2 decomposition in a DC micro-slit sustained glow discharge reactor. Plasma Chemistry and Plasma Processing, 2019, 39(4): 825–844
92. Dębek R, Azzolina-Jury F, Travert A, Maugé F, Thibault-Starzyk F. Low-pressure glow discharge plasma-assisted catalytic CO_2 hydrogenation—the effect of metal oxide support on the performance of the Ni-based catalyst. Catalysis Today, 2019, 337: 182–194
93. Renninger S, Lambarth M, Birke K P. High efficiency CO_2-splitting in atmospheric pressure glow discharge. Journal of CO_2 Utilization, 2020, 42: 101322
94. Wanten B, Maerivoet S, Vantomme C, Slaets J, Trenchev G, Bogaerts A. Dry reforming of methane in an atmospheric pressure glow discharge: confining the plasma to expand the performance. Journal of CO_2 Utilization, 2022, 56: 101869
95. Trenchev G, Nikiforov A, Wang W, Kolev S, Bogaerts A. Atmospheric pressure glow discharge for CO_2 conversion: model-based exploration of the optimum reactor configuration. Chemical Engineering Journal, 2019, 362: 830–841
96. Meng G, Xia L, Cheng Y, Yin Z. AC-driven atmospheric pressure glow discharge co-improves conversion and energy efficiency of CO_2 splitting. Journal of CO_2 Utilization, 2023, 70: 102447
97. Chen G, Wang L, Godfroid T, Snyders R. Progress in plasma-assisted catalysis for carbon dioxide reduction. In: Plasma Chemistry and Gas Conversion. 2018
98. Zhu F, Zhang H, Yan X, Yan J, Ni M, Li X, Tu X. Plasma-catalytic reforming of CO_2-rich biogas over $Ni/\Gamma\text{-}Al_2O_3$ catalysts in a rotating gliding arc reactor. Fuel, 2017, 199: 430–437
99. Chun S, Shin D, Ma S, Yang G, Hong Y. CO_2 microwave plasma-catalytic reactor for efficient reforming of methane to syngas. Catalysts, 2019, 9(3): 1–18
100. Renninger S, Rößner P, Stein J, Lambarth M, Birke K P. Towards high efficiency CO_2 utilization by glow discharge plasma. Processes, 2021, 9(11): 4–9
101. Zhang H, Li L, Xu R, Huang J, Wang N, Li X, Tu X. Plasma-enhanced catalytic activation of CO_2 in a modified gliding arc reactor. Waste Disposal & Sustainable Energy, 2020, 2(2): 139–150
102. Mizuno A, Craven M. Plasma Catalysis Systems. In: Tu X, Whitehead J, Nozaki T, eds. Plasma Catalysis. Springer Series on Atomic, Optical, and Plasma Physics. Berlin: Springer, 2019, 21–46
103. Michielsen I, Uytdenhouwen Y, Pype J, Michielsen B, Mertens J, Reniers F, Meynen V, Bogaerts A. CO_2 dissociation in a packed bed DBD reactor: first steps towards a better understanding of plasma catalysis. Chemical Engineering Journal, 2017, 326: 477–488
104. Butterworth T, Elder R, Allen R. Effects of particle size on CO_2 reduction and discharge characteristics in a packed bed plasma reactor. Chemical Engineering Journal, 2016, 293: 55–67
105. Uytdenhouwen Y, van Alphen S, Michielsen I, Meynen V, Cool P, Bogaerts A. A packed-bed DBD micro plasma reactor for CO_2 dissociation: does size matter? Chemical Engineering Journal, 2018, 348: 557–568
106. Van Laer K, Bogaerts A. How bead size and dielectric constant affect the plasma behaviour in a packed bed plasma reactor: a modelling study. Plasma Sources Science & Technology, 2017, 26(8): 085007
107. Tu X, Whitehead J C. Plasma-catalytic dry reforming of methane in an atmospheric dielectric barrier discharge: understanding the synergistic effect at low temperature. Applied Catalysis B: Environmental, 2012, 125: 439–448
108. Gadkari S, Tu X, Gu S. Fluid model for a partially packed dielectric barrier discharge plasma reactor. Physics of Plasmas, 2017, 24(9): 093510
109. Wang J, AlQahtani M S, Wang X, Knecht S D, Bilén S G, Song C, Chu W. One-step plasma-enabled catalytic carbon dioxide hydrogenation to higher hydrocarbons: significance of catalyst-bed configuration. Green Chemistry, 2021, 23(4): 1642–1647
110. Kim H H, Abdelaziz A A, Teramoto Y, Nozaki T, Hensel K, Mok Y S, et al. Interim report of plasma catalysis: footprints in the past and blueprints for the future. International Journal of Plasma Environmental Science and Technology, 2021, 15: 1–39
111. Oda T, Takahashi T, Kohzuma S. Decomposition of dilute trichloroethylene by using nonthermal plasma processing-frequency and catalyst effects. IEEE Transactions on Industry Applications, 2001, 37(4): 965–970
112. Nguyen D B, Shirjana S, Hossain M M, Heo I, Mok Y S.

Effective generation of atmospheric pressure plasma in a sandwich-type honeycomb monolith reactor by humidity control. Chemical Engineering Journal, 2020, 401: 125970

113. Hossain M M, Mok Y S, Nguyen D B, Kim S-J, Kim Y J, Lee J H, Heo I. Nonthermal plasma in practical-scale honeycomb catalysts for the removal of toluene. Journal of Hazardous Materials, 2021, 404(PB): 123958
114. Cimerman R, Hensel K. Generation of honeycomb discharge assisted by micro-hollow surface dielectric barrier discharge. International Journal of Plasma Environmental Science and Technology, 2021, 15: e01003
115. Nguyen V T, Dinh D K, Mok Y S, Yoon K H, Dao V D, Hossain M M, Saud S, Sosiawati T. High-throughput volatile organic compounds removal in a sandwich-type honeycomb catalyst system combined with plasma. Applied Catalysis B: Environmental, 2022, 310: 121328
116. Taghvaei H, Pirzadeh E, Jahanbakhsh M, Khalifeh O, Rahimpour M R. Polyurethane foam: a novel support for metal oxide packing used in the non-thermal plasma decomposition of CO_2. Journal of CO_2 Utilization, 2021, 44: 101398
117. Bartolomeu R, Foix M, Fernandes A, Tatoulian M, Ribeiro M F, Henriques C, da Costa P. Fluidized bed plasma for pre-treatment of Co-ferrierite catalysts: an approach to NO_x abatement. Catalysis Today, 2011, 176(1): 234–238
118. Foix M, Guyon C, Tatoulian M, Da Costa P. Study of the use of fluidized bed plasma reactors for the treatment of alumina supported palladium catalyst: application for SCR NO_x by CH_4 in stationary sources. Catalysis Communications, 2010, 12(1): 20–24
119. Oberbossel G, Güntner A T, Kündig L, Roth C, Von Rohr P R. Polymer powder treatment in atmospheric pressure plasma circulating fluidized bed reactor. Plasma Processes and Polymers, 2015, 12(3): 285–292
120. Chen G, Chen S, Feng W, Chen W, Yang S Z. Surface modification of the nanoparticles by an atmospheric room-temperature plasma fluidized bed. Applied Surface Science, 2008, 254(13): 3915–3920
121. Chen G, Chen S, Zhou M, Feng W, Gu W, Yang S. Application of a novel atmospheric pressure plasma fluidized bed in the powder surface modification. Journal of Physics D: Applied Physics, 2006, 39(24): 5211–5215
122. Du C, Qiu R, Ruan J. Plasma Fluidized Bed. Singapore: Springer, 2018
123. Andalib M, Zhu J, Nakhla G. Terminal settling velocity and drag coefficient of biofilm-coated particles at high Reynolds numbers. AIChE Journal, 2010, 56(10): 2598–2606
124. Jia Z, Vega-Gonzalez A, Ben Amar M, Hassouni K, Tieng S, Touchard S, Kanaev A, Duten X. Acetaldehyde removal using a diphasic process coupling a silver-based nano-structured catalyst and a plasma at atmospheric pressure. Catalysis Today, 2013, 208: 82–89
125. Pou J O, Colominas C, Gonzalez-Olmos R. CO_2 reduction using non-thermal plasma generated with photovoltaic energy in a fluidized reactor. Journal of CO_2 Utilization, 2018, 27: 528–535
126. Wang Q, Cheng Y, Jin Y. Dry reforming of methane in an atmospheric pressure plasma fluidized bed with Ni/γ-Al_2O_3 catalyst. Catalysis Today, 2009, 148(3-4): 275–282
127. Bouchoul N, Touati H, Fourré E, Clacens J M, Batiot-Dupeyrat C. Efficient plasma-catalysis coupling for CH_4 and CO_2 transformation in a fluidized bed reactor: comparison with a fixed bed reactor. Fuel, 2021, 288: 288
128. Chen X, Sheng Z, Murata S, Zen S, Kim H H, Nozaki T. CH_4 dry reforming in fluidized-bed plasma reactor enabling enhanced plasma-catalyst coupling. Journal of CO_2 Utilization, 2021, 54: 101771
129. Lee H, Sekiguchi H. Plasma-catalytic hybrid system using spouted bed with a gliding arc discharge: CH_4 reforming as a model reaction. Journal of Physics D: Applied Physics, 2011, 44(27): 274008
130. Młotek M, Sentek J, Krawczyk K, Schmidt-Szałowski K. The hybrid plasma-catalytic process for non-oxidative methane coupling to ethylene and ethane. Applied Catalysis A: General, 2009, 366(2): 232–241
131. Schmidt-Szałowski K, Krawczyk K, Młotek M. Catalytic effects of metals on the conversion of methane in gliding discharges. Plasma Processes and Polymers, 2007, 4(7-8): 728–736
132. Zhang H, Tan Q, Huang Q, Wang K, Tu X, Zhao X, Wu C, Yan J, Li X. Boosting the conversion of CO_2 with biochar to clean CO in an atmospheric plasmatron: a synergy of plasma chemistry and thermochemistry. ACS Sustainable Chemistry & Engineering, 2022, 10(23): 7712–7725
133. Martin-Del-Campo J, Uceda M, Coulombe S, Kopyscinski J. Plasma-catalytic dry reforming of methane over Ni-supported catalysts in a rotating gliding arc-spouted bed reactor. Journal of CO_2 Utilization, 2021, 46: 101474
134. Ding W, Xia M, Shen C, Wang Y, Zhang Z, Tu X, Liu C-J. Enhanced CO_2 conversion by frosted dielectric surface with ZrO_2 coating in a dielectric barrier discharge reactor. Journal of CO_2 Utilization, 2022, 61(2): 102045
135. Xia M, Ding W, Shen C, Zhang Z, Liu C J. CeO_2-enhanced CO_2 decomposition via frosted dielectric barrier discharge plasma. Industrial & Engineering Chemistry Research, 2022, 61(29): 10455–10460
136. Subrahmanyam C, Magureanu M, Renken A, Kiwi-Minsker L. Catalytic abatement of volatile organic compounds assisted by non-thermal plasma. Part 1. A novel dielectric barrier discharge reactor containing catalytic electrode. Applied Catalysis B: Environmental, 2006, 65(1-2): 150–156
137. Magureanu M, Mandache N B, Parvulescu V I, Subrahmanyam C, Renken A, Kiwi-Minsker L. Improved performance of non-thermal plasma reactor during decomposition of trichloroethylene: optimization of the reactor geometry and introduction of catalytic electrode. Applied Catalysis B: Environmental, 2007, 74(3-4): 270–277
138. Subrahmanyam C, Renken A, Kiwi-Minsker L. Catalytic abatement of volatile organic compounds assisted by non-thermal plasma. Part II. Optimized catalytic electrode and operating conditions. Applied Catalysis B: Environmental, 2006, 65(1-2): 157–162
139. Belov I, Vermeiren V, Paulussen S, Bogaerts A. Carbon dioxide dissociation in a microwave plasma reactor operating in a wide pressure range and different gas inlet configurations. Journal of

CO_2 Utilization, 2018, 24: 386–397

140. Vialetto L, Van De Steeg A W, Viegas P, Longo S, van Rooij G J, van De Sanden M C M, van Dijk J, Diomede P. Charged particle kinetics and gas heating in CO_2 microwave plasma contraction: comparisons of simulations and experiments. Plasma Sources Science & Technology, 2022, 31(5): 055005
141. Hosseini Rad R, Brüser V, Schiorlin M, Schäfer J, Brandenburg R. Enhancement of CO_2 splitting in a coaxial dielectric barrier discharge by pressure increase, packed bed and catalyst addition. Chemical Engineering Journal, 2023, 456: 141072–141090
142. Yong T, Zhong H, Pannier E, Laux C, Cappelli M A. High-pressure CO_2 dissociation with nanosecond pulsed discharges. Plasma Sources Science & Technology, 2023, 32(11): 115012
143. van Raak T, Li S, Gallucci F. Prevailing surface reactions in the plasma-catalytic ammonia synthesis with Ru/CeO_2 and $Ru/Ti-CeO_2$. Chemical Engineering Journal, 2022, 455: 140691
144. Barboun P M, Daemen L L, Waitt C, Wu Z, Schneider W F, Hicks J C. Inelastic neutron scattering observation of plasma-promoted nitrogen reduction intermediates on $Ni/\gamma\text{-}Al_2O_3$. ACS Energy Letters, 2021, 6(6): 2048–2053
145. Ma X, Li S, Ronda-Lloret M, Chaudhary R, Lin L, van Rooij G, Gallucci F, Rothenberg G, Shiju N R, Hessel V. Plasma assisted catalytic conversion of CO_2 and H_2O over Ni/Al_2O_3 in a DBD reactor. Plasma Chemistry and Plasma Processing, 2018, 39(1): 109–124
146. Li S, Ongis M, Manzolini G, Gallucci F. Non-thermal plasma-assisted capture and conversion of CO_2. Chemical Engineering Journal, 2021, 410: 128335
147. Ozkan A, Dufour T, Silva T, Britun N, Snyders R, Reniers F, Bogaerts A. DBD in burst mode: solution for more efficient CO_2 conversion? Plasma Sources Science & Technology, 2016, 25(5): 55005
148. Chaudhary R, van Rooij G, Li S, Wang Q, Hensen E, Hessel V. Low-temperature, atmospheric pressure reverse water-gas shift reaction in dielectric barrier plasma discharge, with outlook to use in relevant industrial processes. Chemical Engineering Science, 2020, 225: 115803
149. Li S, van Raak T, Kriek R, De Felice G, Gallucci F. Gliding arc reactor under AC pulsed mode operation: spatial performance profile for NO_x synthesis. ACS Sustainable Chemistry & Engineering, 2023, 11(34): 12821–12832
150. Bruggeman P J, Iza F, Brandenburg R. Foundations of atmospheric pressure non-equilibrium plasmas. Plasma Sources Science & Technology, 2017, 26(12): 123002
151. Wong C S, Mongkolnavin R. Methods of plasma generation. In: Elements of Plasma Technology. Singapore: Springer, 2016, 15–48
152. Kogelschatz U, Eliasson B, Egli W. Dielectric-barrier discharges. Principle and applications. Journal de Physique, IV JP, 1997, 7(4): 47–66
153. Peeters F, Butterworth T. Electrical diagnostics of dielectric barrier discharges. In: Chen AN and Z, eds. Atmospheric Pressure Plasma–from Diagnostics to Applications. London: IntechOpen, 2018
154. Peeters F J J, van de Sanden M C M. The influence of partial surface discharging on the electrical characterization of DBDs. Plasma Sources Science & Technology, 2015, 24(1): 15016
155. Pipa A V, Brandenburg R. The equivalent circuit approach for the electrical diagnostics of dielectric barrier discharges: the classical theory and recent developments. Atoms, 2019, 7(1): 14
156. Pipa A V, Hoder T, Brandenburg R. On the role of capacitance determination accuracy for the electrical characterization of pulsed driven dielectric barrier discharges. Contributions to Plasma Physics, 2013, 53(6): 469–480
157. Butterworth T, Allen R W K. Plasma-catalyst interaction studied in a single pellet DBD reactor: dielectric constant effect on plasma dynamics. Plasma Sources Science & Technology, 2017, 26(6): 065008
158. Pipa A V, Koskulics J, Brandenburg R, Hoder T. The simplest equivalent circuit of a pulsed dielectric barrier discharge and the determination of the gas gap charge transfer. Review of Scientific Instruments, 2012, 83(11): 115112
159. Pipa A V, Hoder T, Koskulics J, Schmidt M, Brandenburg R. Experimental determination of dielectric barrier discharge capacitance. Review of Scientific Instruments, 2012, 83(7): 075111
160. Van Raak T. Development of Non-thermal Plasma Reactors For Nitrogen Fixation. 2025
161. Manley T C. The electric characteristics of the ozonator discharge. Transactions of The Electrochemical Society, 1943, 84(1): 83–96
162. Brandenburg R, Jahanbakhsh S, Schiorlin M, Schmidt M. About the development and dynamics of microdischarges in toluene-containing air. Plasma Chemistry and Plasma Processing, 2019, 39(3): 667–682
163. Mujahid Z, Hala A. Plasma dynamics in a packed bed dielectric barrier discharge (DBD) operated in Helium. Journal of Physics D: Applied Physics, 2018, 51(11): 1–6
164. Engeling K W, Kruszelnicki J, Kushner M J, Foster J E. Time-resolved evolution of micro-discharges, surface ionization waves and plasma propagation in a two-dimensional packed bed reactor. Plasma Sources Science & Technology, 2018, 27(8): 085002
165. Kim H, Teramoto Y, Ogata A. Time-resolved imaging of positive pulsed corona-induced surface streamers on TiO_2 and $\gamma\text{-}Al_2O_3$-supported Ag catalysts. Journal of Physics D: Applied Physics, 2016, 49(41): 415204
166. Wang W, Kim H H, Van Laer K, Bogaerts A. Streamer propagation in a packed bed plasma reactor for plasma catalysis applications. Chemical Engineering Journal, 2018, 334: 2467–2479
167. Soldatov S, Link G, Silberer L, Schmedt C M, Carbone E, D'Isa F, Jelonnek J, Dittmeyer R, Navarrete A. Time-resolved optical emission spectroscopy reveals nonequilibrium conditions for CO_2 splitting in atmospheric plasma sustained with ultrafast microwave pulsation. ACS Energy Letters, 2021, 6(1): 124–130
168. Engeln R, Klarenaar B, Guaitella O. Foundations of optical diagnostics in low-temperature plasmas. Plasma Sources Science & Technology, 2020, 29(6): 063001
169. Laux C O, Spence T G, Kruger C H, Zare R N. Optical diagnostics of atmospheric pressure air plasmas. Plasma Sources Science & Technology, 2003, 12(2): 125–138

170. Stancu G D, Kaddouri F, Lacoste D A, Laux C O. Atmospheric pressure plasma diagnostics by OES, CRDS and TALIF. Journal of Physics D: Applied Physics, 2010, 43(12): 124002
171. Bogaerts A, Neyts E C, Guaitella O, Murphy A B. Foundations of plasma catalysis for environmental applications. Plasma Sources Science & Technology, 2022, 31(5): 053002
172. Dilecce G. Optical spectroscopy diagnostics of discharges at atmospheric pressure. Plasma Sources Science & Technology, 2014, 23(1): 015011
173. Ono R. Optical diagnostics of reactive species in atmospheric-pressure nonthermal plasma. Journal of Physics D: Applied Physics, 2016, 49(8): 83001
174. Chen S, Wang H, Dong F. Activation and characterization of environmental catalysts in plasma-catalysis: status and challenges. Journal of Hazardous Materials, 2022, 427: 128150
175. Zhang S, Oehrlein G S. From thermal catalysis to plasma catalysis: a review of surface processes and their characterizations. Journal of Physics D: Applied Physics, 2021, 54(21): 213001
176. Lee G, Go D B, O'Brien C P. Direct observation of plasma-stimulated activation of surface species using multimodal *in situ*/operando spectroscopy combining polarization-modulation infrared reflection-absorption spectroscopy, optical emission spectroscopy, and mass spectrometry. ACS Applied Materials & Interfaces, 2021, 13(47): 56242–56253
177. Clarke R J, Hicks J C. Interrogation of the plasma-catalyst interface via *in situ*/operando transmission infrared spectroscopy. ACS Engineering Au, 2022, 2(6): 535–546
178. Sheng Z, Kim H H, Yao S, Nozaki T. Plasma-chemical promotion of catalysis for CH_4 dry reforming: unveiling plasma-enabled reaction mechanisms. Physical Chemistry Chemical Physics, 2020, 22(34): 19349–19358
179. Saito A, Sheng Z, Nozaki T. *In situ* raman spectroscopy of plasma-catalyst interface for conversion of CO_2 and CH_4 to valuable compounds. International Journal of Plasma Environmental Science and Technology, 2021, 15(2): 1–12
180. Sun Y, Li J, Chen P, Wang B, Wu J, Fu M, Chen L, Ye D. Reverse water-gas shift in a packed bed DBD reactor: investigation of metal-support interface towards a better understanding of plasma catalysis. Applied Catalysis A: General, 2020, 591: 117407
181. Gibson E K, Stere C E, Curran-McAteer B, Jones W, Cibin G, Gianolio D, Goguet A, Wells P P, Catlow C R A, Collier P, et al. Probing the role of a non-thermal plasma (NTP) in the hybrid NTP catalytic oxidation of methane. Angewandte Chemie International Edition, 2017, 56(32): 9351–9355
182. Navascués P, Cotrino J, González-Elipe A R, Gómez-Ramírez A. Plasma assisted dry reforming of methane: syngas and hydrocarbons formation mechanisms. Fuel Processing Technology, 2023, 248: 107827
183. Morillo-Candas A S, Klarenaar B L M, Guerra V, Guaitella O. Fast O atom exchange diagnosed by isotopic tracing as a probe of excited states in nonequilibrium CO_2-CO-O_2 plasmas. Journal of Physical Chemistry C, 2023, 127(13): 6135–6151
184. Janssen C, Tuzson B. Isotope evidence for ozone formation on surfaces. Journal of Physical Chemistry A, 2010, 114(36): 9709–9719
185. Marinov D, Guaitella O, De Los Arcos T, Von Keudell A, Rousseau A. Adsorption and reactivity of nitrogen atoms on silica surface under plasma exposure. Journal of Physics D: Applied Physics, 2014, 47(47): 475204
186. Parastaev A, Hoeben W F L M, van Heesch B E J M, Kosinov N, Hensen E J M. Temperature-programmed plasma surface reaction: an approach to determine plasma-catalytic performance. Applied Catalysis B: Environmental, 2018, 239: 168–177
187. Alves L L, Becker M M, van Dijk J, Gans T, Go D B, Stapelmann K, Tennyson J, Turner M M, Kushner M J. Foundations of plasma standards. Plasma Sources Science & Technology, 2023, 32(2): 023001
188. Sakai O, Kawaguchi S, Murakami T. Complexity visualization, dataset acquisition, and machine-learning perspectives for low-temperature plasma: a review. Japanese Journal of Applied Physics, 2022, 61(7): 070101
189. He M, Bai R, Tan S, Liu D, Zhang Y. Driven plasma science: a new perspective on modeling diagnostics and application through machine learning. Plasma Processes and Polymers, 2024, 21(9): 2400020
190. Dobbelaere M R, Plehiers P P, van de Vijver R, Stevens C V, van Geem K M. Machine learning in chemical engineering: strengths, weaknesses, opportunities, and threats. Engineering, 2021, 7(9): 1201–1211
191. Bonzanini A D, Shao K, Graves D B, Hamaguchi S, Mesbah A. Foundations of machine learning for low-temperature plasmas: methods and case studies. Plasma Sources Science & Technology, 2023, 32(2): 024003
192. Anirudh R, Archibald R, Asif M S, Becker M M, Benkadda S, Bremer P T, Budé R H S, Chang C S, Chen L, Churchill R M, et al. 2022 review of data-driven plasma science. IEEE Transactions on Plasma Science, 2023, 51(7): 1750–1838
193. Shen Y, Fu C, Luo W, Liang Z, Wang Z R, Huang Q. Machine learning for CO_2 conversion driven by dielectric barrier discharge plasma and Cs_2TeCl_6 photocatalysts. Green Chemistry, 2023, 25(19): 7605–7611
194. Cai Y, Mei D, Chen Y, Bogaerts A, Tu X. Machine learning-driven optimization of plasma-catalytic dry reforming of methane. Journal of Energy Chemistry, 2024, 96: 153–163
195. Rashvand M, Altieri G, Abbaszadeh R, Matera A, Genovese F, Feyissa A H, di Renzo G C. Prediction of CO_2 and ethylene produced in-packaged apricot under cold plasma treatment by machine learning approach. Journal of Food Process Engineering, 2023, 46(9): 1–17
196. Mei D, Zhang P, Duan G, Liu S, Zhou Y, Fang Z, Tu X. CH_4 reforming with CO_2 using a nanosecond pulsed dielectric barrier discharge plasma. Journal of CO_2 Utilization, 2022, 62: 102073
197. Pan J, Liu Y, Zhang S, Hu X, Liu Y, Shao T. Deep learning-assisted pulsed discharge plasma catalysis modeling. Energy Conversion and Management, 2023, 277: 116620
198. Chen Y, Feng J, Wang X, Zhang C, Ke D, Zhu H, Wang S, Suo H, Liu C. Iterative approach of experiment-machine learning for efficient optimization of environmental catalysts: an example of NO_x selective reduction catalysts. Environmental Science &

Technology, 2023, 57(46): 18080–18090

199. Wilkinson M D, Dumontier M, Aalbersberg Ij J, Appleton G, Axton M, Baak A, Blomberg N, Boiten J W, da Silva Santos L B, Bourne P E, et al. Comment: the FAIR guiding principles for scientific data management and stewardship. Scientific Data, 2016, 3(1): 1–9
200. Bai R, Zhu H, Li J, Liu D, Lu X. Exploring the potential of ChatGPT in enhancing atmospheric pressure plasma research techniques. Plasma Processes and Polymers, 2024, 21(7): 1–12
201. Von Keudell A. Large language models for plasma research: curse or blessing? Plasma Processes and Polymers, 2024, 21(7): 2–3
202. Rouwenhorst K H R, Mani S, Lefferts L. Improving the energy yield of plasma-based ammonia synthesis with *in situ* adsorption. ACS Sustainable Chemistry & Engineering, 2022, 10(6): 1994–2000
203. Vertongen R, De Felice G, van den Bogaard H, Gallucci F, Bogaerts A, Li S. Sorption-enhanced dry reforming of methane in a DBD plasma reactor for single-stage carbon capture and utilization. ACS Sustainable Chemistry & Engineering, 2024, 12(29): 10841–10853
204. Attri P, Koga K, Razzokov J, Okumura T, Kamataki K, Nozaki T, Shiratani M. Plasma-ionic liquid-assisted CO_2 capture and conversion: a novel technology. Applied Physics Express, 2024, 17(4): 046001
205. Fitriani S W, Okumura T, Kamataki K, Koga K, Shiratani M, Attri P. Capture and conversion of CO_2 from ambient air using ionic liquid-plasma combination. Plasma Chemistry and Plasma Processing, 2024, 44(6): 2153–2162
206. Veng V, Tabu B, Simasiku E, Landis J, Mack J H, Carreon M, Trelles J P. Design and characterization of a membrane dielectric-barrier discharge reactor for ammonia synthesis. Plasma Chemistry and Plasma Processing, 2023, 43(6): 1921–1940
207. Hayakawa Y, Kambara S, Miura T. Hydrogen production from ammonia by the plasma membrane reactor. International Journal of Hydrogen Energy, 2020, 45(56): 32082–32088
208. Zheng Q, Xie Y, Tan J, Xu Z, Luo P, Wang T, Liu Z, Liu F, Zhang K, Fang Z, et al. Coupling of dielectric barrier discharge plasma with oxygen permeable membrane for highly efficient low-temperature permeation. Journal of Membrane Science, 2022, 641: 119896
209. Chen G, Buck F, Kistner I, Widenmeyer M, Schiestel T, Schulz A, Walker M, Weidenkaff A. A novel plasma-assisted hollow fiber membrane concept for efficiently separating oxygen from CO in a CO_2 plasma. Chemical Engineering Journal, 2019, 392: 123699
210. Chen G, Widenmeyer M, Yu X, Han N, Tan X, Homm G, Liu S, Weidenkaff A. Perspectives on achievements and challenges of oxygen transport dual-functional membrane reactors. Journal of the American Ceramic Society, 2024, 107(3): 1490–1504
211. Li S, De Felice G, Eichkorn S, Shao T, Gallucci F. A review on plasma-based CO_2 utilization: process considerations in the development of sustainable chemical production. Plasma Science & Technology, 2024, 26(9): 094001
212. Rabinovich A, Nirenberg G, Kocagoz S, Surace M, Sales C, Fridman A. Scaling up of non-thermal gliding arc plasma systems for industrial applications. Plasma Chemistry and Plasma Processing, 2022, 42(1): 35–50
213. Okubo M. Recent development of technology in scale-up of plasma reactors for environmental and energy applications. Plasma Chemistry and Plasma Processing, 2022, 42(1): 3–33
214. Tsonev I, Ahmadi Eshtehardi H, Delplancke M P, Bogaerts A. Importance of geometric effects in scaling up energy-efficient plasma-based nitrogen fixation. Sustainable Energy & Fuels, 2024, 8(10): 2191–2209
215. O'Modhrain C, Trenchev G, Gorbanev Y, Bogaerts A. Upscaling plasma-based CO_2 conversion: case study of a multi-reactor gliding arc plasmatron. ACS Engineering Au, 2024, 4(3): 333–344
216. Van Raak T, van den Bogaard H, De Felice G, Emmery D, Gallucci F, Li S. Numbering up and sizing up gliding arc reactors to enhance the plasma-based synthesis of NO_x. Catalysis Science & Technology, 2024, 14(18): 5405–5421
217. Winter L R, Chen J G. N_2 fixation by plasma-activated processes. Joule, 2021, 5(2): 300–315
218. Van Rooij G J, Akse H N, Bongers W A, van de Sanden M C M. Plasma for electrification of chemical industry: a case study on CO_2 reduction. Plasma Physics and Controlled Fusion, 2018, 60(1): 014019
219. Kaufmann S J, Rößner P, Renninger S, Lambarth M, Raab M, Stein J, Seithümmer V, Birke K P. Techno-economic potential of plasma-based CO_2 splitting in power-to-liquid plants. Applied Sciences, 2023, 13(8): 4839
220. Delikonstantis E, Scapinello M, Stefanidis G D. Process modeling and evaluation of plasma-assisted ethylene production from methane. Processes, 2019, 7(2): 68